

# **Glycopolymers for Biomedical Applications**

by

Bo Yuan

A dissertation submitted to the Graduate Faculty of  
Auburn University  
in partial fulfillment of the  
requirements for the Degree of  
Doctor of Philosophy

Auburn, Alabama  
May 04, 2013

Keywords: glycopolymer, biodecomposition, hydrogel, micelle, drug delivery

Copyright 2013 by Bo Yuan

Approved by

Gisela Buschle-Diller, Chair, Professor of Polymer and Fiber Engineering  
Peter Schwartz, Professor of Polymer and Fiber Engineering  
Maria Lujan Auad, Associate Professor of Polymer and Fiber Engineering  
Xinyu Zhang, Assistant Professor of Polymer and Fiber Engineering

## Abstract

Glycopolymers are synthetic polymers containing carbohydrate groups. They may play an important role in a wide range of biomolecular events such as adhesion, inflammation, cellular recognition, cell growth regulation, and cancer cell metastasis. They may play an important role in a wide range of biomolecular events such as adhesion, inflammation, cellular recognition, cell growth regulation, and cancer cell metastasis. In this study, three glycopolymers were synthesized and their application as biomedical materials was evaluated.

In the first project, a glycomonomer with amide linkage: (maleic acid monoamido)-2-D-glucopyranose (MAMG) was first synthesized within a one-step reaction in 4 h with relatively high yield. The product was isolated by precipitation in ethyl acetate. Copolymerization of MAMG and styrene was conducted in DMSO using AIBN as initiator with different initial monomer ratios.  $^1\text{H-NMR}$  was used to characterize the chemical structure of MAMG. The chemical structure of copolymer PMAMG-ST was confirmed by FTIR and  $^1\text{H-NMR}$ . Molecular weight and final monomer ratio on PMAMG-ST was determined by GPC and elemental analysis, respectively. The biodecomposition and release of the sugar of glycomonomer, glycopolymer and control sample was evaluated by an oxidative-fermentative test.

In the second project, glucosamine was grafted onto poly(vinyl methyl ether-alt-maleic acid) to produce a glycopolymer, Glu-PMVE-MAc, with high yield. The product was isolated by precipitation in ethyl acetate. The chemical structure of the glycopolymer was confirmed by FTIR and  $^1\text{H-NMR}$ . Elemental analysis was utilized to determine the amount of grafted

glucosamine groups. Glu-PMVE-MAc was crosslinked by poly(ethylene glycol) (PEG 400 or PEG 600). Swelling of the Glu-PMVE-MAc hydrogels in aqueous solution at pH of 1.2 to 7.4 was investigated. The mesh size of the hydrogels was calculated from swelling data using Peppas–Merrill equation. The drug delivery profile of fluorescein isothiocyanate-dextran (FITC-dextran)-loaded hydrogels in enzyme-free simulated gastric fluid (pH 1.2) and simulated intestinal fluid (pH 6.8) was studied.

In the third project, a thermo-responsive amphiphilic glycopolymer: poly(2-{{(D-glucosamine-2N-yl)carbonyl]-oxy}ethylmethacrylate)-b-poly(propylene oxide) (PHEMAGI-PPO) was synthesized via atom transfer radical polymerization (ATRP). The chemical structure of glycomonomer (HEMAGI), macroinitiator (PPO-Br), and glycopolymer was confirmed by <sup>1</sup>H-NMR or <sup>13</sup>C-NMR spectra. Degree of functionalization of PPO-Br was determined to be more than 99%. Molecular weight of glycopolymers was estimated from integral ratio of specific peaks on NMR spectra. The critical micelle concentration (CMC) of the glycopolymer was measured by dye micellization method and the diameter of the formed micelles was determined by transmission electron microscopy (TEM). The lectin recognition property was evaluated using Con A as a model lectin.

## Acknowledgments

The author would like to express his thanks to his advisor and mentor, Dr. Gisela Buschle-Diller, for her guidance, encouragement, support and valuable advice. The author is also grateful to his committee member, Dr. Peter Schwartz, Dr. Maria Auad, and Dr. Xinyu Zhang for their suggestions and help.

The author is owed a tremendous appreciation to Dr. Zhiwei Xie for his teachings, discussion, and brilliant advice. Thanks also go to group members: Dr. M. A. Karaasalan, Kai Wang, and Mei Li. Thanks to Dr. Michael Meadows for being the outside reader and advisor on the NMR study, and Dr. Michael Miller for his help with microscopic testing methods. Thanks to the Department of Polymer and Fiber Engineering for providing support and exciting research environment.

He would like to express his most sincere thanks to his parents, Dixiang Yuan and Chun Liu; his wife, Rui Liu, for the love and encouragement throughout the years.

## Table of Contents

Abstract .....	ii
Acknowledgments.....	iv
List of Figures .....	viii
List of Tables .....	xii
Chapter 1 Synthesis and Biodecomposition of Glycopolymer: Poly((maleic acid monoamido)-2-D-glucopyranose-co-styrene) (PMAMG-ST).....	1
1.1 Introduction.....	1
1.1.1 Glycopolymers.....	1
1.1.2 Synthesis of glycomonomers.....	2
1.1.3 Free radical copolymerization of glycomonomer and styrene.....	9
1.1.4 Approach to a convenient synthesis of a glycopolymer in this project .....	18
1.2 Experimental Part.....	18
1.2.1 Materials .....	18
1.2.2 Synthesis of glycomonomer and glycopolymer.....	19
1.2.3 Characterization: .....	20
1.3 Results and Discussion: .....	21
1.4 Conclusions.....	28
1.5 References.....	28
Chapter 2 Synthesis of Glucosamine-Grafted Poly(methyl vinyl ether-alt-maleic acid) (Glu-PMVE-MAc) and pH-Responsive Hydrogel for Drug Delivery Application .....	33
2.1 Introduction.....	33

2.1.1 Glycopolymers.....	33
2.1.2 Sugar derivatives grafted onto maleic groups that are connected to polymers.....	33
2.1.3 pH-responsive glycopolymer hydrogels .....	42
2.1.4 Approach.....	44
2.2 Experimental Part.....	45
2.2.1 Materials .....	45
2.2.2 Synthesis of glucosamine grafted poly(methyl vinyl ether-alt-maleic acid) .....	45
2.2.3 Synthesis of PEG crosslinked hydrogels .....	46
2.2.4 Characterization of Glu-PMVE-MAc and hydrogels .....	48
2.2.5 Determination of network mesh size .....	49
2.2.6 Drug release studies .....	50
2.3 Results and Discussion .....	52
2.4 Conclusions.....	60
2.5 References.....	61
Chapter 3 Synthesis of Amphiphilic Glycopolymer (PHEMAGI-PPO) Using Atom Transfer Radical Polymerization (ATRP) for Drug Delivery Application .....	65
3.1 Introduction.....	65
3.1.1 Glycopolymers in micelle formation .....	65
3.1.2 Synthesis of amphiphilic glycopolymers.....	67
3.1.3 Formation of glycopolymer micelles.....	69
3.1.4 CMC of amphiphilic glycopolymrs .....	72
3.1.5 Hydrodynamic diameter of glycopolymer micelles and interaction with lectins .....	73
3.1.6 Drug-loaded glycopolymer micelles.....	75
3.1.7 Approach.....	80

3.2 Experimental part.....	80
3.2.1 Materials .....	80
3.2.2 Synthesis of 2- {[ (D-glucosamine-2N-yl) carbonyl] oxy} ethyl methacrylate.....	81
3.2.3 Synthesis of end-group bromized poly(propylene glycol) (PPO-Br) .....	82
3.2.4 Atom transfer radical polymerization of amphiphilic glycopolymer .....	83
3.2.5 Characterization .....	84
3.3 Results and Discussion .....	86
3.4 Conclusions.....	98
3.5 References.....	99

## List of Figures

Figure 1.1 Synthesis of AGA and MAG.....	4
Figure 1.2 Synthesis of Glycomonomers: 3 (4-O- $\beta$ -D-galactopyranosyl-1-(acrylamido)-1-deoxyglucitol).....	4
Figure 1.3 Synthesis of 2-{{(D-glucosamine-2-N-yl)carbonyl} oxy} ethyl methacrylate.....	5
Figure 1.4 Synthesis of Glycomonomers: 5a, 5b.....	6
Figure 1.5 Synthesis of VLA (N-p-vinylbenzyl-[O- $\alpha$ -D-glucopyranosyl-(1 $\rightarrow$ 4)]-D-glucanamide).....	7
Figure 1.6 Synthesis of LAMA and GAMA.....	8
Figure 1.7 Synthesis of Glycomonomer: 8 (N-p-vinylbenzyl-D-glucuronamide).....	8
Figure 1.8 CHMA (6-(methacryloyloxy)hexyl $\beta$ -D-cellobioside).....	9
Figure 1.9 LIMA (11-(N-p-vinylbenzyl) amidoundecanoyl maltobionamide).....	10
Figure 1.10 Glycomonomers: 11, 12, 13, 14, and 15.....	11
Figure 1.11 VLA, VM5A, and VAA.....	12
Figure 1.12 LVO (D-lactose-O-(vinylbenzyl)oxime).....	13
Figure 1.13 Glycomonomers: 20, 21, 22, 23, and 24.....	14
Figure 1.14 GEMA (Glucosyloxyethyl methacrylate).....	15
Figure 1.15 Glycomonomer: 26 (2,4,6,-tri-O-acetyl-3-deoxy-D-erythro-hex-2-enono-1,5-lactone).....	15
Figure 1.16 Glycomonomers: 27, 28, and 29.....	16
Figure 1.17 Glycomonomers: 30, 31, 32, 33, 34, and 35.....	17
Figure 1.18 HEAGI (2-{{(D-glucosamine-2-N-yl) carbonyl}oxy} ethyl acrylate).....	17



Figure 1.19 <sup>1</sup> H-NMR spectra of (maleic acid monoamido)-2-D-glucopyranose (MAMG).....	22
Figure 1.20 FT-IR spectra of poly((maleic acid monoamido)-2-D-glucopyranose-co-styrene) (PMAMG-ST).....	23
Figure 1.21 <sup>1</sup> H-NMR spectra of poly((maleic acid monoamido)-2-D-glucopyranose-co-styrene) (PMAMG-ST).....	24
Figure 1.22 GPC spectra of poly((maleic acid monoamido)-2-D glucopyranose-co-styrene) (PMAMG-ST).....	25
Figure 1.23 Biodecomposition evaluation of MAMG, PSMA, and PMAMG-ST by oxidative-fermentative test (OF test) via pH change .....	27
Figure 2.1 Grafting D-galactopyranosyl- $\alpha$ -(1 $\rightarrow$ 3)-galactopyranosyl- $\alpha$ -p-aminophenol (1) onto poly(styrene-co-maleic acid) (PSMAC) .....	34
Figure 2.2 Grafting (2), (3) and (4) onto poly(styrene-co-maleic anhydride) (PSMAH).....	35
Figure 2.3 Grafting (5) – (11) onto poly(styrene-co-maleic anhydride) (PSMAH) .....	36
Figure 2.4 Grafting of (12) and (13) onto poly{styrene-co-[(maleic anhydride)-alt-styrene]} (PST-PSMAH).....	37
Figure 2.5 Grafting of N-(4-aminobutyl)-O- $\beta$ -D-galactopyranosyl-(1 $\rightarrow$ 4)-D-gluconamide (14) onto poly(N-vinylpyrrolidone-co-maleic acid) (PNVP-MAC) .....	38
Figure 2.6 Grafting of (15), (16) and (17) onto poly(ethylene-atl-maleic anhydride) (PEMAH) .....	39
Figure 2.7 Grafting of (18), (19) and (20) onto poly(propylene-alt-maleic anhydride) (PPMAH) thin film.....	40
Figure 2.8 Grafting of glucosamine (21) onto poly(isobutylene-alt-maleic acid) (PIMAC).....	41
Figure 2.9 FT-IR spectra of glucosamine grafted poly(methyl vinyl ether-alt-maleic acid) (Glu-PMVE-MAc).....	52
Figure 2.10 <sup>1</sup> H-NMR spectra of glucosamine grafted poly(methyl vinyl ether-alt-maleic acid) (Glu-PMVE-MAc).....	53
Figure 2.11 Equilibrium swelling ratio of Glu-PMVE-MAc and PMVE-MAc hydrogels in aqueous solution from pH of 1.2 to 7.4 .....	55
Figure 2.12 Mesh size of Glu-PMVE-MAc hydrogels in aqueous solution from pH of 1.2 to 7.4.....	56

Figure 2.13 Drug release profile of FITC-dextran-loaded Glu-PMVE-MAc hydrogels in enzyme-free simulated gastric fluid (SGF) (pH=1.2) or simulated intestinal fluid (SIF) (pH=6.8) within 240 min .....	59
Figure 2.14 Drug release profile of FITC-dextran-loaded Glu-PMVE-MAc hydrogels in enzyme-free simulated gastric fluid (SGF) (pH=1.2) or simulated intestinal fluid (SIF) (pH=6.8) within 120 h.....	60
Figure 3.1 Star-shaped poly( $\epsilon$ -caprolactone)-b-poly(D-gluconamidoethyl methacrylate) glycopolymers (SPCL-PGAMA).....	67
Figure 3.2 Star-shaped poly( $\epsilon$ -caprolactone)-b-poly(D-lactobionamidoethyl methacrylate) glycopolymers (SPCL-PLAMA) .....	68
Figure 3.3 Poly(2- {[D-glucosamin-2N-yl]carbonyl}-oxy}ethyl methacrylate-b-poly(n-butyl acrylate) (PHEMAGI-PBA).....	69
Figure 3.4 Poly(2-( $\beta$ -D-galactosyloxy)ethyl methacrylate-co-styrene)-b-polystyrene (P(GalEMA-co-S)-b-PS).....	69
Figure 3.5 Poly(ethylene oxide)-poly(D-gluconamidoethyl methacrylate)-poly(2-(diethylamino)ethyl methacrylate) (PEO-GAMA-DEA) and poly(propylene oxide)-poly(D-gluconamidoethyl methacrylate) (PPO-GAMA) .....	70
Figure 3.6 Poly(3-O-methacryloyl- $\alpha,\beta$ -D-glucopyranose)-b-poly(2-(diethylamino)ethyl methacrylate) (PMAGlc-PDEA).....	71
Figure 3.7 Poly(2'-(4-vinyl-[1,2,3]-triazol-1-yl)ethyl-O- $\alpha$ -D-mannopyranoside)-b-poly(N-isopropyl acrylamide) .....	71
Figure 3.8 Peracetylated maltoheptaose-b-poly(2-ethyl-2-oxazoline)-b-peracetylated maltoheptaose (AcMH-b-PEtOz-b-AcMH).....	72
Figure 3.9 Star-shaped poly( $\gamma$ -benzyl L-glutamate)-b-poly(D-gluconamidoethyl methacrylate) (SPBLG-PGAMA).....	77
Figure 3.10 Star poly(amido amine)-b-poly( $\epsilon$ -caprolactone)-b-poly(D-gluconamidoethyl methacrylate) (PAMAM- PCL-PGAMA).....	78
Figure 3.11 Poly(6-O-(2'-formyl-4'-vinylphenyl)-D-galactopyranose-b-5,6-benzo-2-methylene-1,3-dioxepane) (PVDG-BMDO) .....	79
Figure 3.12 $^{13}\text{C}$ -NMR spectra of HEMAN.....	86
Figure 3.13 $^1\text{H}$ -NMR spectra of HEMAGI.....	87
Figure 3.14 $^1\text{H}$ -NMR spectra of PPO-Br .....	88

Figure 3.15 $^1\text{H-NMR}$ spectra of PHEMAGI-PPO .....	89
Figure 3.16 CMC determination of PHEMAGI <sub>62</sub> -PPO <sub>41</sub> (A), PHEMAGI <sub>46</sub> -PPO <sub>41</sub> (B), PHEMAGI <sub>31</sub> -PPO <sub>41</sub> (C), and PHEMAGI <sub>15</sub> -PPO <sub>41</sub> (D) .....	92
Figure 3-17 Optical transmittance measurement as a function of temperature for PHEMAGI-PPO micelles .....	94
Figure 3-18 TEM images of PHEMAGI <sub>62</sub> -PPO <sub>41</sub> (A), PHEMAGI <sub>46</sub> -PPO <sub>41</sub> (B), PHEMAGI <sub>31</sub> - PPO <sub>41</sub> (C), and PHEMAGI <sub>15</sub> -PPO <sub>41</sub> (D) .....	95
Figure 3.19 Lectin binding ability test of PHEMAGI-PPO using Con A (0.5 mg/mL) as model lectin.....	98

## List of Tables

Table 1.1 Molecular weight and PDI of PMAMG-ST .....	25
Table 1.2 Monomer ratio on PMAMG-ST .....	26
Table 2.1 Amount of utilized reagents and yield for synthesis of Glu-PMVE-MAc .....	46
Table 2.2 Amount of reagents in synthesis of PMVE-MAc or Glu-PMVE-MAc hydrogels.....	47
Table 2.3 Glucosamine substitution rate on Glu-PMVE-MAc.....	54
Table 2.4 Actual weight and weight percentage of released Glu-PMVE-MAc of G2-400 hydrogels after immersing in SGF or SIF in 240 minutes .....	57
Table 3.1 CMC of amphiphilic glycopolymers and common surfactant.....	72
Table 3.2 $D_h$ of glycopolymer aggregates determined by DLS and lectins that can interact with them.....	74
Table 3.3 Amount of utilized reagents for synthesis of PHEMAGI-PPO .....	84
Table 3.4 Characteristics of PHEMAGI-PPO glycopolymers synthesized by ATRP .....	90
Table 3.5 CMC and concentration at onset of linear course.....	93
Table 3.6 Lower critical solution temperature (LCST) of PHEMAGI-PPO.....	94
Table 3.7 Size of the micelles and the concentration of the glycopolymer solutions.....	96

**CHAPTER 1 SYNTHESIS AND BIODECOMPOSITION OF GLYCOPOLYMER:  
POLY((MALEIC ACID MONOAMIDE)-2-D-GLUCOPYRANOSE-CO-  
STYRENE) (PMAMG-ST)**

**1.1 Introduction**

**1.1.1 Glycopolymers**

Glycopolymers are synthetic polymers with carbohydrate groups; they form a bridge between purely synthetic polymers and polysaccharides. Other terms for glycopolymers are polyvinyl saccharides, carbohydrate-containing polymers and synthetically modified sugar-based polymers. The sugar units can be monomeric, dimeric or oligomeric and built into the polymer backbone or grafted onto the synthetic polymer.

Applications of glycopolymers in the biomedical area can be found in areas of virus inhibition, drug delivery, hydrogel and micelle formation, etc. For instance, the infection of the Influenza virus starts from interaction between hemagglutinins on the surface of the virus with sialosides on the cell surface. If such an interaction can be prevented, infection might be stopped at this stage. Sigal and the co-researchers synthesized two glycopolymers containing sialoside pendent groups by polymerization or grafting (Sigal et al., 1996).  $K_i$  value is the minimum concentration of sialoside groups (not the concentration of glycopolymer) required to prevent hemagglutination of chicken red blood cells caused by virus. The lower the  $K_i$  value, the prevalent is the interaction. The  $K_i$  value decreased with the increasing molecular weight of the glycopolymers. Compared to single sialoside, the  $K_i$  value was lower by a factor of  $10^{-3}$ .

Glycopolymer-drug conjugates were synthesized for targeted drug delivery to minimize undesirable side effects. A glycopolymer containing galactose pendent groups was conjugated with doxorubicin, which is a common anti-cancer drug that causes significant side effects. Animal survival tests were performed to evaluate the toxicity (Hopwell et al. 2001). All animals survived after 12 weeks with glycopolymer-doxorubicin conjugate treatment of 4, 8, and 12 mg/kg. However, animal survival rate was reduced with an increasing dose of free doxorubicin. Only 4 mg/kg free doxorubicin resulted 100% death after 12 weeks. The system was then assessed in a Phase I clinical trial involving patients with solid hepatic tumors (Seymour et al. 2002). Uptake of the conjugate into hepatic tumors was significantly higher than the control due to the interaction of galactose groups with corresponding receptors on the tumors.

Glycopolymers were usually synthesized by four different methods: polymerization of glycomonomers or copolymerization of glycomonomers with vinyl monomers, ring-opening polymerization of anhydro-sugars, enzyme-mediated polymerization, and grafting of sugars onto functionalized synthetic polymers (Varma et al. 2004). In this paper, the focus is on the synthesis of amide linked glycomonomers and free radical copolymerization of glycomonomers with styrene.

### **1.1.2 Synthesis of glycomonomers**

Sugars have been linked to vinyl molecules to synthesize glycomonomers by amide linkage, ester linkage, ether linkage, and other linkages. Since the glycomonomer used in this paper contains amide linked sugar, the main focus is on the introduction of glycomonomers synthesized by amide linkage. Most sugar precursors that were commonly used in glycomonomer synthesis are not commercially available. Synthesis of those precursors might

occur via one or more reactions. Similarly, most vinyl precursors are commercially unavailable as well and need to be synthesized. Therefore, the overall synthesis can be tedious and time-consuming.

Masutda and co-workers developed a glycomonomer: N-acryloyl-D-glucosamine (AGA, **1**) (Fig. 1.1) within one reaction with a yield of 38% (Masutda et al., 1996). The glycomonomer was obtained by reacting D-glucosamine hydrochloride with acryloyl chloride in potassium carbonate aqueous solution using sodium nitrite as polymerization inhibitor. The total reaction time was 24 h. The glycomonomer was separated by pouring the reaction solution to ethanol and recrystallized in a mixed solvent. Bernard and co-workers synthesized the same glycomonomer with minor change (Bernard et al. 2006). They isolated the product by passing the reaction mix through a silica chromatography column followed by recrystallization. In this case a yield of only 20% was achieved. Further redesign of synthesis of AGA led to a slightly different glycomonomer: 2-(methacrylamido)glucopyranose (MAG, **2**) (Fig. 1.1) by the same synthesis and separation method as AGA within 24 h. Methacryloyl chloride was linked with D-glucosamine hydrochloride to produce such product. A yield of 32% and 58% was reported in two different papers for this product, respectively (Pearson et al., 2009 and Ting et al., 2010).

Wilson et al. (1998) reported the synthesis of 4-O- $\beta$ -D-galactopyranosyl-1-(acrylamido)-1-deoxyglucitol (**3**) (Fig. 1.2). A sugar precursor containing an amine group was obtained by treatment of lactose with hydrazine hydrate for 24 h and then with hydrogen gas for another 24 h. A similar synthetic strategy as the production of AGA was applied to produce **3** from sugar precursor and acryl chloride. Extraction and precipitation were utilized to obtain the final product. The total yield, which is defined as the product of yield of each reaction was calculated to be 58.9%.

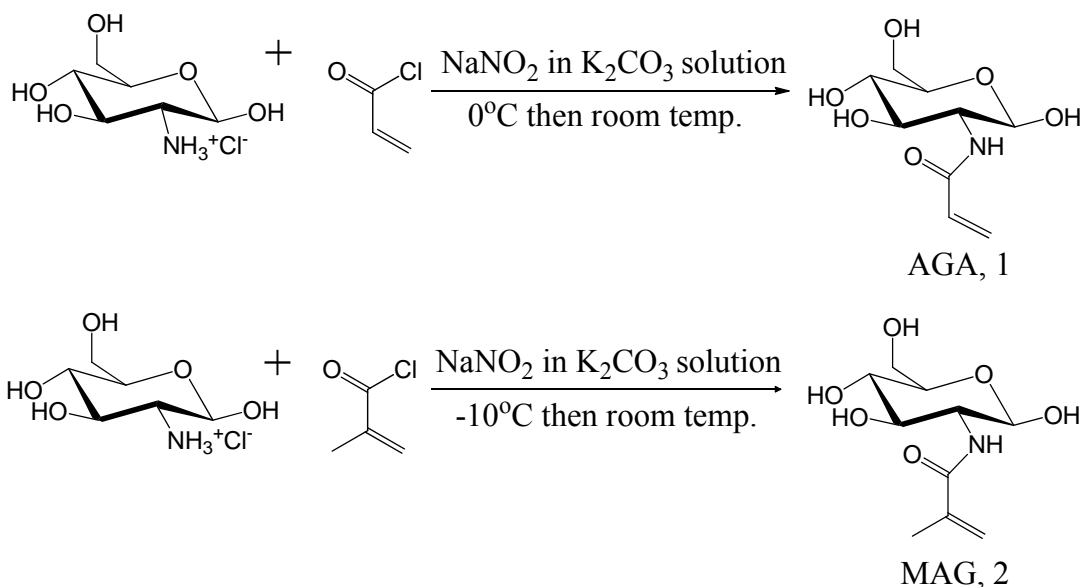


Figure 1-1 Synthesis of AGA and MAG (Masutda et al., 1996 and Pearson et al., 2009)

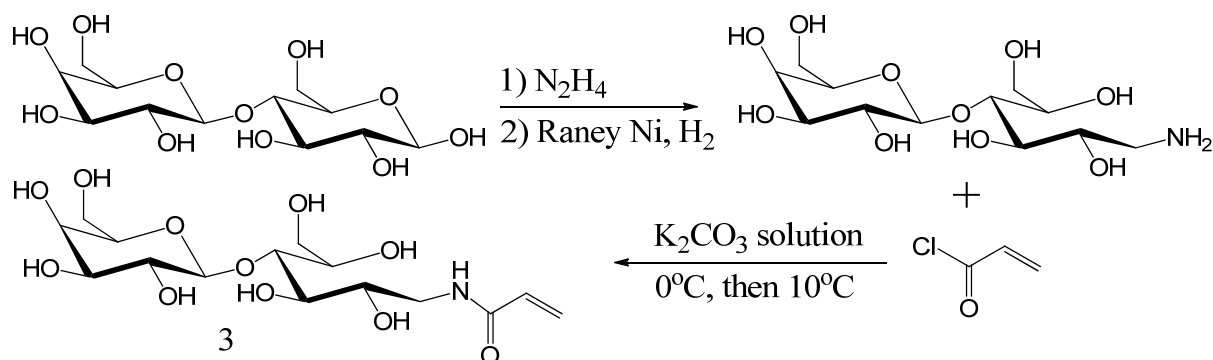
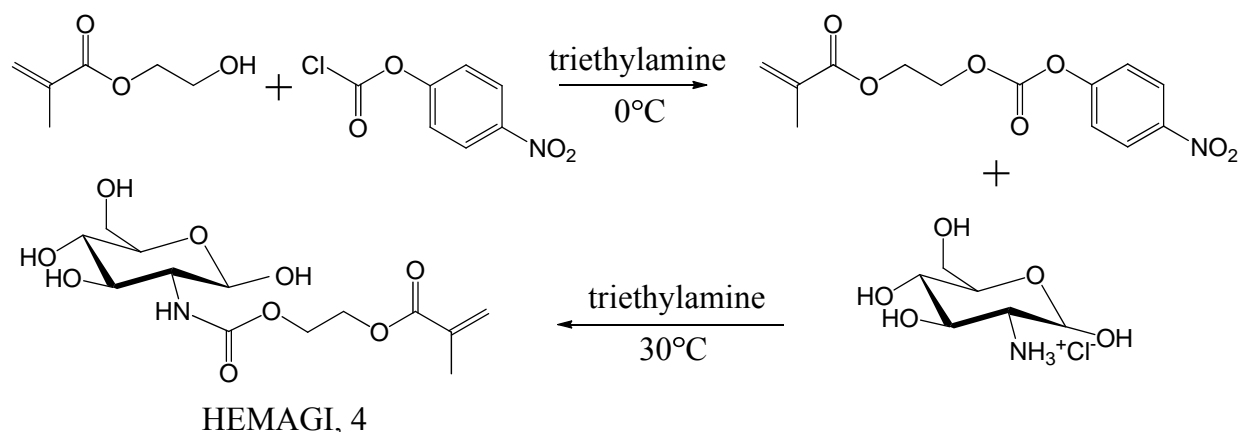


Figure 1-2 Synthesis of Glycomonomers: 3 (4-O-β-D-galactopyranosyl-1-(acrylamido)-1-deoxyglucitol; Wilson et al. 1998)

Another glycomonomer 2-{[(D-glucosamine-2-N-yl)carbonyl] oxy}ethyl methacrylate (HEMAGI, 4) (Fig. 1.3) was produced by researchers in Garcia's group (Leon et al., 2010). The vinyl precursor was synthesized by reaction between 2-hydroxyethyl methacrylate and p-nitrophenyl chloroformate for 24 h and isolated by precipitation in cold methanol. D-glucosamine hydrochloride was then linked to the vinyl precursor and purified by precipitation in a solvent mixture. The total reaction took 48 h with total yield of 57%.





**Figure 1-3 Synthesis of 2-[(D-glucosamine-2-N-yl)carbonyl]oxyethyl methacrylate (HEMAGI; Leon et al., 2010)**

Mixture of sialyllactose isomers isolated from bovine milk was aminated and reacted with p-vinylbenzyl chloride to synthesize two glycomonomers: N-p-vinylbenzoyl-b-sialyllactosylamine (**5a**, **5b**) (Fig. 1.4) within two reactions (Tsuchida et al., 1998<sup>a</sup>). Sialyllactosylamine was obtained from reaction between sialyllactose and ammonium hydrogen carbonate in 72 h. Excess ammonium hydrogen carbonate was removed by dilution of the residue with water, concentration of the solution and then filtration. Reaction of sialyllactosylamine with p-vinylbenzyl chloride took 5 h. The product was purified by chromatography. Total yield was reported to be 88%. Three enzymatically synthesized oligosaccharides were aminated and linked with p-vinylbenzyl chloride in the same way by the same research group (Tsuchida et al. 1998<sup>b</sup>).

Kobayashi et al. (1985) produced N-p-vinylbenzyl-[O- $\alpha$ -D-glucopyranosyl-(1 $\rightarrow$ 4)]-D-glucanamide (VLA, **6**) (Fig. 1.5) within four reactions. They first oxidized D-maltose-1-hydrate to maltono-1,5-lactone. Separation of the sugar precursor required precipitation, recrystallization and purification by passing through a chromatography column. The vinyl precursor p-vinylbenzylamine was prepared from p-vinylbenzyl chloride with two steps. To synthesize the

glycomonomer, the oxidized six-membered ring on sugar precursor was opened; and an amide linkage was formed between the sugar precursor and the vinyl precursor. The total reaction time was estimated to be 72 h; and the total yield was calculated to be 42.4%.

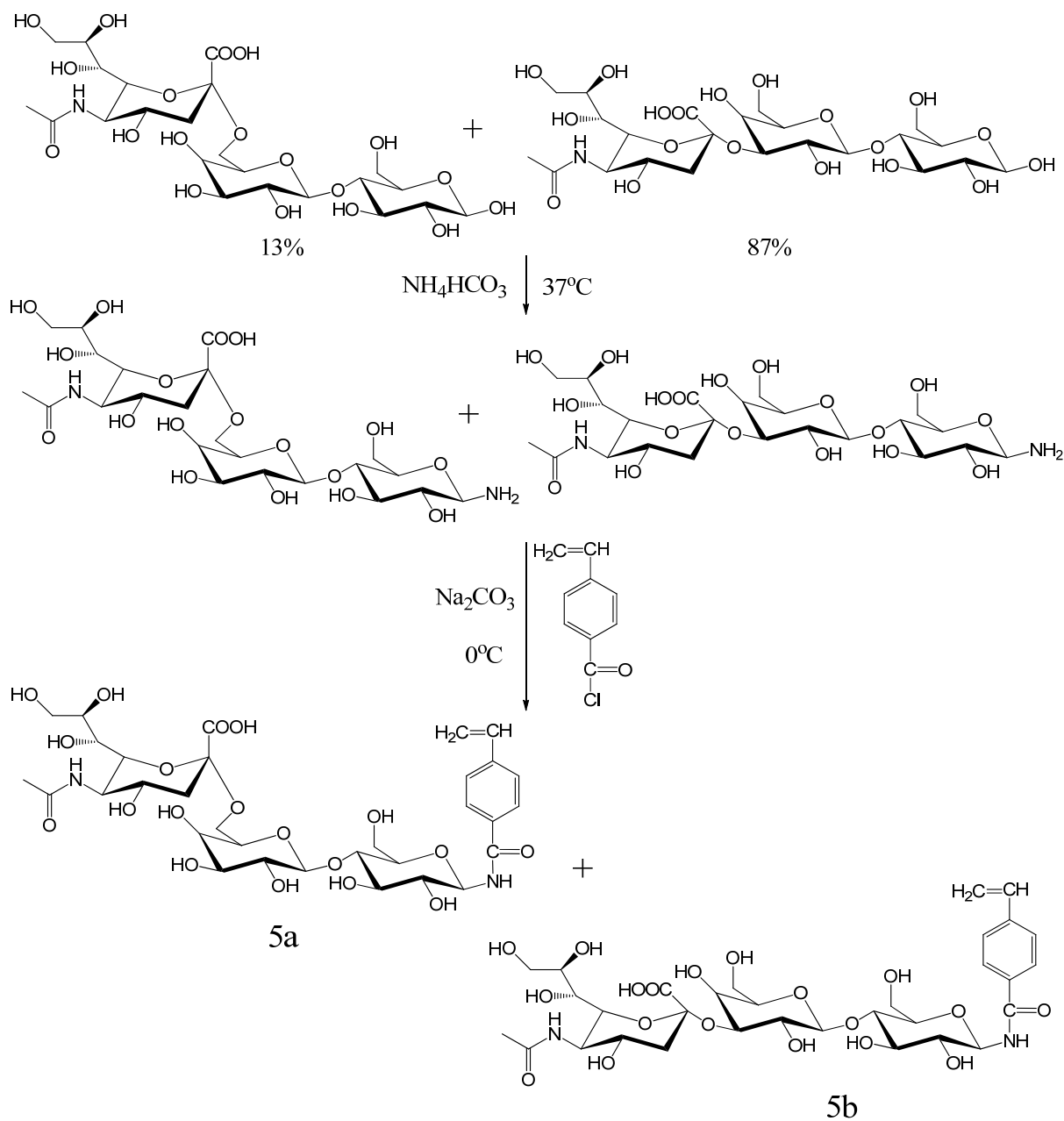
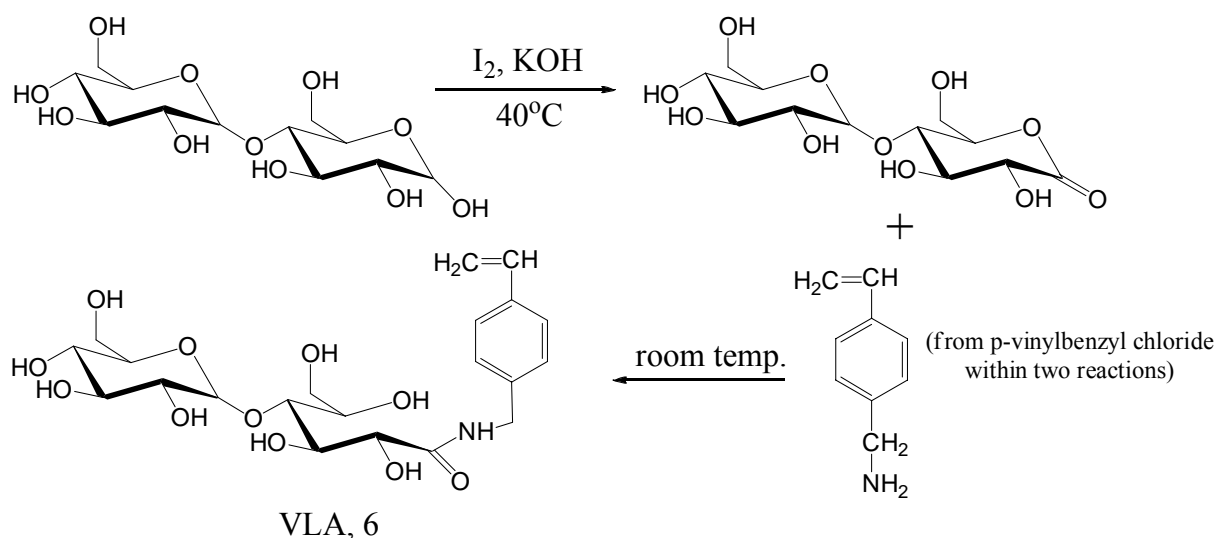


Figure 1-4 Synthesis of Glycomonomers: 5a, 5b (Tsuchida et al., 1998<sup>3</sup>)

A similar synthetic method as for the production of VLA was utilized to prepare 2-lactobionamidoethyl methacrylate (LAMA, **7a**) (Fig. 1.6) with three steps (Narain et al., 2003). The vinyl precursor 2-aminoethyl methacrylate was obtained by reaction of ethanolamine and methacryl chloride followed by precipitation and recrystallization. The sugar precursor lactobionolactone was converted from lactobionic acid by vacuum distillation at 50°C. The total yield was reported to be 54.6%. Another glycomonomer, D-gluconamidoethyl methacrylate (GAMA, **7b**) (Fig. 1.6), was synthesized in the same manner.



**Figure 1-5** Synthesis of VLA (N-p-vinylbenzyl-[O- $\alpha$ -D-glucopyranosyl-(1 $\rightarrow$ 4)]-D-glucanamide; Kobayashi et al. 1985)

N-p-vinylbenzyl-D-glucuronamide (**8**) (Fig. 1.7) was synthesized by Kim et al. (2000) by a four step reaction. D-glucuronolactone was first acetalized in acetone using  $\text{H}_2\text{SO}_4$  as catalyst. The ester bond on the sugar precursor was opened when reacting with p-vinylbenzylamine, which was prepared from p-vinylbenzyl chloride as the glycomonomer. The total reaction time was estimated to be 48 h and the total yield was calculated to be 34.5%. Glycomonomers having D-glucuronic moieties were obtained by a similar approach (Hashimoto et al., 1999)

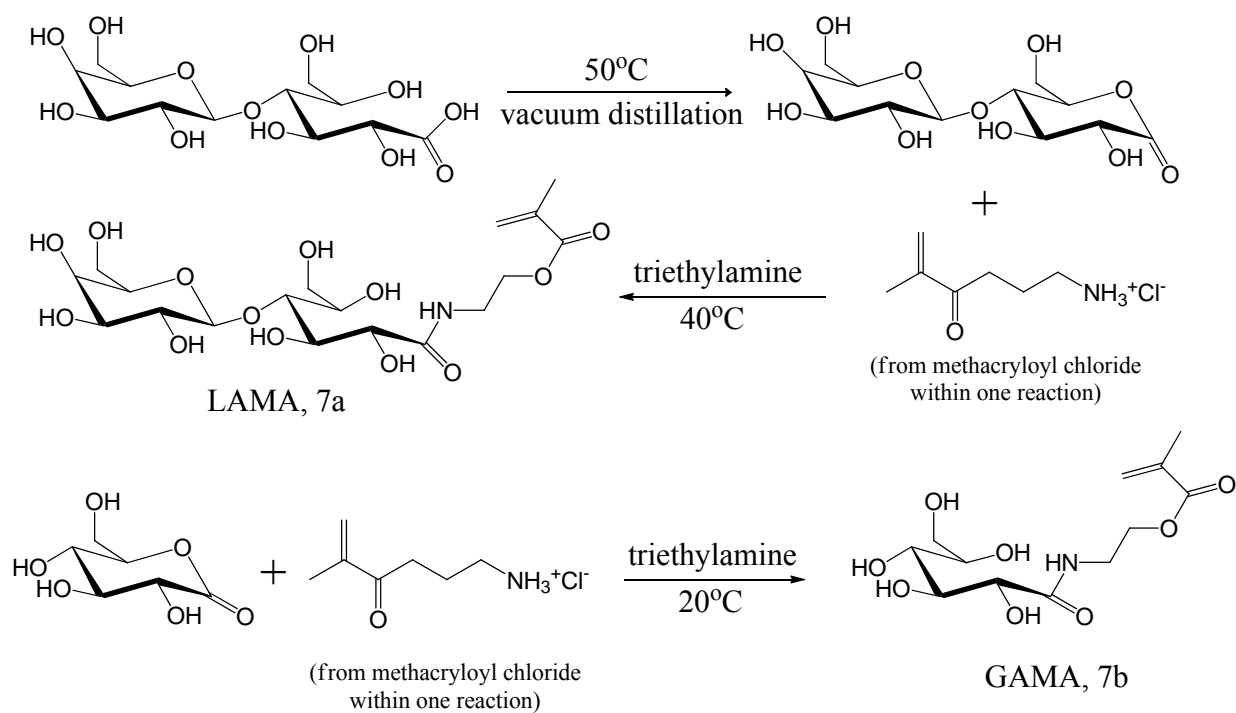


Figure 1-6 Synthesis of LAMA and GAMA (Narain et al., 2003)

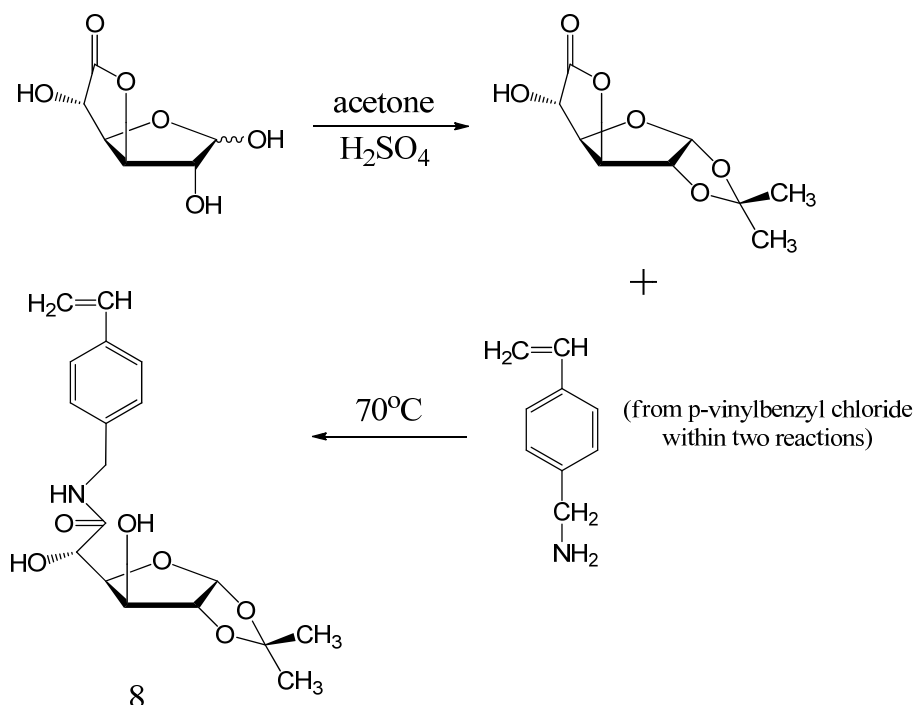


Figure 1-7 Synthesis of Glycomonomer: 8 (N-p-vinylbenzyl-D-glucuronamide; Kim et al. 2000)

Glycomonomers containing ester linkages were synthesized by several researchers (Ye et al., 2001, Gotz, et al., 2002, Malinova et al., 2005, Muthukrishnan et al., 2005<sup>a,b</sup>, Ting et al., 2007, Cameron et al., 2008, Borges et al., 2009, Ting et al., 2009<sup>a</sup>, Suriano et al., 2010). Glycomonomers having ether linkage were reported in various papers as well (Yamada et al., 2001, D'Agosto et al., 2002, Lu et al., 2005, Guo et al., 2006, Cameron et al., 2008, Broyer et al., 2008, Ting et al., 2009<sup>b</sup>, Xu et al., 2009, Otman et al., 2010, Ke et al., 2010, Hu et al., 2010).

### 1.1.3 Free radical copolymerization of glycomonomer and styrene

A glycopolymer containing styrene was first reported by Charreyre et al. (1993). The glycomonomer 6-(methacryloyloxy)hexyl  $\beta$ -D-cellobioside (CHMA, **9**) (Fig. 1.8) was copolymerized with styrene at different monomer ratios in DMSO using AIBN as initiator. After 20 h, conversion of CHMA reached about 80%; and conversion of styrene varied from about 60% to about 100% with different initial monomer ratios. Composition of two monomers in glycopolymers agreed well with theoretical value.

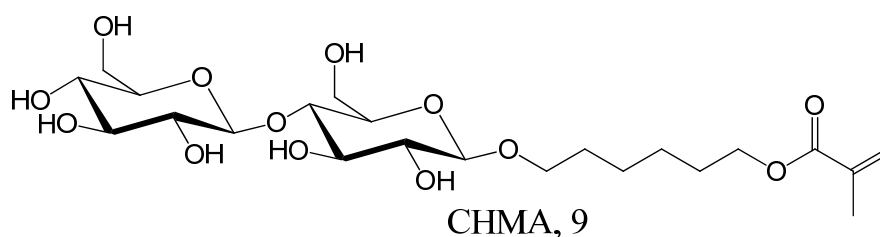
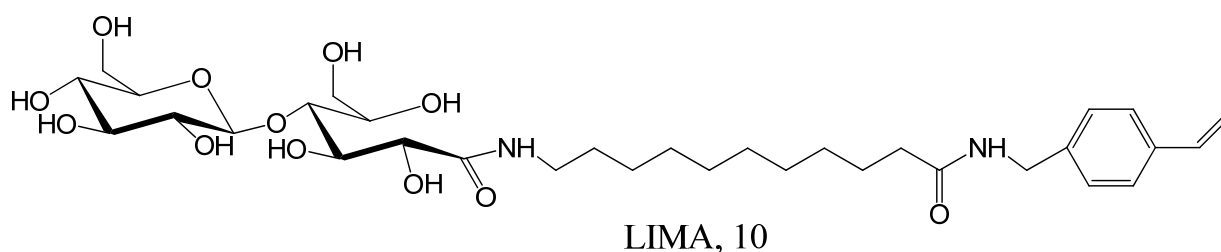


Figure 1-8 CHMA (6-(methacryloyloxy)hexyl  $\beta$ -D-cellobioside; Charreyre et al. 1993)

Copolymerization of glycomonomer 11-(N-p-vinylbenzyl) amidoundecanoyl maltobionamide (LIMA, **10**) (Fig. 1.9) and styrene in DMSO was reported in 1996 (Revilla et al. 1996). AIBN was used as initiator. Conversion of LIMA was about 80%; and styrene of about 60%. Copolymerization reactivity ratio was calculated to be  $r_S = 1.23 \pm 0.09$  and  $r_{LIMA} = 0.86 \pm 0.1$ .

Furthermore, LIMA was used as polymerizable emulsifier for production of sugar functionalized polystyrene nanoparticles (Revilla et al., 1993). Critical micelle concentration (CMC) of LIMA was first determined by surface tension measurement as well as fluorescence emission spectra. Batch emulsion polymerization of styrene was carried out using LIMA as emulsifier, potassium persulfate as initiator, and dipotassium phosphate as buffer. Various concentrations of LIMA led to different sizes of nanoparticles ranging from 130 to 330 nm. Seeded emulsion polymerization of styrene was also conducted.



**Figure 1-9 LIMA (11-(N-p-vinylbenzyl) amidoundecanoyl maltobionamide; Revilla et al. 1996)**

Wulff and colleagues synthesized a protected glycomonomer: 2,3;4,5-di-*O*-isopropylidene-1-(4-vinylphenyl)-D-gluco(D-manno)pentitol (**11**) (Fig. 1.10) and copolymerized **11** with styrene in bulk and solution using AIBN as initiator (Wulff et al. 1997). Bulk polymerization achieved a yield of more than 85%. Mol fraction of **3** in glycopolymers agreed well with feed monomer ratio in bulk as well as solution polymerization. Films and plates of glycopolymers were produced by casting and hot pressing, respectively. The water contact angle of deprotected films decreased with increasing amount of sugar moieties. Later on, the same researchers copolymerized four glycomonomers: (**11**), 7,8-dideoxy-1,2;3,4-di-*O*-isopropylidene- $\alpha$ -D-galacto-oct-7-en-1,5-pyranose-6-ulose (**12**), 1,2;5,6-di-*O*-isopropylidene-3-*O*-methacryloyl- $\alpha$ -D-glucofuranose (**13**), and 2,3;5,6-di-*O*-isopropylidene-1-(4-vinylphenyl)-keto-D-glucose (**14**)

(Fig. 1.10) to study the surface properties of deprotected glycopolymers (Wulff et al. 1999). The copolymerization reactivity ratio of these four polymerizations was calculated. The water contact angle and the surface resistance of the produced films and plates were also measured. In 2002, a glycomonomer was deprotected to produce 4-vinylphenyl-D-gluco(D-manno)hexitol (**15**) (Fig. 1.10) by Narain et al. (2002). Compound **15** was copolymerized with styrene in DMF and the copolymerization initiated by AIBN.

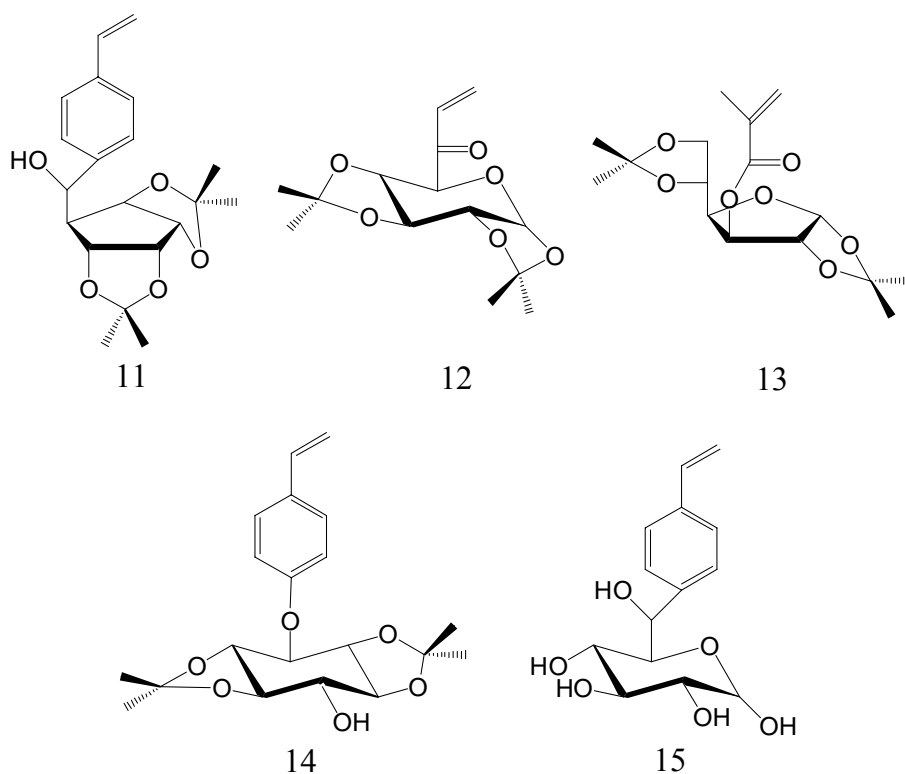


**Figure 1-10 Glycomonomers: 11, 12, 13, 14, and 15 (Wulff et al. 1997, Wulff et al. 1999 and Narain et al. 2002)**

Glycomonomers containing a disaccharide: N-p-vinylbenzyl-[O- $\beta$ -D-galactopyranosyl-(1-4)]-D-gluconamide (VLA, **16**), a penta-saccharide: N-p-vinylbenzyl-[O- $\alpha$ -D-glucopyranosyl-(1-4)]-4-D-gluconamide (VM5A, **17**), and a polysaccharide: N-p-vinylbenzyl-[O- $\alpha$ -D-glucopyranosyl-(1-4)]-p-1-D-gluconamide (VAA, **18**) (Fig. 1.11) were synthesized by Kobayashi and Kamiya

(Kobayashi et al., 1997). The copolymerization of these glycomonomers and styrene was carried out in DMSO using AIBN as initiator. It was found that with only 0.18 mol % of VAA, the glycopolymer turned to be insoluble in chloroform whereas pure polystyrene is soluble. Methyl orange which is insoluble in chloroform was soluble in chloroform containing little amount of glycopolymers. Hence, methyl orange was solubilized into chloroform with the help of glycopolymers.

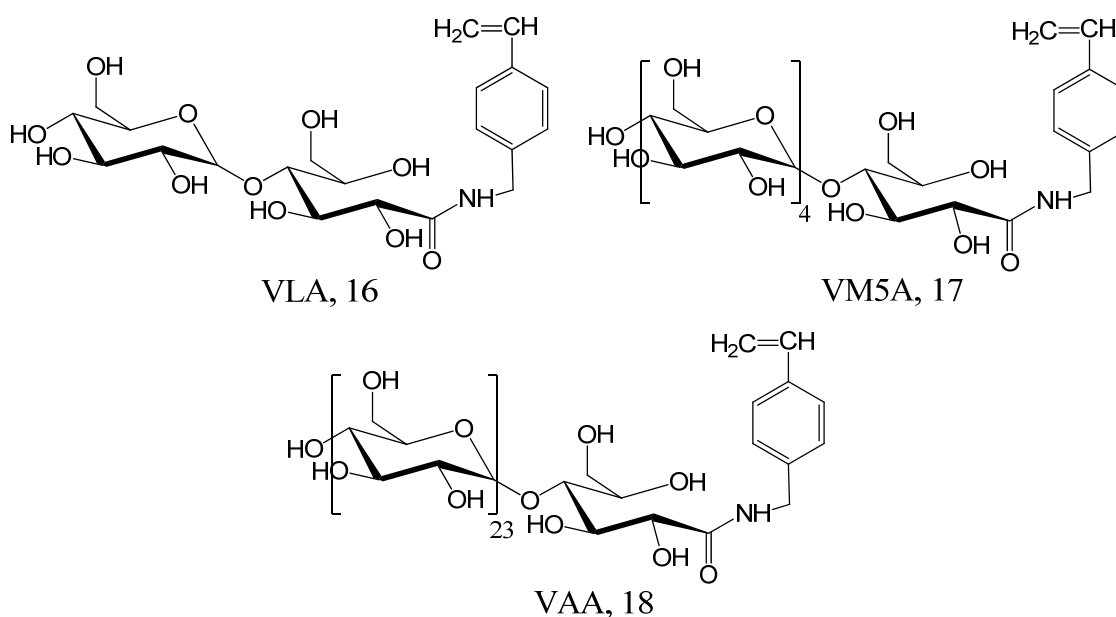


**Figure 1-11 VLA, VM5A, and VAA (Kobayashi et al., 1997)**

A thorough study of copolymerization of D-lactose-O-(vinylbenzyl)oxime (LVO, **19**) (Fig. 1.12) with styrene was reported by Zhou et al. (1998). The reaction was performed in a mixed solvent (DMSO/toluene=1:1) and initiated by AIBN. The relationship between conversion and initial monomer ratio at 65°C was studied. Conversion of copolymerization at 55°C, 65°C, 75°C was measured too. TGA characterization showed that pendent disaccharide moieties compromised the thermal stability of the glycopolymers.



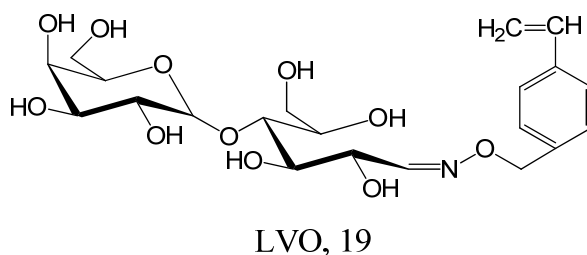
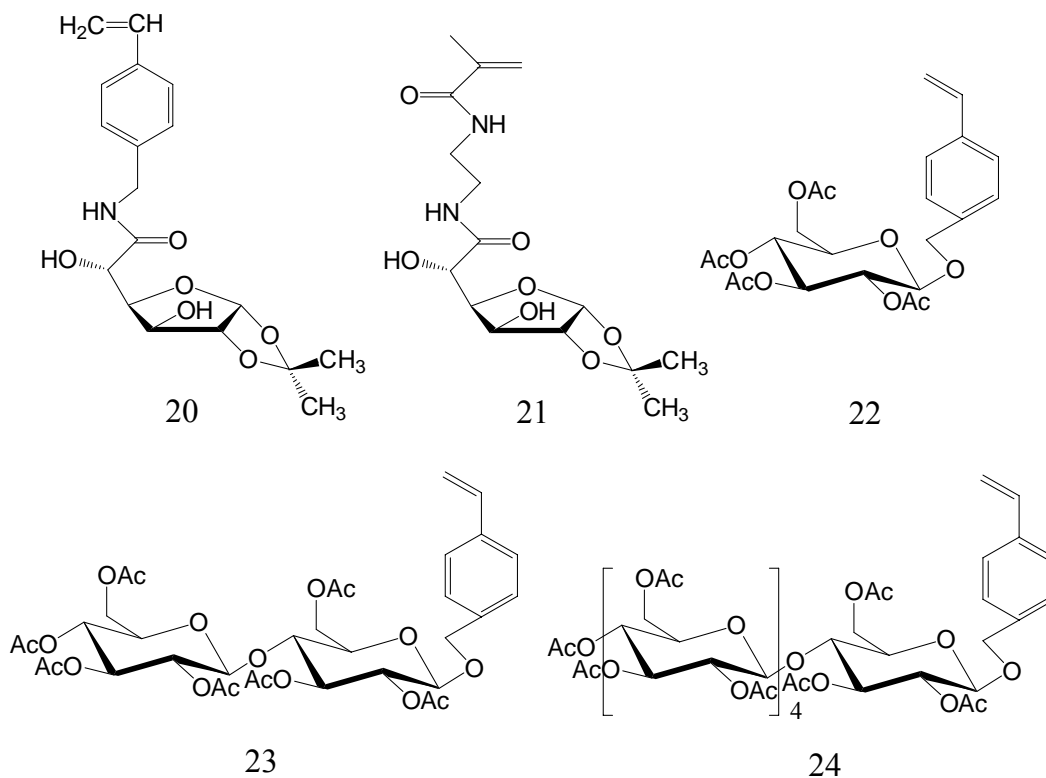


Figure 1-12 LVO (D-lactose-O-(vinylbenzyl)oxime; Zhou et al. 1998)

The solubility of glycopolymers containing styrene in various solvents was investigated by two Japanese research groups. Two protected glycomonomers, *N*-(*p*-vinylbenzyl)-1,2-*O*-isopropylidene-6-*D*-glucofuranuronamide (**20**) and *N*-(2-methacryloylamino)ethyl-1,2-*O*-isopropylidene-6-*D*-glucofuranuronamide (**21**) (Fig. 1.13), were copolymerized with styrene with various initial feed ratios in DMSO and initiated by AIBN (Shimura et al. 2001). The solubility of the product glycopolymers with different amounts of glycomonomers at the backbone after deprotection was studied in ten solvents from hexane to water with increasing solubility parameters. Three glycomonomers with acetylated monosaccharide, disaccharide, and penta-saccharide pendent groups, 4-vinylbenzyl 2,3,4,6-tetra-*O*-acetyl- $\beta$ -*D*-glucopyranoside (**22**), 4-vinylbenzyl *O*-(2,3,4,6-tetra-*O*-acetyl- $\alpha$ -*D*-glucopyranosyl)-(1 $\rightarrow$ 4)-*O*-2,3,6-tri-*O*-acetyl- $\beta$ -*D*-glucopyranoside (**23**), and 4-vinylbenzyl *O*-(2,3,4,6-tetra-*O*-acetyl- $\alpha$ -*D*-glucopyranosyl)-(1 $\rightarrow$ 4)-[(*O*-2,3,6-tri-*O*-acetyl- $\alpha$ -*D*-glucopyranosyl)-(1 $\rightarrow$ 4)]<sub>4</sub>-*O*-2,3,6-tri-*O*-acetyl- $\beta$ -*D*-glucopyranoside (**24**) (Fig. 1.13), were copolymerized with styrene in DMF using AIBN as initiator (Narumi et al. 2001). Varying the initial molar ratios led to various glycopolymers with different glycomonomer mol fractions. After deacetylation, the solubility of deprotected glycopolymers in toluene, chloroform, THF, and water was studied. With a  $W_g$  value, which is weight percentage of glucose residue in the glycopolymer, greater than about 50%, the glycopolymers dissolved in water. However, with  $W_g$  value less than about 40%, the

glycopolymers precipitated in water.



**Figure 1-13 Glycomonomers: 20, 21, 22, 23, and 24 (Shimura et al. 2001 and Narumi et al. 2001)**

Serizawa et al. (2001) reported an interesting amphiphilic glycopolymers which had a polystyrene hydrophobic block and a glycopolymers hydrophilic block. The author first initiated the glycomonomer: glucosyloxyethyl methacrylate (GEMA, **25**) (Fig. 1.14) by ammonium peroxydisulfate in DMF. The resulting oligomer was modified by reacting with 4-vinylbenzoic acid to produce a macromonomer which further copolymerized with styrene in an ethanol/water mixture using AIBN as initiator. Micelles were obtained by dialysis against distilled water. From dynamic light scattering (DLS) and transmission electron microscopy (TEM) images, the mean diameter of micelles was determined to be 300 to 620 nm depending on the molar ratio of styrene and the macromonomer. The author also found that the micelles could recognize Con A, which is a lectin that interacts specifically with glucose.

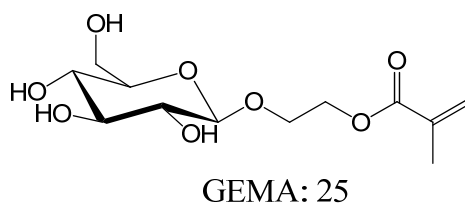


**Figure 1-14 GEMA (Glucosyloxyethyl methacrylate; Serizawa et al. 2001)**

A unique acetylated glycolmonomer, 2,4,6,-tri-O-acetyl-3-deoxy-D-erythro-hex-2-enono-1,5-lactone (**26**) (Fig. 1.15), which has a double bond in its six-membered ring was synthesized by Glumer et al. (2004). It was copolymerized with equal amounts of styrene in benzene. AIBN and dibenzoyl peroxide were used as initiators. The copolymerization was conducted at 60°C for 120 h. The sugar moiety served as the backbone in the glycopolymer rather than as pendent group in most glycopolymers. Because of styrene's high reactivity, the glycopolymer only contained 5 mol% of **26**. The yield was also limited.

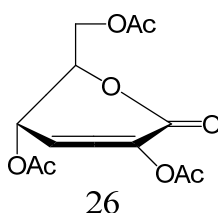


**Figure 1-15 Glycomonomer: 26 (2,4,6,-tri-O-acetyl-3-deoxy-D-erythro-hex-2-enono-1,5-lactone; Glumer et al. 2004)**

Researchers in Barros's group developed a series of polymerizable sucrose ether derivatives. For example, 1',2,3,3',4,4',6-hepta-O-benzyl-6'-O-vinyl sucrose (**27**), 1',2,3,3',4,4',6-hepta-O-benzyl-6'-O-vinylbenzyl sucrose (**28**), and hepta-O-acetyl-monovinylbenzyl sucrose (**29**) (Fig. 1.16) were copolymerized with styrene in toluene using AIBN as initiator at 60°C (Crucho et al. 2008). Ziegler-Natta catalyzed polymerization was carried out in 2009 (Barros et al. 2009). The compounds 1',2,3,3',4,4',6-hepta-O-benzyl-6'-O-crotonyl-sucrose (**30**) and 1',2,3,3',4,4',6-hepta-O-benzyl-6'-O-methacryloyl-sucrose (**31**) (Fig. 1.17) were copolymerized with styrene in

hexane at 40°C.  $\text{TiCl}_4$  and  $\text{AlEt}_3$  were used as catalysts. Molar rate of Ti/Al was 8:1 and sugar/styrene was 1, 0.5, 0.1, and 0.05. The relationship of mol fraction of glycomonomers to glycopolymers and molecular weight of glycopolymers with initial molar ratios of monomers was studied. In 2010, copolymerization of styrene with 6-O-methacryloyl sucrose (**32**), 6-O-crotonoyl sucrose (**33**), 1',2,3,3',4,4',6'-hepta-O-acetyl-6-O-methacryloyl-sucrose (**34**), and 1',2,3,3',4,4',6'-hepta-O-acetyl-6-O-crotonoyl-sucrose (**35**) (Fig. 1.17) were conducted in DMF for the first two and in toluene for the last two compounds, respectively (Barros et. al 2010). The relationship of molecular weights of the glycopolymers, degree of monomer conversion, and mol fraction of glycomonomers to glycopolymers with feed monomer ratios was investigated. A biodegradation test on the glycopolymers by a fungal (*Aspergillus niger*) culture method showed a fungal growth  $\geq 60\%$ , indicating good biodegradability.

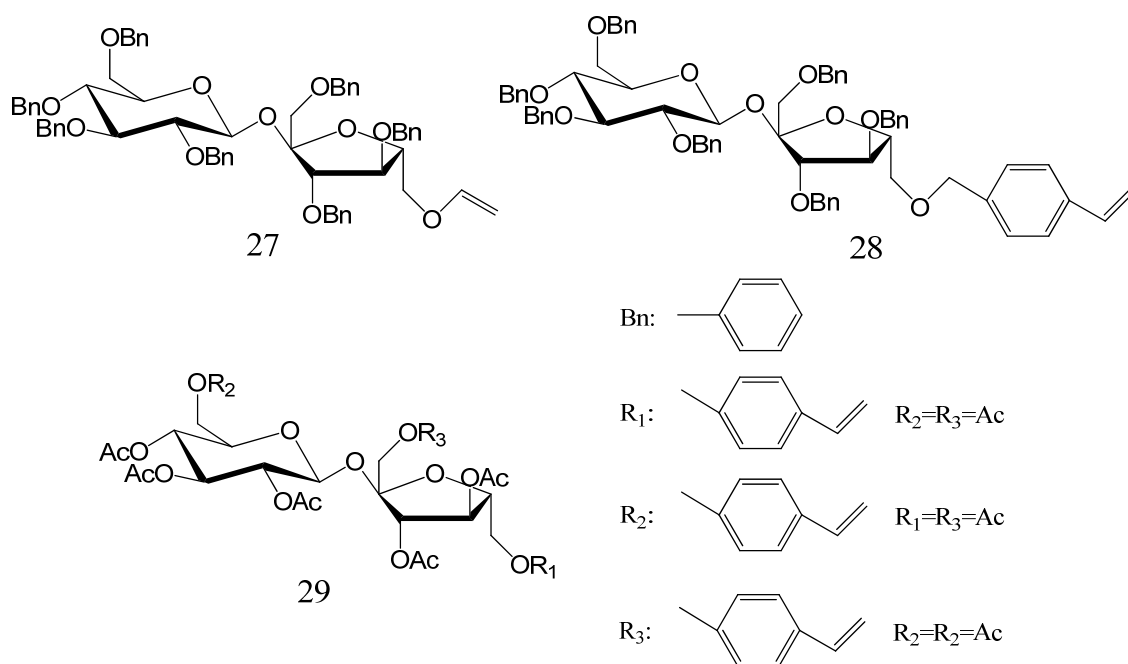


Figure 1-16 Glycomonomers: 27, 28, and 29 (Crucho et al. 2008)

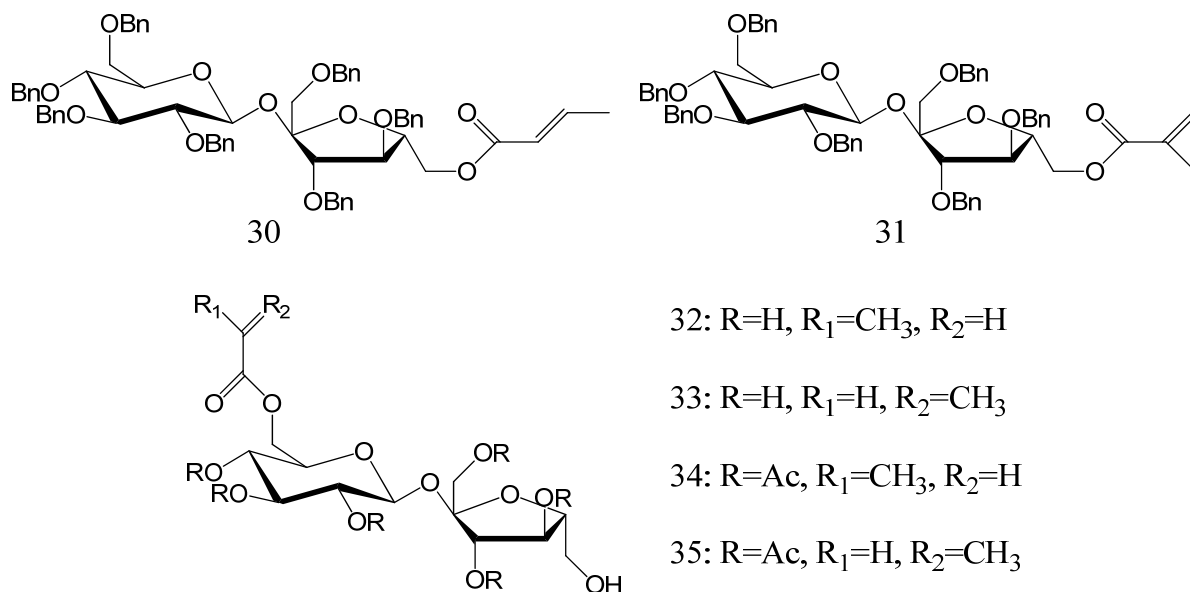


Figure 1-17 Glycomonomers: 30, 31, 32, 33, 34, and 35 (Barros et al. 2009 and Barros et. al 2010)

A glycopolymer composed of 2-[[*(D*-glucosamine-2-*N*-yl) carbonyl]oxy}ethyl acrylate (HEAGI, **36**) (Fig. 1.18) and styrene was made by copolymerization in DMF using AIBN as initiator (Munoz-Bonilla et al., 2010). A blend of glycopolymer and polystyrene was spin-coated onto a silicon wafer to fabricate honeycomb-structured films. From AFM study, the diameter of holes depended on composition of the blend. It was also found from fluorescence microscope imaging that FITC-Con A could recognize the sugar moiety on the film.

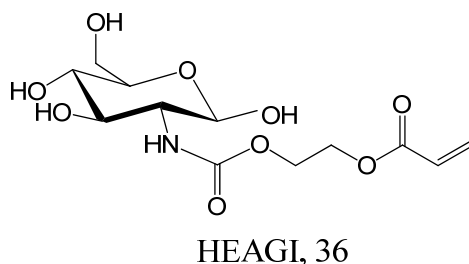


Figure 1-18 HEAGI (2-[[*(D*-glucosamine-2-*N*-yl) carbonyl]oxy}ethyl acrylate; Munoz-Bonilla et al., 2010)

#### **1.1.4 Approach to a convenient synthesis of a glycopolymer in this project**

In this project, an attempt was made to offer a faster, less cumbersome synthesis route with reasonable product yield. A glycomonomer with amide linkage: (maleic acid monoamido)-2-D-glucopyranose (MAMG) was first synthesized within a one-step reaction in 4 h with relatively high yield. The product was isolated by precipitation in ethyl acetate. Copolymerization of MAMG and styrene was conducted in DMSO using AIBN as initiator with different initial monomer ratios. <sup>1</sup>H-NMR was used to characterize the chemical structure of MAMG. The chemical structure of copolymer PMAMG-ST was confirmed by FTIR and <sup>1</sup>H-NMR. Molecular weight and final monomer ratio on PMAMG-ST was determined by GPC and elemental analysis, respectively. The biodecomposition and release of the sugar of glycomonomer, glycopolymer and control sample was evaluated by an oxidative-fermentative test.

### **1.2 Experimental Part**

#### **1.2.1 Materials**

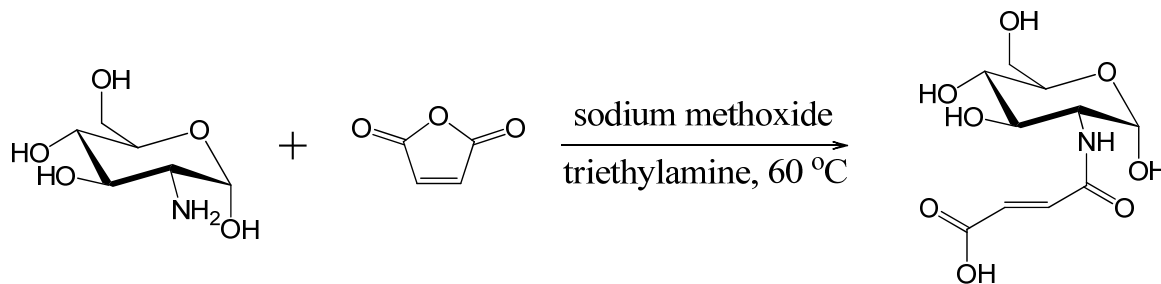
D-Glucosamine hydrochloride (99.9%, Calbiochem), maleic anhydride (98%, Alfa Aesar), sodium methoxide (98%, Alfa Aesar), methanol (99.9%, Acros), triethylamine (99%, Alfa Aesar), ethyl acetate (99.5%, Mallinckrodt Chemicals), anhydrous magnesium sulfate (MgSO<sub>4</sub>) (99%, Strem Chemicals) and sodium hydroxide (NaOH) (technical, Spectrum) were used as received. Styrene (99%, stabilized 10-15 ppm 4-tert-butylcatechol, Alfa Aesar) was purified from inhibitor by washing with 10% aqueous solution of sodium hydroxide and then with deionized water; after drying over anhydrous MgSO<sub>4</sub>, it was filtered and distilled under vacuum. (2,2'-azobisisobutyronitrile) (AIBN) (98%, Sigma Aldrich) was recrystallized from methanol.

Dimethyl sulfoxide (DMSO) (99.9% Malinckrodt) was dried over anhydrous  $\text{MgSO}_4$  before reaction.

## 1.2.2 Synthesis of glycomonomer and glycopolymer

### 1.2.2.1 Synthesis of (maleic acid monoamido)-2-D glucopyranose (MAMG)

The (maleic acid monoamido)-2-D-glucopyranose was synthesized by modifying the procedure previously reported (Jin et al., 2009). Maleic anhydride (2.3 g, 23.45 mmol) was added to a 250 ml three neck flask containing D-glucosamine hydrochloride (10.0 g, 46.35 mmol), sodium methoxide (2.5 g, 46.3 mmol), and methanol (125 ml) while stirring. After stirring at 60°C for 30 min, maleic anhydride (2.3 g, 23.45 mmol) and triethylamine (9.3 ml, 66.8 mmol) were added. The reaction was stopped after 4 h. The solution was filtered and the filtrate was slowly added to 250 ml ethyl acetate. The precipitation was isolated by filtration and dried under vacuum at 35 °C for 12 h to yield 8.9138 g MAMG (yield: 69.4%)

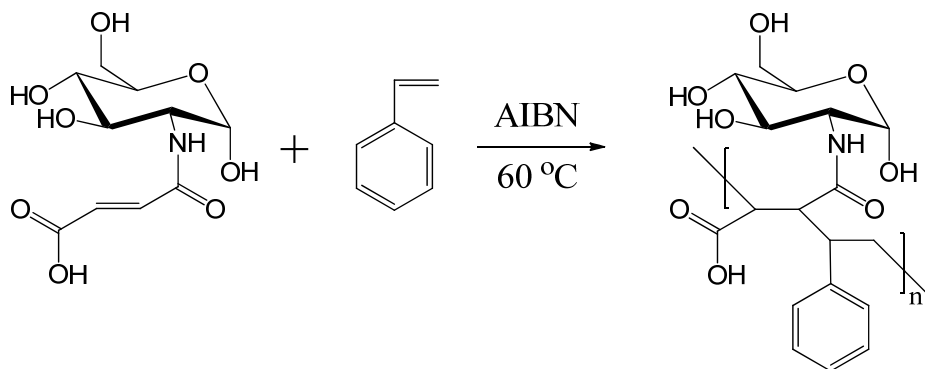


Scheme 1.1. Synthesis of (maleic acid monoamido)-2-D-glucopyranose (MAMG)

### 1.2.2.2 Copolymerization of (maleic acid monoamido)-2-D glucopyranose and styrene

MAMG (3.885 g, 15 mmol), styrene (1.56 g, 15 mmol), AIBN (0.136 g, 0.829 mmol) and 15 ml DMSO were added to a 100 ml Schlenk flask. Air was removed by vacuum and nitrogen was injected in to create nitrogen atmosphere in the Schlenk flask. After stirring at 60°C for 15 h,

copolymers were isolated by precipitation in methanol, then filtrated and dried under vacuum for 12 h at 35°C. MAMG and styrene feed ratio was 1:3 or 1:1. P1 (0.25 MAMG – 0.75 ST) and P2 (0.5 MAMG – 0.5 ST) were obtained. Poly(styrene-co-maleic anhydride) was also obtained using previous described method as control sample.



**Scheme 1.2. Synthesis of poly((maleic acid monoamido)-2-D-glucopyranose-co-styrene) (PMAMG-ST)**

### 1.2.3 Characterization:

#### 1.2.3.1 Fourier Transform Infrared Spectroscopy (FT-IR)

The FT-IR of PMAMG-ST was recorded in powder form. The spectra were recorded on a Thermo Scientific Nicolet 6700 at resolution of  $4\text{ cm}^{-1}$  and the number of scans was 32.

#### 1.2.3.2 Nuclear Magnetic Resonance (NMR) Spectroscopy

$^1\text{H}$  NMR was used to determine the chemical structures of synthesized products. Spectra were recorded at room temperature with deuterated dimethyl sulfoxide (DMSO- $d_6$ ) as a solvent. A Bruker 400 NMR spectrometer was used. Typical parameters for the proton spectra were a 15 s pulse delay, a 3 s acquisition time, a 20.68 ppm spectral width, and 16 scans.

#### 1.2.3.3 Gel permeation chromatography (GPC)



The number-average weight ( $M_n$ ) and polydispersity indexes ( $M_w / M_n$ ) were measured by a Viscotek GPC assembly which includes a VE 1122 solvent delivery system, a VE 7510 GPC degasser, a 270 dual detector, VE 3580 RI detector, and a Viscogel GMHhr-M column. Tetrahydrofuran (THF) containing 126 ppm of BHT as stabilizer was used as fluent at flow rate of 1 ml/min at room temperature. Polystyrene standards (Polycal) of 99448 g/mol ( $M_n$ ) were used to calibrate the columns.

#### **1.2.3.4 Elemental analysis**

Elemental analysis was done by MICRO ANALYSIS INC. using carbon, oxygen, nitrogen method.

#### **1.2.3.5 Biodecomposition evaluated by Oxidative-fermentative test (OF test)**

In OF basal medium at 37°C and under aerobic conditions, glycopolymer, glycomonomer or control sample were used as only carbon source for growth of Escherichia coli (E. coli). Biodecomposition was evaluated by pH change caused by the acid E coli produced upon biodegradation of the substrate. The pH change was followed for 48 h.

### **1.3 Results and Discussion:**

#### **1.3.1 <sup>1</sup>H-NMR characterization of (maleic acid monoamido)-2-D-glucopyranose (MAMG)**

<sup>1</sup>H-NMR spectra of MAMG is shown in Fig. 1.19. Hydrogen and OH groups on sugar moiety were observed in the spectra from 2.69 ppm to 5.4 ppm and at 5.74 ppm. The peak for the amide group at 8.39 ppm and 8.62 ppm confirmed that glucosamine has been linked to maleic anhydride via the amide linkage. The band of the carboxylic acid group at 10.92 ppm showed the

anhydride group was opened; only one carboxylic acid group reacted with amine group on glucosamine during the reaction. H-8 and H-9 proved the double bond on maleic anhydride remained after the reaction.

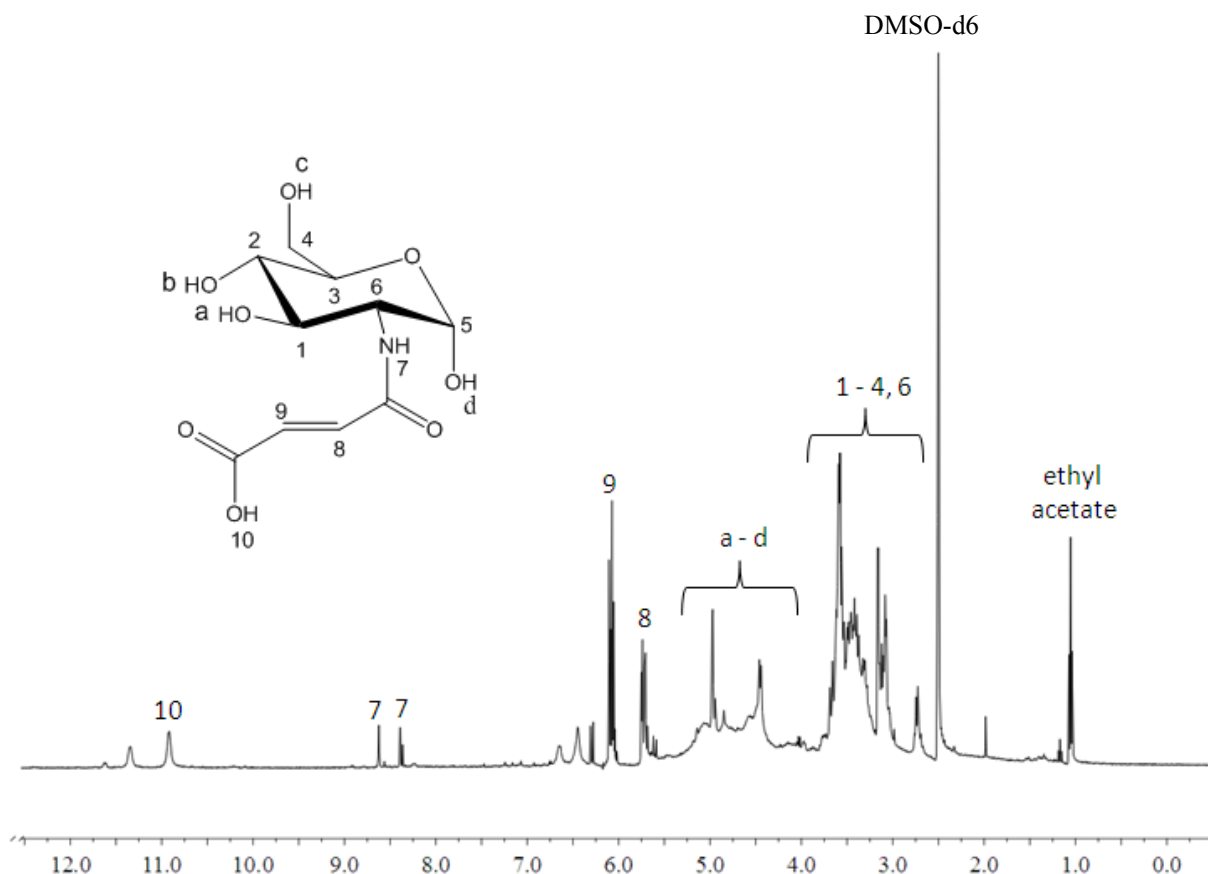


**Figure 1-19**  $^1\text{H-NMR}$  spectra of (maleic acid monoamido)-2-D-glucopyranose (MAMG); MAMG: (400MHz, DMSO-d),  $\delta(\text{ppm})$ : 2.69 - 3.8 (H-1 - H-4, H-6), 4.36 – 5.4 (H-a - H-d), 5.74 (H-8), 6.07 (H-9), 8.39, 8.62 (H-7), 10.92 (H-10)

### 1.3.2 FT-IR characterization of poly((maleic acid monoamido)-2-D-glucopyranose-co-styrene) (PMAMG-ST)

FT-IR spectra of poly((maleic acid monoamido)-2-D-glucopyranose-co-styrene) (PMAMG-ST) and poly(styrene-maleic anhydride) (PSMA) are shown in Fig. 1.20. The C-OH groups on sugar at  $1017.0\text{ cm}^{-1}$  and OH groups between  $2339.0\text{ cm}^{-1}$  and  $3685.4\text{ cm}^{-1}$  confirmed the sugar moiety

on PMAMG-ST. Peaks for the amide group at  $1572.8\text{ cm}^{-1}$  and  $3260.4\text{ cm}^{-1}$  also proved the presence of the sugar moiety. The peak at  $3027.5\text{ cm}^{-1}$  which designates the aromatic C-H groups indicated benzene ring was on PMAMG-ST as well.

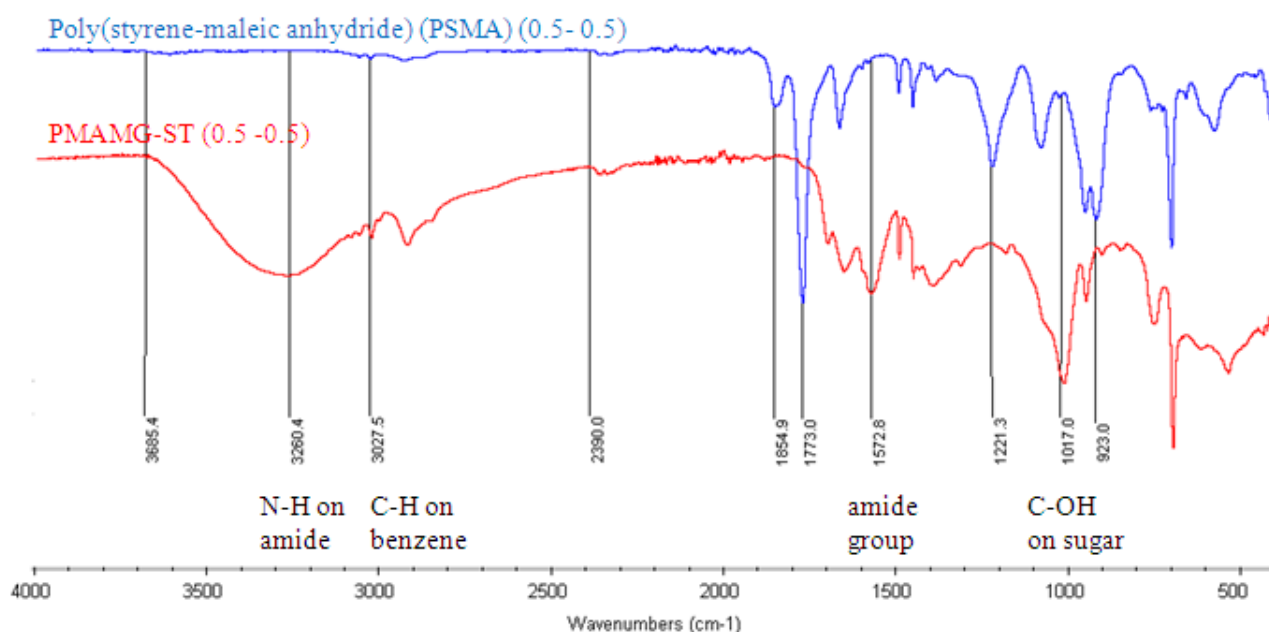


**Figure 1-20 FT-IR spectra of poly((maleic acid monoamido)-2-D-glucopyranose-co-styrene) (PMAMG-ST) (P2); PMAMG-ST: wavelength ( $\text{cm}^{-1}$ ): 1017.0 (C-OH on sugar), 1572.8 (C=O on amide group), 2390.0 – 3685.4 (OH on sugar), 3027.5 (aromatic C-H on benzene ring), 3260.4 (N-H on amide group); in comparison PSMA: wavelength ( $\text{cm}^{-1}$ ): 923.0 (C-O-C on cyclic anhydride), 1221.3 (C-O-C), 1773.0, 1854.9 (C=O on 5-ring anhydride), 3027.5 (aromatic C-H on benzene ring)**

### 1.3.3 $^1\text{H-NMR}$ characterization of poly((maleic acid monoamido)-2-D-glucopyranose-co-styrene) (PMAMG-ST)

Since spectral data confirmed the successful synthesis of the glycomonomer, the copolymerization with styrene was attempted. The product was confirmed by  $^1\text{H-NMR}$  analysis. Fig. 1.21 shows  $^1\text{H-NMR}$  spectra of poly((maleic acid monoamido)-2-D-glucopyranose-co-styrene) (PMAMG-ST). H-8 to H-12 designate the backbone of PMAMG-ST. H-1 to H-7 and H-a to H-d proved the sugar moiety on PMAMG-ST. H-13 to H-17 confirmed the presence of

benzene ring on PMAMG-ST. The H-8 peak on the glycomonomer MAMG was the identification peak of the double bond at 6.07 ppm. It disappeared in the spectra of the glycopolymer, suggesting that the reaction has occurred.

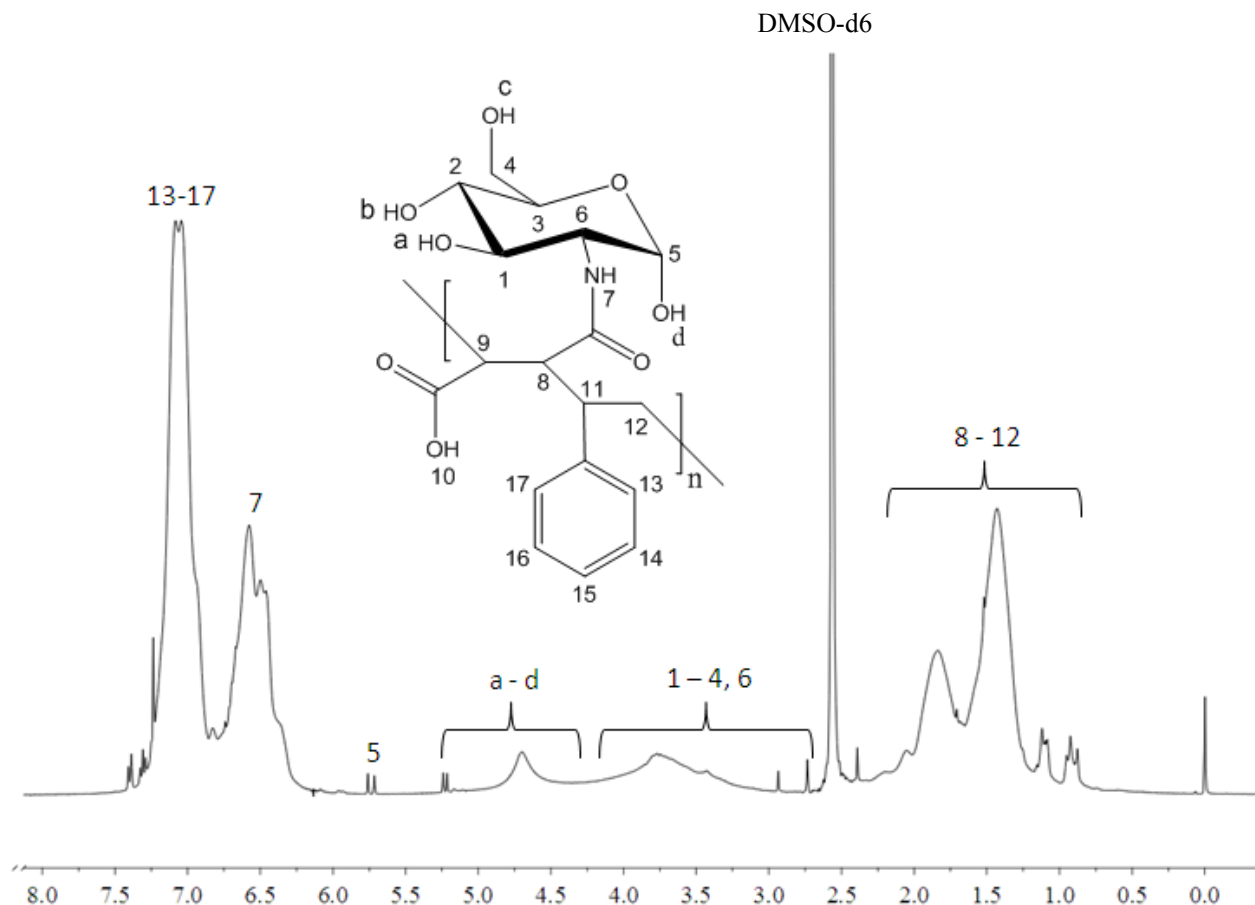


**Figure 1-21**  $^1\text{H-NMR}$  spectra of poly((maleic acid monoamido)-2-D-glucopyranose-co-styrene) (PMAMG-ST) (P2); PMAMG-ST: (400MHz, DMSO-d,  $\delta$ (ppm): 0.78 – 2.39 (H-8 - H-12), 2.71 – 4.29 (H-1 - H-4, H-6), 4.45 – 5.24 (H-a – H-d), 5.74 (H-5), 6.59 (H-7), 6.81 – 7.37 (H-13 – H-17)

### 1.3.4 Molecular weight ( $M_n$ ) and polydispersity index (PDI) of poly((maleic acid monoamido)-2-D glucopyranose-co-styrene) (PMAMG-ST)

Copolymerization of MAMG and ST with two different initial monomer ratios was carried out: P1 (0.25 MAMG – 0.75 ST) and P2 (0.5 MAMG – 0.5 ST). Gel permeation chromatography (GPC) was used to provide proof for P1 and P2. The GPC spectra are shown in Fig. 1.22. The

number average molecular weight ( $M_n$ ) and the polydispersity index (PDI) are given in Table 1. P1 (0.25 MAMG - 0.75 ST) had a  $M_n$  of 10,288 and the PDI was 1.31. The  $M_n$  of P2 (0.5 MAMG - 0.5 ST) was much higher with 18,380, but its PDI with 1.28 was almost the same. Since MAMG has a larger molecular weight than ST, the higher ratio of MAMG produced a glycopolymer with higher molecular weight as expected.

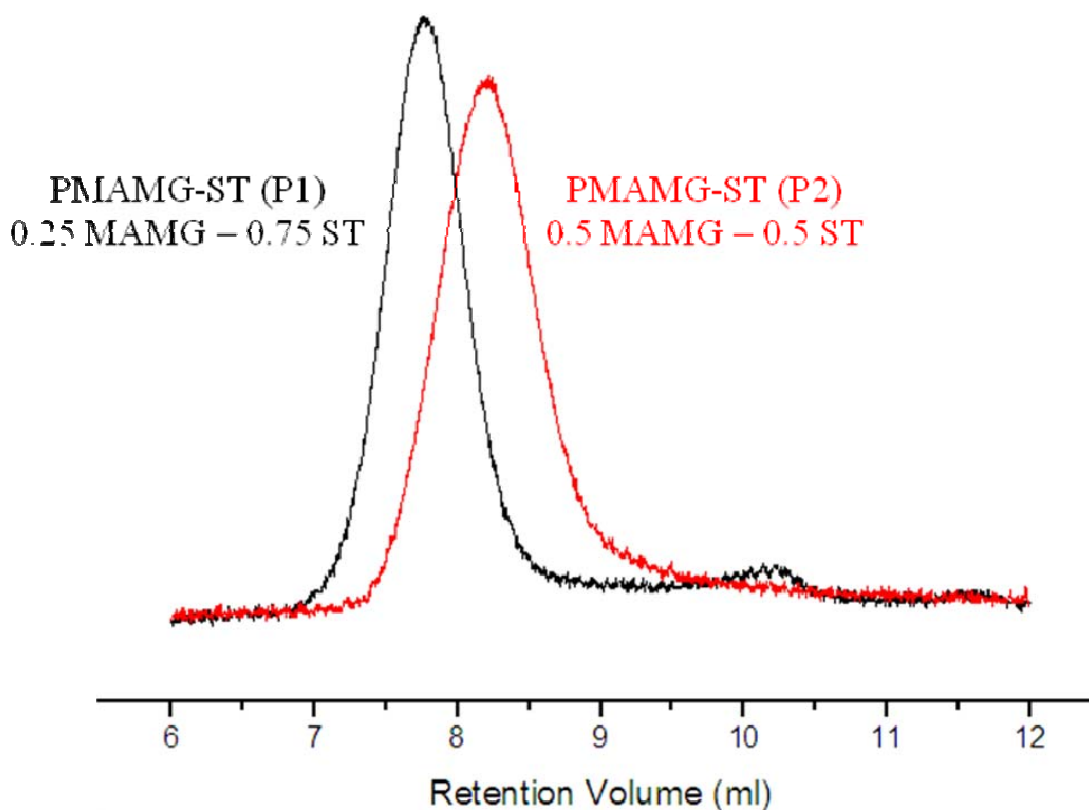


Figure 1-22 GPC spectra of poly((maleic acid monoamido)-2-D glucopyranose-co-styrene) (PMAMG-ST), black: P1 (0.25 MAMG - 0.75 ST) and red: P2 (0.5 MAMG - 0.5 ST)

Table 1.1 Molecular weight and PDI of PMAMG-ST

	$M_n$	PDI
P1 (0.25 MAMG - 0.75 ST)	10,288	1.31
P2 (0.5 MAMG - 0.5 ST)	18,380	1.28

### 1.3.5 Monomer ratio on poly((maleic acid monoamido)-2-D glucopyranose-co-styrene) (PMAMG-ST)

Data from elemental analysis are reported in Table 2 as C%, H% and N%. With further calculation, the monomer ratio of MAMG and ST on PMAMG-ST is given in Table 2 as well. The MAMG segment on P1 (0.25 MAMG - 0.75 ST) was 20.35%, and on P2 (0.5 MAMG – 0.5 ST) was 47.63%. The monomer ratio on glycopolymer agreed well with the initial monomer ratio.

Table 1.2 Monomer ratio on PMAMG-ST

	C%	H%	N%	MAMG%	ST %
P1 (0.25 MAMG - 0.75 ST)	50.6%	5.98%	1.67%	20.35%	79.65%
P2 (0.5 MAMG – 0.5 ST)	60.4%	6.51%	3.72%	47.63%	52.37%

### 1.3.6 Biodecomposition evaluation by oxidative-fermentative test (OF test)

A biodecomposition test was performed to evaluate the release of glucose from the products. If sugar can be released, it may act as a sensor for a multitude of applications since glucose is easily detected by simple means. An oxidative-fermentative test was utilized to investigate this aspect of the presented research.

PSMA, PMAMG-ST or MAMG were the only carbon sources in the medium for growth of *E. coli*. Acid is produced when these materials are consumed by the microorganism. The acid can be traced back to the original compounds and used as an indicator for their biodegradation. Therefore, the pH value was used as an indicator for growth of *E. coli*. The results of OF test are shown in Fig. 1.23. *E. coli* produced much higher amounts of acid when consuming PMAMG-

ST (P2) than when exposed to PSMA. Moreover, *E. coli* produced even more acid when consuming MAMG. Thus, it can be assumed that pendent sugar groups on PMAMG-ST were removed by *E. coli* and utilized as carbon source for their growth. In other words, the OF test indicated that sugar was released from PMAMG-ST. Glucose units could fulfill various functions in the biomedical field.

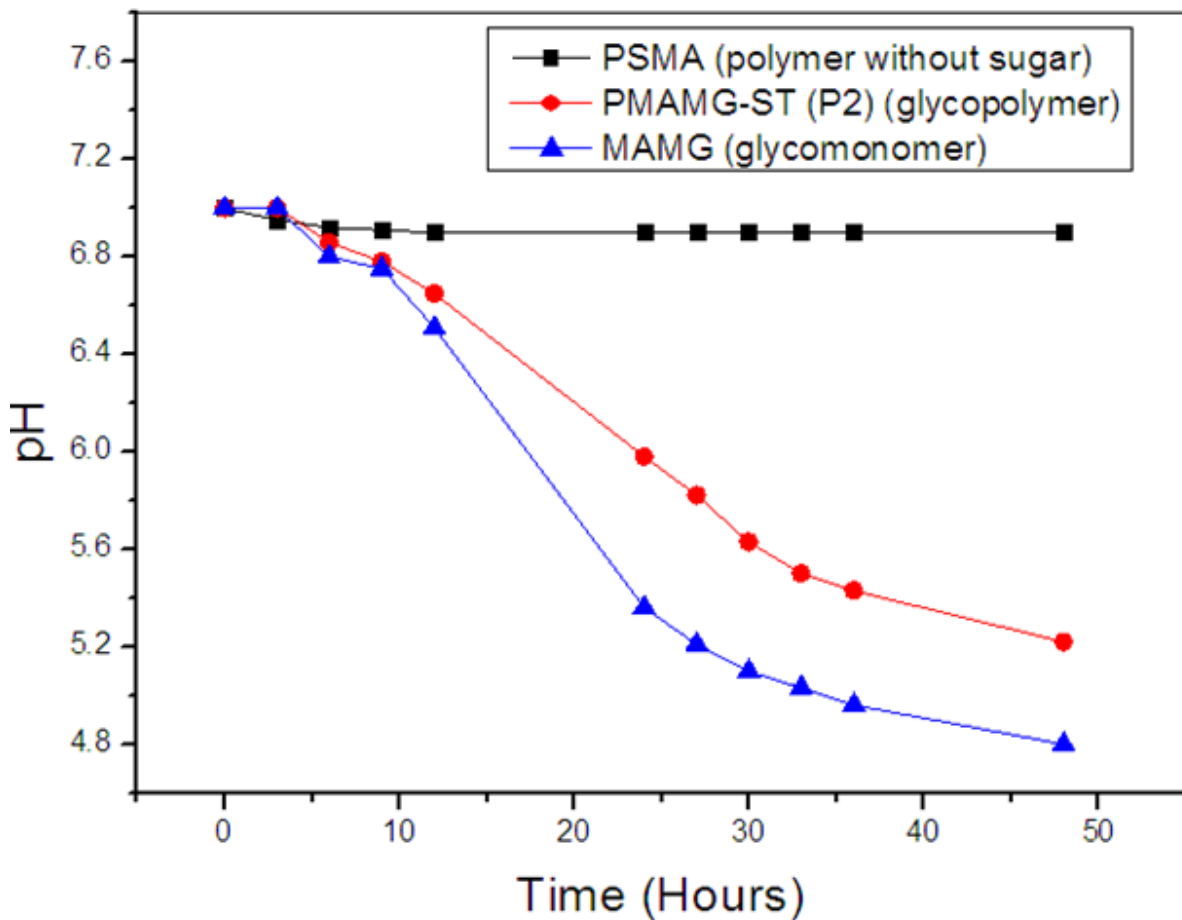


Figure 1-23 Biodecomposition evaluation of MAMG, PSMA, and PMAMG-ST by oxidative-fermentative test (OF test) via pH change

### **1.3.7 Increasing the yield**

The synthesis of PMAMG-ST and analysis of the intermediate and final products have been described in the previous sections and it could be shown that in fact PMAMG-ST was obtained. However, the yield of the glycomonomer had still been fairly low with less than 20%. Therefore, the synthesis route had to be modified to lead to a more attractive yield. A better result was obtained by doubling the amount of catalyst (triethylamine) and changing the method of adding the reaction solution to ethyl acetate. With these process modifications the yield of the glycomonomer could be increased to almost 70%.

### **1.4 Conclusions**

With the methods used in this research, it could be shown that (maleic acid monoamido)-2-D glucopyranose (MAMG) could be synthesized in a one-step reaction that is more efficient with relatively high yield. The chemical structure of MAMG was confirmed by <sup>1</sup>H-NMR. MAMG could then be used to produce poly((maleic acid monoamido)-2-D glucopyranose-co-styrene) (PMAMG-ST) successfully. The chemical structure of PMAMG-ST was confirmed by FTIR and <sup>1</sup>H-NMR. Molecular weight and PDI of PMAMG-ST was determined by GPC. Elemental analysis and further calculation showed monomer ratio on glycopolymer agreed well with initial monomer ratio. Biodecomposition evaluated by oxidative-fermentative test indicated sugar was released from PMAMG-ST. Glucose units could fulfill various functions in the biomedical field.

### **1.5 References**

Barros MT, Petrova KT, and Raj-Singh TR. *European Polymer Journal*, **2010**, 46, 1151–1157



Bernard J, Hao Xj, Davis PT, Barner-Kowollik C, and Stenzel MH. *Biomacromolecules*, **2006**, 7, 232-238

Borges MR, Dos Santos JA, Vieira M, and Balaban R. *Materials Science and Engineering C*, **2009**, 29 519–523

Broyer RM., Quaker GM., and Heather D, and Maynard J. *AM. CHEM. SOC.*, **2008**, 130, 1041-1047

Cameron NR., Spain SG, Kingham JA, Weck S, Albertin L, Barker CA, Battaglia G, Smart T, and Blanz A. *Faraday Discuss.*, **2008**, 139, 359–368

Charreyre MT, and Boullanger P. *Makromol. Chem.*, **1993**, 194, 117-135

Crucho C, Petrova K, Pinto R, and Barros M. *Molecules*, **2008**, 13, 762-770

D'Agosto F, Charreyre MT, Pichot C, and Mandrand B. *Macromol. Chem. Phys.*, **2002**, 203, 146-154

Gotz H, Harth E, Schiller SM., Frank CW, Knoll W, and Hawker CJ. *Journal of Polymer Science: Part A: Polymer Chemistry*, **2002**, 40, 3379–3391

Guo Ty, Liu P, Zhu Jw, Song Md, and Zhang Bh. *Biomacromolecules*, **2006**, 7, 1196-1202

Hashimoto K, Ohsawa R, Imai N, and Okada M. *Journal of Polymer Science: Part A: Polymer Chemistry*, **1999**, 37, 303–312

Hopwell JW, Duncan R, Wilding D and Chakrabarti K, *Hum. Exp. Toxicol.*, **2001**, 20, 461-470

Hu Zg, Fan Xs, and Zhang Gs. *Carbohydrate Polymers*, **2010**, 79, 119–124

Ke Bb, Wan Ls, Zhang Wx, and Xu Zk. *Polymer*, **2010**, 51, 2168-2176

Kim SH, Goto M, Cho CS and Akaike T. *Biotechnology Letters*, **2000**, 22, 1049–1057

Kobayashi K, Sumitomo H, and Ina Y. *Polymer Journal*, **1985**, 17, 567-575

Kobayashi K, and Kamiya S. *Macromol. Symp.*, **1997**, 120, 139-146

Leon O, Bordege V, Munoz-Bonilla A, Sanchez-Chaves M, and Fernandez-Garcia M. *Journal of Polymer Science: Part A: Polymer Chemistry*, **2010**, 48, 3623–3631

Lu Fz, Meng Jq, Du Fs, Li Zc, and Zhang By. *Macromol. Chem. Phys.* **2005**, 206, 513–520

Malinova V, and Rieger B. *Macromol. Rapid Commun.*, **2005**, 26, 945–949

Matsuda T, and Sugawara T. *Macromolecules*, **1996**, 29, 5375-5383

Muthukrishnan S, Jutz G, Andre X, Mori H, and Muller A HE. *Macromolecules*, **2005<sup>a</sup>**, 38, 9-18

Muthukrishnan S, Mori H, and Muller A HE. *Macromolecules*, **2005<sup>b</sup>**, 38, 3108-3119

Narain R, Jhurry D, and Wulff G. *European Polymer Journal*, **2002**, 38, 273-280

Narain R and Armes SP. *Biomacromolecules*, **2003**, 4, 1746-1758

Otman O, Boullanger P, Drockenmuller E, and Hamaide T. *Beilstein J. Org. Chem.*, **2010**, 6, No. 58

Pearson S, Allen N, and Stenzel MH. *Journal of Polymer Science: Part A: Polymer Chemistry*, **2009**, 47, 1706–1723

Revilla J, Elaissari A, Pichot C, and Gallot B. *Polymers for Adv. Tech.*, **1995**, 6, 455-464

Revilla J, Delair T, Gallot B, and Pichot C. *Polymer*, **1996**, 37, 687-698

Serizawa T, Yasunaga S, and Akashi M. *Biomacromolecules*, **2001**, 2, 469-475

Seymour LW., Ferry DR, Anderson D, Hesslewood S, Julyan P J, Poyner R, Doran J, Young AM, Burtles S, and Kerr DJ, *Journal of Clinical Oncology*, **2002**, 20, 1668-1676

Shimura Y, Hashimoto K, Yamanaka C, and Setojima D. *Journal of Polymer Science: Part A: Polymer Chemistry*, **2001**, 39, 3893–3901

Sigal GB, Mammen M, Dahmann G, and Whitesides, GM. *J. Am. Chem. Soc.*, **1996**, 118, 3789-3800

Suriano F, Coulembier O, and Dubois P. *Reactive & Functional Polymers*, **2010**, 70, 747-754

Ting SR S, Granville AM, Quemener D, Davis TP, Stenzel MH, and Barner-Kowollik C. *Aust. J. Chem.*, **2007**, 60, 405–409

Ting SR S, Gregory AM., and Stenzel MH. *Biomacromolecules*, **2009<sup>a</sup>**, 10, 342–352

Ting SR S, Min EH, Escale P, Save M, Billon L, and Stenzel MH. *Macromolecules*, **2009<sup>b</sup>**, 42, 9422–9434

Ting SR S, Min EH, Zetterlund PB, and Stenzel MH. *Macromolecules*, **2010**, 43, 5211–5221

Tsuchida A, Akimoto S, Usui T, and Kobayashi K. *J. Biochem.*, **1998<sup>a</sup>**, 123, 715-721

Tsuchida A, Kobayashi K, Matsubara N, Muramatsu T, Suzuki T, and Suzuki Y. Glycoconjugate Journal, **1998**<sup>b</sup>, 15, 1047–1054

Varma AJ, Kennedy JF, and Galgali P. Carbohydrate Polymers, **2004**, 56, 429-445

Wilson ME, Najdi S, Krochta JM, Hsieh YL, and Kurth MJ. Macromolecules, **1998**, 31, 4486-4492

Wulff G, Zhu Lm, and Schmidt H. Macromolecules, **1997**, 30, 4533-4539

Wulff G, Schmidt H, and Zhu Lm. Macromol. Chem. Phys., **1999**, 200, 774–782

Xu N, Wang R, Du Fs, and Li Zc. Journal of Polymer Science: Part A: Polymer Chemistry, **2009**, 47, 3583–3594

Yamada K, Minoda M, Fukuda T, and Miyamoto T. Journal of Polymer Science: Part A: Polymer Chemistry, **2001**, 39, 459–467

Ye Wj, Wells S, and Desimone JM. Journal of Polymer Science: Part A: Polymer Chemistry, **2001**, 39, 3841–3849

Zhou Wj, Naik SS, Kurth MJ, Hsieh Y, and Krochta JM. Journal of Polymer Science: Part A: Polymer Chemistry, **1998**, 36, 2971–2978

## CHAPTER 2 SYNTHESIS OF GLUCOSAMINE-GRAFTED POLY(METHYL VINYL ETHER-ALT-MALEIC ACID) (GLU-PMVE-MAC) AND PH-RESPONSIVE HYDROGEL FOR DRUG DELIVERY APPLICATION

### 2.1 Introduction

#### 2.1.1 Glycopolymers

Glycopolymers are synthetic polymers that incorporate carbohydrate groups. Generally they can be synthesized by four different methods: polymerization of glycomonomers or copolymerization of glycomonomers with vinyl monomers, ring-opening polymerization of anhydro-sugars, enzyme-mediated polymerization, and grafting of sugars onto functionalized synthetic polymers (Varma et al. 2004). In the previous chapter, synthesis of an amide linked glycomonomer and free radical copolymerization of glycomonomer with styrene was reported. In the present work, glycopolymers were synthesized from grafting sugar onto a maleic acid-containing synthetic polymer. The properties of the resulting glycopolymers were studied. Very interesting aspects of this work are the formation and use of these materials as pH-responsive hydrogel for controlled drug delivery applications.

#### 2.1.2 Sugar derivatives grafted onto maleic groups that are connected to polymers

Vetere et al. (2002) first reported grafting a sugar derivative onto a maleic group-containing polymer. D-Galactopyranosyl- $\alpha$ -(1 $\rightarrow$ 3)-galactopyranosyl- $\alpha$ -p-aminophenol (**1**) (Fig. 2.1) was grafted onto poly(styrene-co-maleic acid) (PSMAC) in 2-(N-morpholino)ethanesulfonic acid (MES) buffer solution with N-(3-dimethylaminopropyl)-N'-ethylcarbodiimide hydrochloride (EDC) and N-hydroxysuccinimide (NHS) as catalysts. The glycopolymer was aimed at

applications for removing natural antibodies that cause hyperacute rejection when implanting an organ from animals such as a pig or a monkey into the human body. Researchers in the same group synthesized three amino sugars: 1-amino-1-deoxy- $\beta$ -D-galactose (**2**), 1-amino-1-deoxy- $\beta$ -D-glucose (**3**), and 1-amino-1-deoxy- $\beta$ -D-lactose (**4**) (Fig. 2.2) and grafted them onto poly(styrene-co-maleic anhydride) (PSMAH) in sodium bicarbonate buffer solution (Donati, et al. 2002). The potential application of these glycopolymers as matrix for hepatic cell cultures was evaluated.

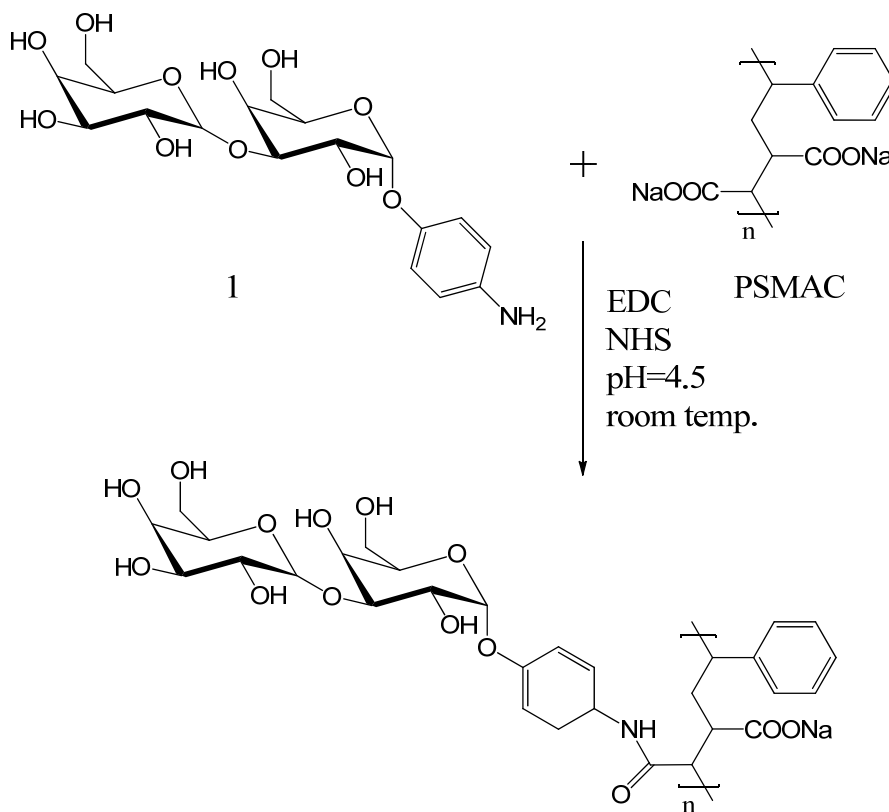


**Figure 2-1 Grafting D-galactopyranosyl- $\alpha$ -(1 $\rightarrow$ 3)-galactopyranosyl- $\alpha$ -p-aminophenol (**1**) onto poly(styrene-co-maleic acid) (PSMAC) (Vetere et al. 2002)**

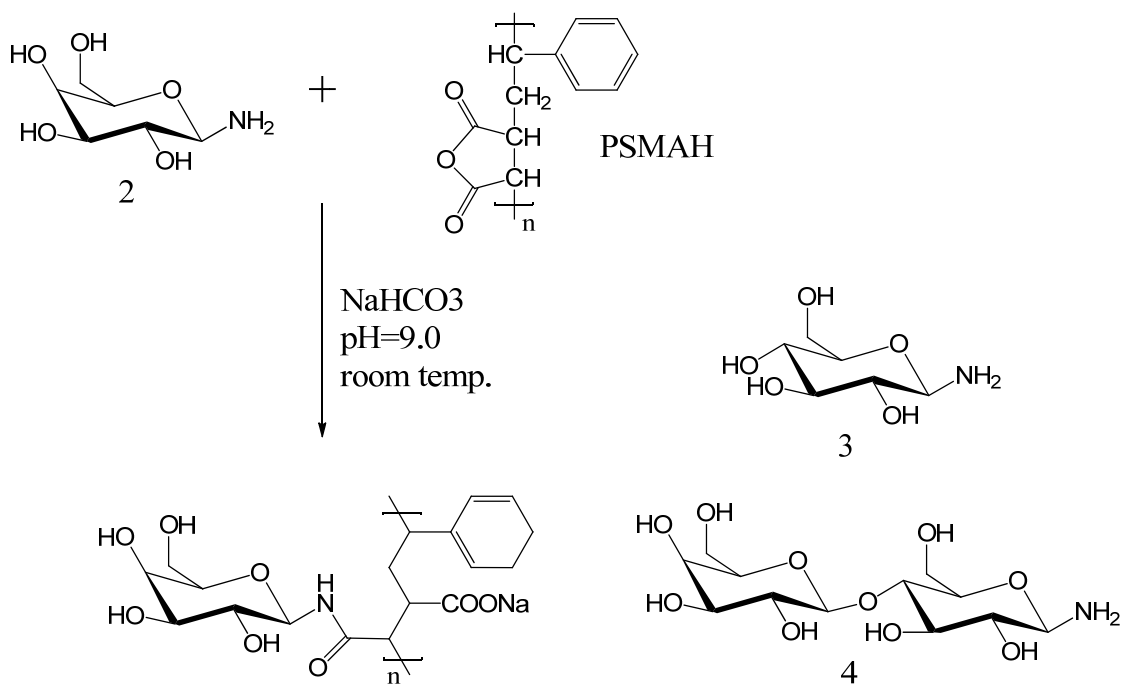


**Figure 2-2 Grafting (2), (3) and (4) onto poly(styrene-co-maleic anhydride) (PSMAH) (Donati et al. 2002)**

Gagali and co-workers grafted glucose (5), lactose (6), and sucrose (7) (Fig. 2.3) directly to poly(styrene-co-maleic anhydride) (PSMAH) via esterification reaction using 4-dimethylaminopyridine (DMAP) as catalyst. Fungal degradation tests showed good biodegradability. FT-IR was utilized to study the structural changes of the glycopolymers after fungal treatment (Galgali, et al. 2002 and 2004). In 2007, D-glucose (5), 6-O-trityl glucose (8), methyl glucoside (9), 1,2-5,6-diisopropylidene-D-glucose (10), and 1,2,3,4-tetraacetyl-D-glucose (11) (Fig. 2.3) grafted poly(styrene-co-maleic anhydride) were synthesized and investigated by FT-IR (Galgali et al. 2007). Fourier deconvolution was used for the assignment of the different ester carbonyls formed by the reaction of the different hydroxyl groups on those sugars with the maleic anhydride compound of PSMAH.

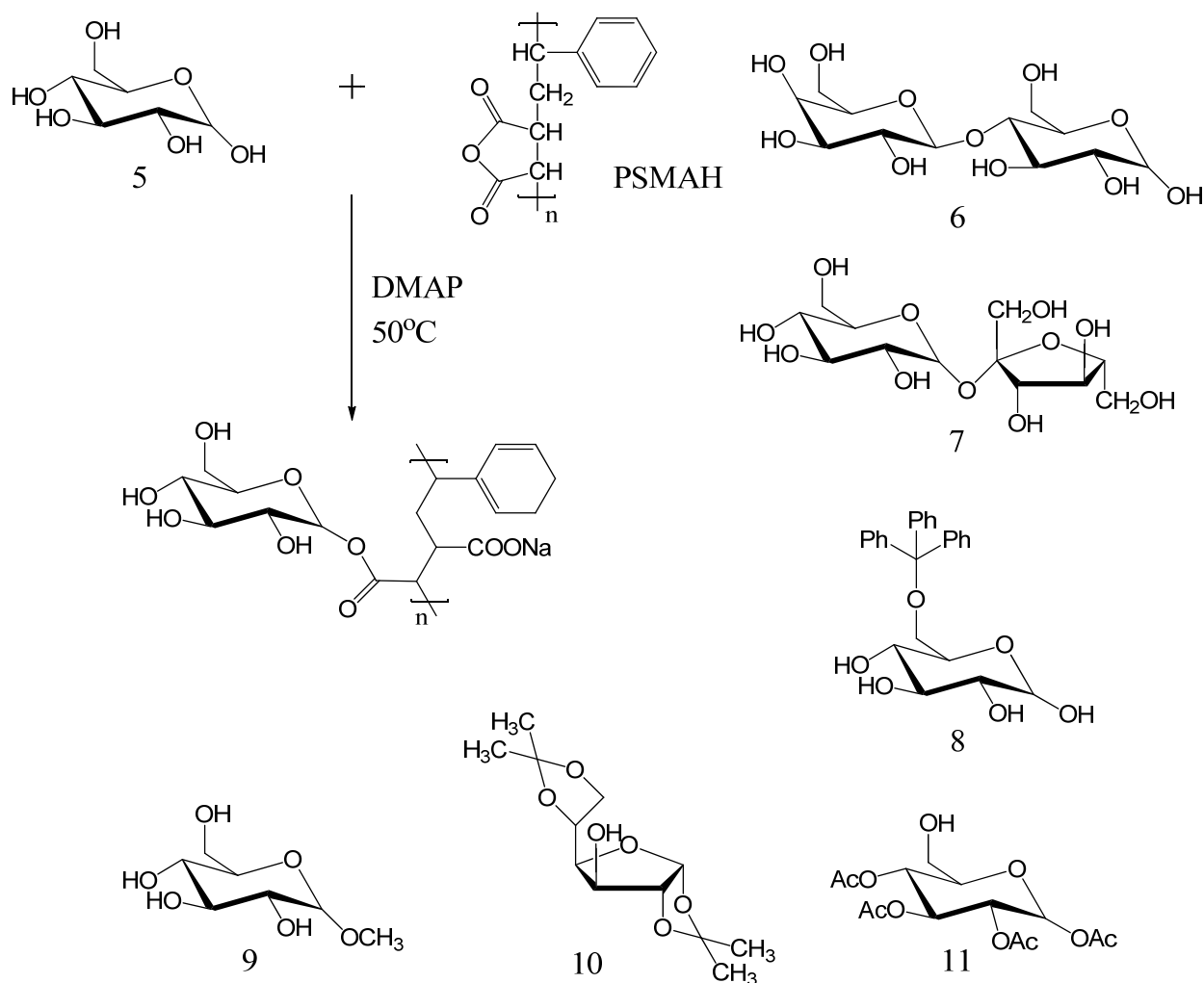


**Figure 2-3 Grafting (5) – (11) onto poly(styrene-co-maleic anhydride) (PSMAH) (Galgali et al. 2002, 2004, and 2007)**

Two sugar derivatives,  $\alpha$ -1-O-(2'-aminoethyl)-D-mannopyranoside (**12**) and  $\beta$ -1-O-(2'-aminoethyl)-D-galactopyranoside (**13**) (Fig. 2.4) were grafted onto poly{styrene-co- [(maleic anhydride)-alt-styrene]} (PST-PSMAH) (Su et al. 2009). Methyl red or rhodamine 6G doped nanoparticles were formed by sonication. The mannose containing nanoparticle interacted with concanavalin A which is a lectin that specifically recognizes glucose and mannose.



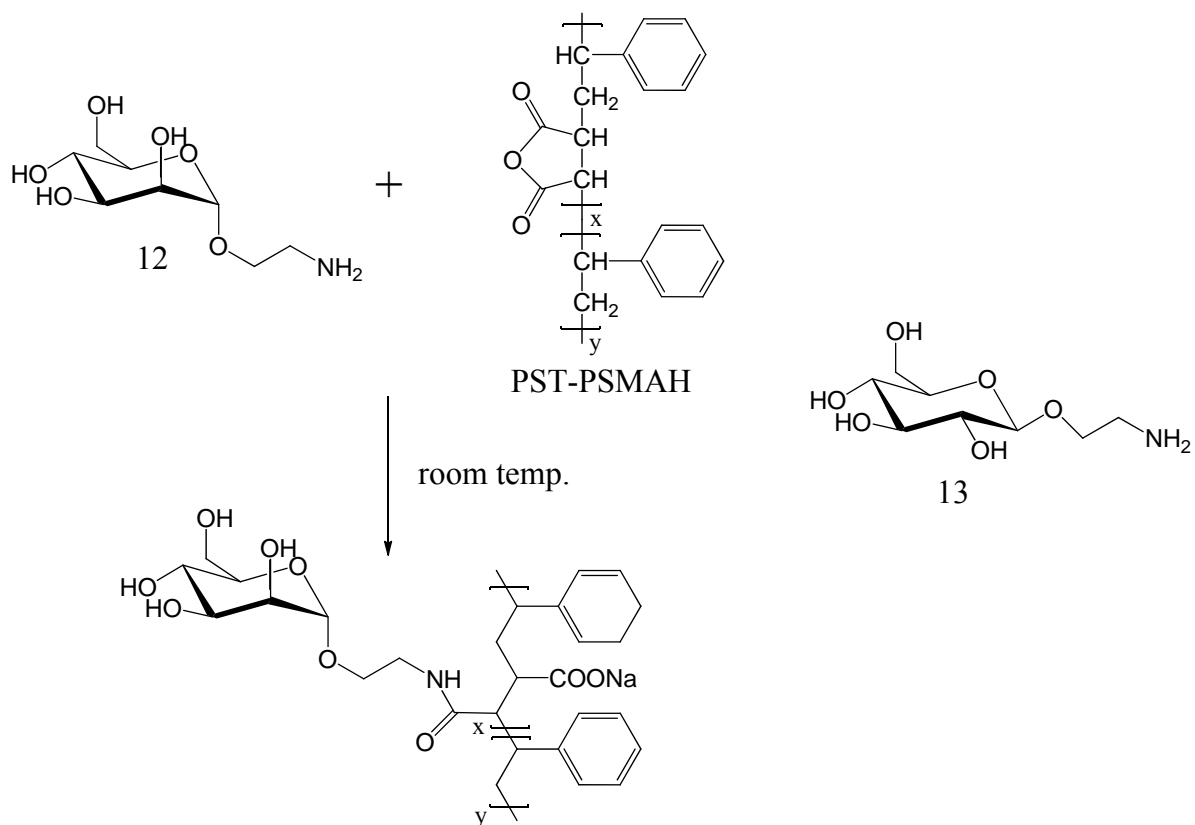


**Figure 2-4 Grafting of (12) and (13) onto poly{styrene-co-[(maleic anhydride)-alt-styrene]} (PST-PSMAH) (Su et al. 2009)**

Researchers in Auzely-Velty's group developed a lactose derivative: N-(4-aminobutyl)-O-β-D-galactopyranosyl-(1→4)-D-gluconamide (**14**) (Fig. 2.5) and grafted it onto poly(N-vinylpyrrolidone-co-maleic acid) (PNVP-MAC) with NaOH treatment (Auzely-Velty et al., 2002). The glycopolymer was reported to interact with a lectin (Ricinus Communis Agglutinin, RCA<sub>120</sub>). Amphiphilic copolymers were produced by grafting (**14**) and dodecylamine onto PNVP-MAC via the previously described method (Cade et al. 2004). Nanoparticles were prepared by an emulsification–diffusion procedure. The nanoparticle interacted with RCA<sub>120</sub> as well.

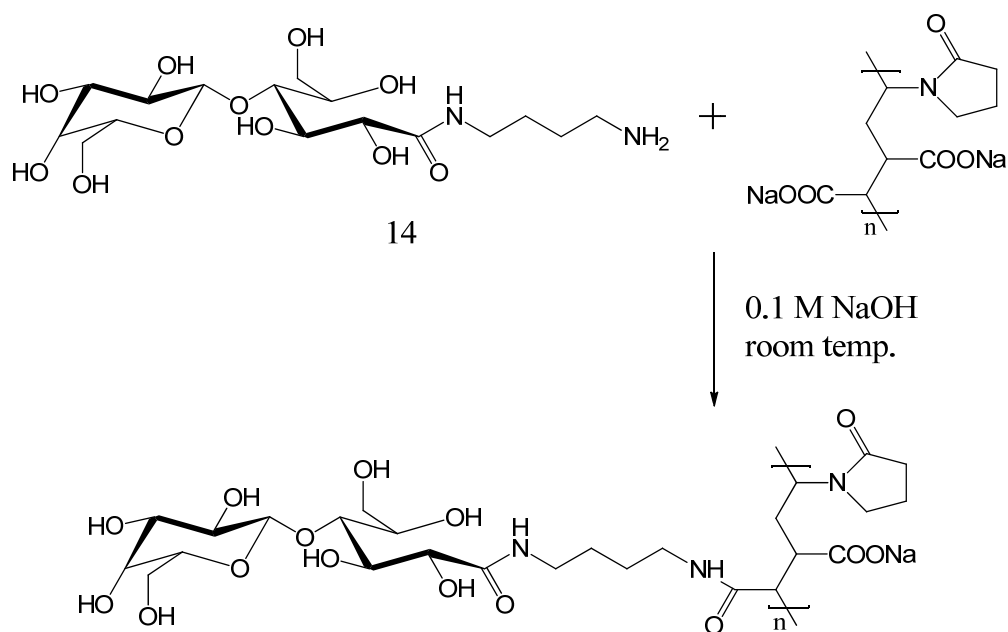


**Figure 2-5 Grafting of N-(4-aminobutyl)-O-β-D-galactopyranosyl-(1→4)-D-gluconamide (14) onto poly(N-vinylpyrrolidone-co-maleic acid) (PNVP-MAC) (Auzely-Velty et al. 2002)**

Uzawa et al. (2005) grafted three sugar derivatives: 10-aminodecyl O-(α-D-galactopyranosyl)-(1→4)-β-D-galactopyranoside (**15**), 4-aminophenyl-O-β-lactoside (**16**), and 4-aminophenyl-O-α-D-mannopyranoside (**17**) (Fig. 2.6) onto poly(ethylene-alt-maleic anhydride) (PEMAH). Layer-by-layer membranes on gold substrate surface were fabricated by polyanionic glycopolymer together with polycationic polymer. The derived glycosyl arrays were aimed to detect Shiga toxin produced by *Escherichia coli* O-157.

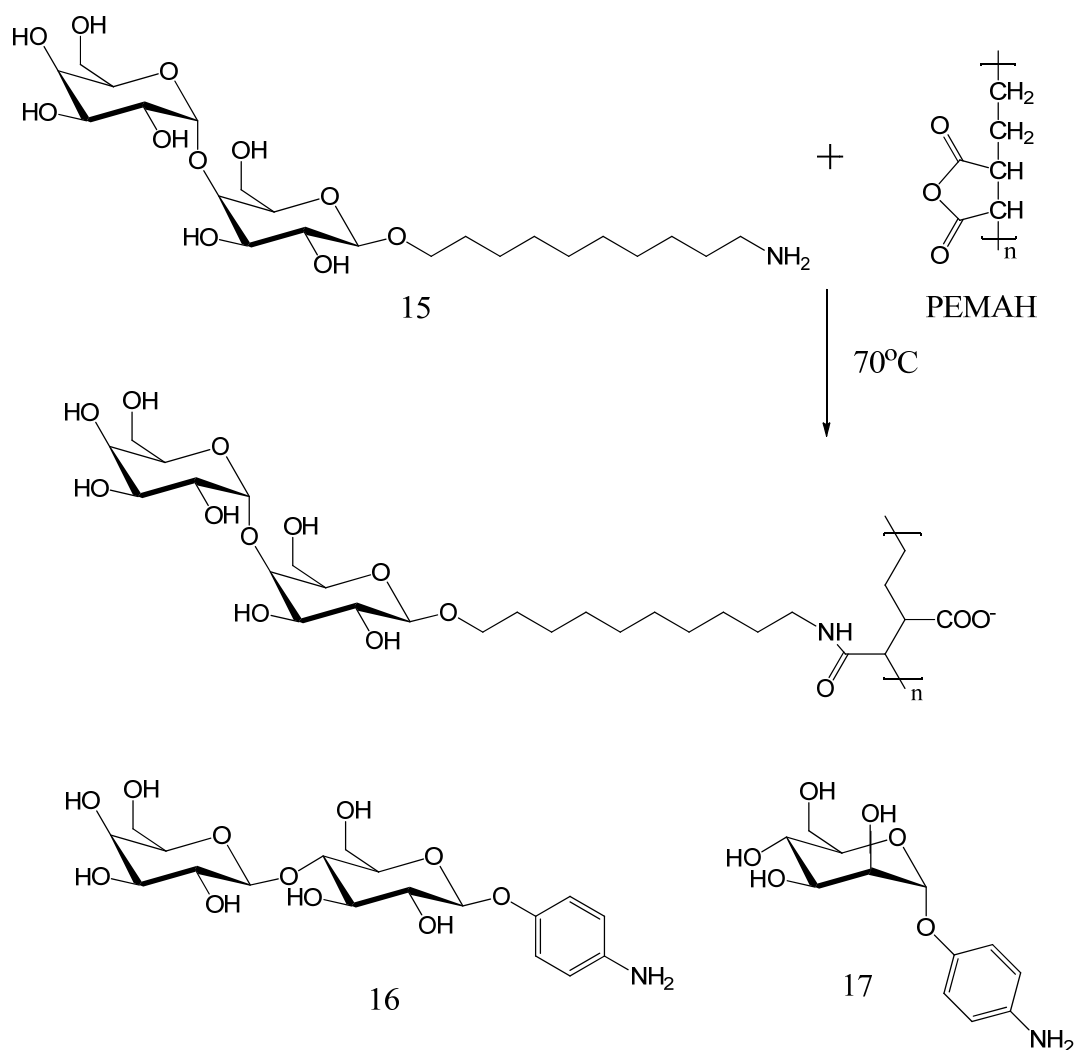


**Figure 2-6 Grafting of (15), (16) and (17) onto poly(ethylene-alt-maleic anhydride) (PEMAH) (Uzawa et al. 2005)**

A glucose derivative, 2-aminoethyloxyl- $\beta$ -D-glucopyranoside (**18**) (Fig. 2.7), was grafted onto spin-coated poly(propylene-alt-maleic anhydride) (PPMAH) thin film (Grombe et al., 2006). A set of sugar derivatives such as sulfated 2-[2-(2-aminoethyl)-ethyl]-ethyl- $\beta$ -D-glucopyranoside (**19**), sulfated 2-[2-(2-aminoethyl)-ethyl]-ethyl-4-( $\alpha$ -D-glucopyranosyl)- $\beta$ -D-glucopyranoside (**20**) (Fig. 2.7), sulfated cellulose, and heparin was grafted onto PEMAH or PPMAH thin films

(Grombe et al. 2007). Antithrombin binding tests and whole blood incubation assays indicated that those glycopolymers have potential to be used as anticoagulant.

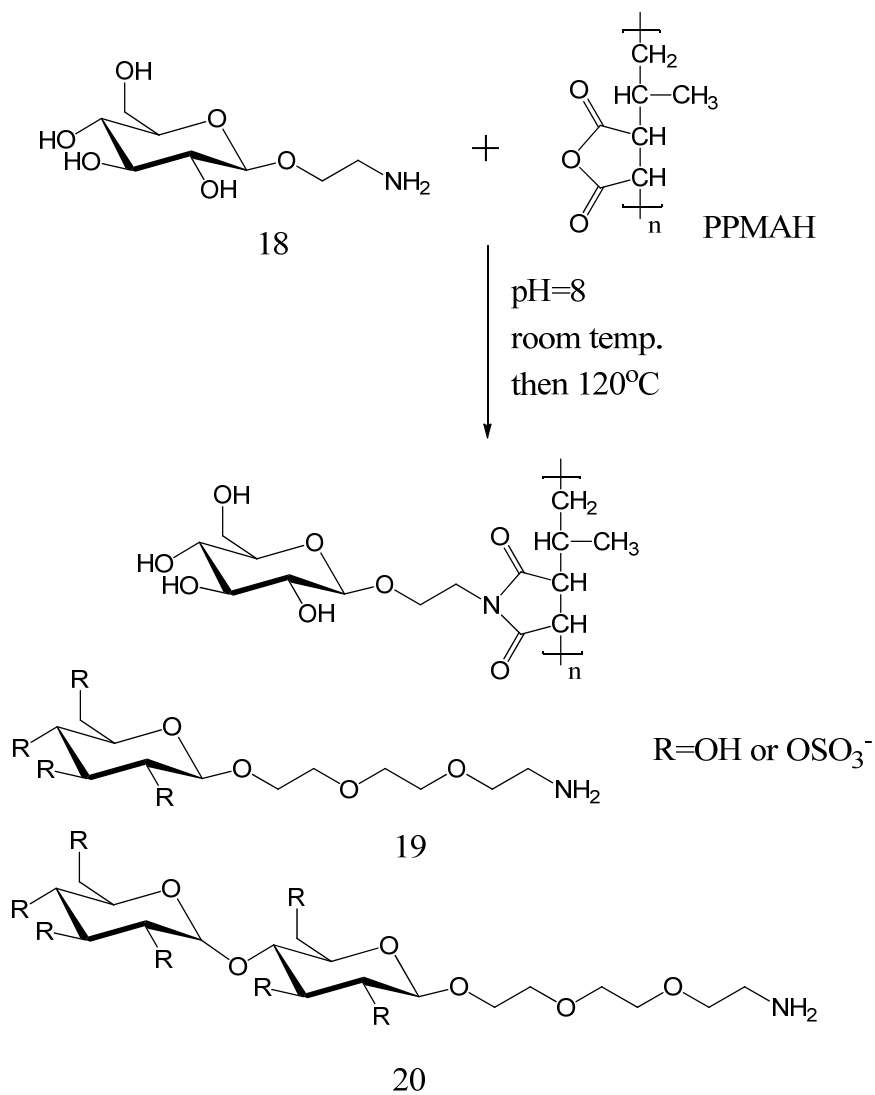


**Figure 2-7 Grafting of (18), (19) and (20) onto poly(propylene-alt-maleic anhydride) (PPMAH) thin film (Grombe et al. 2006, 2007)**

Paraskar and colleagues (2010) reported a sugar containing nanoparticle to enhance antitumor efficacy. Glucosamine (**21**) (Fig. 2.8) was grafted onto poly(isobutylene -alt-maleic acid) (PIMAC) using diaza(1,3)bicyclo[5.4.0]undecane (DBU) as catalyst. A chemotherapy drug,

cisplatin, was complexed with the glycopolymer via a monocarboxylato and O→platinum (Pt) coordinate bond. At a certain Pt to glycopolymer ratio, the complex self-assembled into a nanoparticle that released cisplatin in a pH-dependent manner. *In vivo* treatment to lung and breast cancer and biodistribution tests showed that the nanoparticles delayed tumor growth and decreased biodistribution of platinum to the kidney. Nanoparticles fabricated by oxaliplatin complex with glucosamine functionalized PIMAC for better antitumor efficacy were also studied (Paraskar et al. 2012).

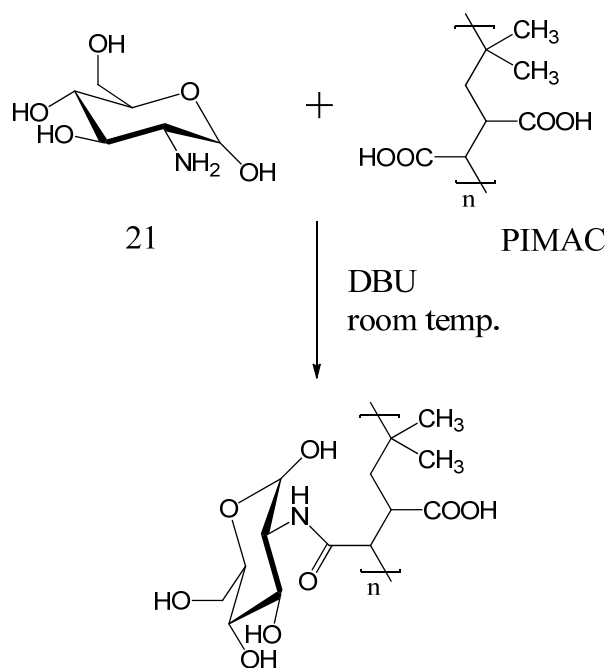


**Figure 2-8 Grafting of glucosamine (21) onto poly(isobutylene-alt-maleic acid) (PIMAC) (Paraskar et al. 2010)**

As a biocompatible material, poly (methyl vinyl ether-co-maleic acid) (PVME-MAc) was mostly used as denture adhesive. It is the base compound in Super Poligrip®. Because of the strong reactivity of carboxylic acid groups on the polymer, several natural compounds such as peptides (Ladaviere et al. 2000) and proteins (Koyama et al. 1992, Allard et al. 2001) have been grafted

onto PVME-MAc via amide linkage. Glucosamine, which is a monosaccharide containing an amine group, is a good candidate to be grafted onto PVME-MAc for specific biological properties. Meanwhile, PVME-MAc could also be crosslinked by ethylene glycol, 1,4-butanediol, 1,6-hexandiol, 1,8-octanediol, 1,10-decanediol, 1,12-dodecanediol (Luppi et al. 2003), partially hydrolyzed poly(vinyl acetate) (Guo et al. 2008), cellulosic nanowhisker (Goetz et al. 2009, 2010), and poly(ethylene glycol) (Raj Singh et al. 2009, 2010, Garland et al. 2011). Applications of those hydrogels were investigated, including topical vehicles for hydrophilic and hydrophobic drugs (Luppi et al. 2003), tunable denture adhesives to both hydrophobic and hydrophilic surfaces (Guo et al. 2008), nanocomposites (Goetz et al. 2009, 2010), and controlled drug delivery devices (Raj Singh et al. 2009, 2010, Garland et al. 2011).

### **2.1.3 pH-responsive glycopolymer hydrogels**

Hydrogels are some of the most common drug carriers. They are three-dimensional, cross-linked polymers that swell in water or aqueous solvent systems. Because of their high water uptake, they are generally biocompatible. Drugs are either loaded into the hydrogel during hydrogel synthesis or diffuse into the hydrogel upon swelling of the hydrogel. Drug delivery is governed by diffusion of the drug, interaction of drug and hydrogel, and degradation of the matrix. Therefore, several factors such as pore size and biodegradability of the hydrogel as well as interaction between drug and matrix influence the speed of drug delivery.

Depending on the pH of the environment, pH-responsive hydrogels naturally display big differences in swelling properties. They contain pendent acidic (e.g. carboxylic and sulfonic acids) or basic (e.g. ammonium salt) groups that either accept or release protons in response to changes in environmental pH. At this event, expulsion of charges on pendent groups increases

swelling of hydrogels. pH-responsive hydrogels that stay in collapsed state at low pH and swell at neutral pH may be used as oral drug delivery devices for pH-sensitive drugs such as proteins. Researchers have reported that sugar such as lactose, glucose, and sucrose could stabilize different proteins by a “preferential hydration” mechanism (Arakawa et al. 1982, Lee et al. 1975, 1981), while glucose can prevent the aggregation of insulin (Jeffrey 1974). Thus, pH-responsive glycopolymer hydrogels as drug delivery devices may better protect proteins in the matrix.

Although hydrogels have been studied insensitively, just a few glycopolymer hydrogels have been developed. Nakamae and colleagues obtained a glycopolymer hydrogel containing glucose pendent moieties as drug delivery device for insulin (Miyata et al. 1996). N,N'-methylene bisacrylamide was used as chemical crosslinking agent and concanavalin A served as physical crosslinking agent. In glucose solution, physical crosslinks were opened due to prevented interaction between concanavalin A with pendent glucose groups caused by a surplus of glucose in the solution. The swelling ratio increased with increasing glucose concentration in the solution; therefore drugs in the hydrogel may be released upon swelling of the hydrogel. An insulin-loaded hydrogel can be used as a smart device to control the glucose level in the blood by itself.

Zhang et al. (2006) synthesized a glycopolymer hydrogel containing blood B group epitope pendent groups for norovirus treatment. Because of the interaction between norovirus and blood B group epitope, the hydrogel absorbed most norovirus from the solution. This hydrogel might be administered to patients with the goal of removing most of the norovirus in the digestive system, thus reduce the possibility of getting infected.

Three pH-responsive glycopolymer hydrogels have been reported by different research groups. Kim et al. (2002) synthesized a poly(methacrylic acid-co-2-methacyloxyethyl glucoside) based hydrogel by free-radical photopolymerization. It swelled dramatically above pH 5, which is the  $pK_a$  of poly(methacrylic acid) (PMAA). The mesh size of the hydrogel which is the distance between adjacent crosslinks was calculated by Peppas–Merrill equation (Peppas et al. 1977).

Mahkam (2007) obtained a hydrogel which also contained the PMAA block. It remained in collapsed state at strongly acidic conditions and swelled in neutral solution. The author loaded a prodrug named oslalazine into the hydrogel and studied the drug release profile at the pH of 1 and 7.4. As expected, much more drug was released from the hydrogel at pH of 7.4.

A multi-component drug delivery system was developed by Polikarpov et al. (2010). It was constructed by a thermo- and pH-responsive hydrogel matrix with incorporated maltosylated hyperbranched poly(ethylene imine) (PEI-Mal). A small, hydrophilic dye (Rose Bengal) was used as model compound to investigate the drug loading behavior. It was found that PEI-Mal formed complexes with up to 130 dye molecules per polymer. These complexes were absorbed by the hydrogel and released quickly at basic and neutral conditions; however, most of them remained in the matrix at acidic condition.

#### **2.1.4 Approach**

In this project, glucosamine was grafted onto poly(vinyl methyl ether-atl-maleic acid) to produce a glycopolymer, Glu-PMVE-MAc, with high yield. The product was isolated by precipitation in ethyl acetate. The chemical structure of the glycopolymer was confirmed by FTIR and  $^1H$ -NMR. Elemental analysis was utilized to determine the amount of grafted glucosamine groups. Glu-PMVE-MAc was crosslinked by poly(ethylene glycol) (PEG 400 or PEG 600). Swelling of the



Glu-PMVE-MAc hydrogels in aqueous solution at pH of 1.2 to 7.4 was investigated. The mesh size of the hydrogels was calculated from swelling data using Peppas–Merrill equation. The drug delivery profile of fluorescein isothiocyanate-dextran (FITC-dextran)-loaded hydrogels in enzyme-free simulated gastric fluid (pH 1.2) and simulated intestinal fluid (pH 6.8) was studied.

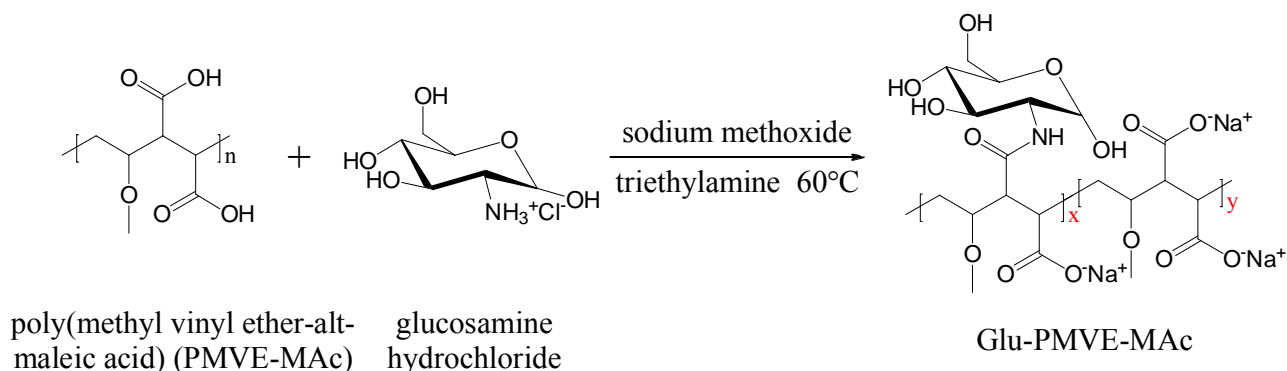
## **2.2 Experimental Part**

### **2.2.1 Materials**

Poly(methyl vinyl ether-alt-maleic acid) (PMVE-MAc) (Mn 80,000) (Sigma-Aldrich), methanol (99.8%, BDH), D-Glucosamine hydrochloride (99.9%, Calbiochem), sodium methoxide (98%, Alfa Aesar), triethylamine (99%, Alfa Aesar), anhydrous magnesium sulfate ( $\text{MgSO}_4$ ) (99%, Strem Chemicals), ethyl acetate (99.5%, Mallinckrodt Chemicals) and poly(ethylene glycol) (PEG) (400 and 600, Alfa Aesar) were used as received. Fluorescein isothiocyanate–dextran (FITC–Dextran) (10000, Sigma-Aldrich) was used as model drugs for drug release studies.

### **2.2.2 Synthesis of glucosamine grafted poly(methyl vinyl ether-alt-maleic acid) (Glu-PMVE-MAc)**

The overall scheme of the grafting reaction is shown in Scheme 2.1; the concentration of the reagents is listed in Table 2.1. PMVE-MAc in methanol was added dropwise to a mixture of D-glucosamine hydrochloride, sodium methoxide, and methanol at 60°C. Subsequently, triethylamine and anhydrous magnesium sulfate were added. The reaction was terminated after 4 h. The solution was filtered and the filtrate was concentrated using a rotary evaporator. The product was precipitated by pouring the concentrated filtrate into ethyl acetate. The precipitation was then collected and dried overnight under vacuum at 35°C.



**Scheme 2.1** Synthesis of glucosamine grafted poly(methyl vinyl ether-alt-maleic acid) (Glu-PMVE-MAC)

**Table 2.1** Amount of utilized reagents and yield for synthesis of Glu-PMVE-MAC

Glu-PMVE-MAC (1:1) (G1)		Glu-PMVE-MAC (1:2) (G2)	
glucosamine hydrochloride	23.2 mmol	glucosamine hydrochloride	11.6 mmol
PMVE-MAC (base polymer)	23.2 mmol (repeating units)	PMVE-MAC (base polymer)	23.2 mmol (repeating units)
glucosamine: maleic acid	1 : 1	glucosamine: maleic acid	1 : 2
Yield	71.4%	Yield	86.4%

### 2.2.3 Synthesis of PEG crosslinked hydrogels

A predetermined amount of Glu-PMVE-MAC or PMVE-MAC, poly(ethylene glycol) (PEG) and water was mixed to make a brown solution (Table 2.2). A film was prepared by pouring the solution into a petri dish on a leveled surface and left at room temperature for 72 h. After drying, the film was cured at 80°C for 24 h to induce chemical crosslinking (Raj Singh et al., 2009).

**Table 2.2 Amount of reagents in synthesis of PMVE-MAc or Glu-PMVE-MAc hydrogels**

Glu-PMVE-MAc Hydrogel (G1-400)		Glu-PMVE-MAc Hydrogel (G1-600)	
Glu-PMVE-MAc (1:1) (G1)	5.894 mmol (repeating units) (1.974 g)	Glu-PMVE-MAc (1:1) (G1)	5.894 mmol (repeating units) (1.974 g)
PEG 400	2.813 mmol (1.125 g)	PEG 600	2.813 mmol (1.688 g)
Water	16.901 g	Water	16.338 g
Glu-PMVE-MAc Hydrogel (G2-400)		Glu-PMVE-MAc Hydrogel (G2-600)	
Glu-PMVE-MAc (1:2) (G2)	5.894 mmol (repeating units) (1.5 g)	Glu-PMVE-MAc (1:2) (G2)	5.894 mmol (repeating units) (1.5 g)
PEG 400	2.813 mmol (1.125 g)	PEG 600	2.813 mmol (1.688 g)
Water	17.375 g	Water	16.813 g
PMVE-MAc Hydrogel (P-400)		PMVE-MAc Hydrogel (P-600)	
PMVE-MAc	5.894 mmol (repeating units) (1.026 g)	PMVE-MAc	5.894 mmol (repeating units) (1.026 g)
PEG 400	2.813 mmol (1.125 g)	PEG 600	2.813 mmol (1.688 g)
Water	17.849 g	Water	17.287 g

## **2.2.4 Characterization of Glu-PMVE-MAc and hydrogels**

### **2.2.4.1 Fourier Transform Infrared Spectroscopy (FT-IR)**

The FT-IR spectra of Glu-PMVE-MAc was recorded in powder form, using a Thermo Scientific Nicolet 6700 FT-IR spectrometer at resolution of  $4\text{ cm}^{-1}$ ; the number of scans was 32.

### **2.2.4.2 Nuclear Magnetic Resonance Spectroscopy (NMR)**

$^1\text{H}$  NMR was used to determine the structure of the synthesized products. Spectra were recorded at room temperature from a solution in deuterated dimethyl sulfoxide (DMSO- $d_6$ ) with a Bruker 400 spectrometer at 400 MHz. Typical parameters for the proton spectra were a 15 s pulse delay, a 3 s acquisition time, a 20.68 ppm spectral width, and 32 scans.

### **2.2.4.3 Elemental analysis**

Elemental analysis was performed by MICRO ANALYSIS INC. using carbon, oxygen, nitrogen method.

### **2.2.4.4 Equilibrium swelling study**

Prewighed dry hydrogels were immersed in various buffer solutions at a pH range from 1.2 to 7.4. After the swelling equilibrium was reached, the swollen hydrogels were taken out of the solution, gently taped with filter paper to remove the surface water, and weighed. All swelling tests were performed three times on three hydrogels made from three individually synthesized glycopolymers (Glu-PMVE-MAc) for each kind of hydrogels. The equilibrium swelling ratio ESR was calculated using the following equation:

$$\text{ESR (\%)} = (W_s - W_d) / W_d \times 100 \quad (1)$$

where  $W_s$  is the mass of the hydrogel at swelling equilibrium and  $W_d$  is the initial mass of dry hydrogel.

Preparation of buffer solutions: NaCl/HCl, pH 1.2-2.0; Na<sub>2</sub>HPO<sub>4</sub>/citric acid, pH 2.5-7.4. The ionic strength was maintained at 0.2 mol/L by adding NaCl to the buffer solutions.

### 2.2.5 Determination of network mesh size

In order to estimate the mesh size, which is the distance between adjacent crosslinks, of the swollen hydrogel, the Peppas–Merrill equation (Peppas et al., 1977) was used to calculate the number average molecular weight between crosslinks. Parameters involved in mesh size calculation are shown in Table 2.3.

$$\frac{1}{M_c} = \frac{2}{M_n} - \frac{(\bar{v}/V_1)[\ln(1-v_{2,s}) + v_{2,s} + \chi_1 v_{2,s}^2]}{v_{2,s} \left[ \left( \frac{v_{2,s}}{v_{2,r}} \right)^{1/3} - \frac{1}{2} \left( \frac{v_{2,s}}{v_{2,r}} \right) \right]} \quad (2)$$

Here,  $\bar{M}_n$  is the number average molecular weight of the uncross-linked polymer,  $\bar{v}$  is the specific volume of the polymer,  $V_1$  is the molar volume of the swelling agent,  $v_{2,r}$  is the polymer volume fraction after crosslinking but before swelling (the relaxed polymer volume fraction),  $v_{2,s}$  is the polymer volume fraction after equilibrium swelling (swollen polymer volume fraction), and  $\chi$  is the Flory polymer-solvent interaction parameter. The values of  $v_{2,r}$  and  $v_{2,s}$  were determined by an equilibrium swelling experiment.

After calculation of  $\overline{M}_c$ , mesh size  $\xi$  of the polymer network was calculated by the equation (3):

$$\xi = \nu_{2,s}^{-1/3} \sqrt{C_n} \sqrt{\frac{2\overline{M}_c}{M_r}} l \quad (3)$$

Where  $C_n$  is the characteristic ratio of the polymer,  $M_r$  is the average molecular weight of the repeating unit,  $l$  is the carbon-carbon bond length.

**Table 2.3 Parameters involved in mesh size calculation**

Parameters	Physical meaning	Value
$\overline{M}_n$	number average molecular weight of the uncross-linked polymer	G1 = 154,000 Da
		G2 = 117,000 Da
$\bar{v}$	specific volume of the uncross-linked polymer	0.769 cm <sup>3</sup> / g
$V_1$	molar volume of the swelling agent (water)	18 cm <sup>3</sup> / mol
$\chi$	Flory polymer-solvent interaction parameter	0.5 ( $\chi_{\text{polyacrylic acid}} = 0.5^a$ )
$C_n$	characteristic ratio of the uncross-linked polymer (glucosamine grafted poly(vinyl methyl ether-alt-maleic acid))	6.5 (estimated value) ( $C_{n-\text{poly(acrylic acid)}} = 6.7^a$ , $C_{n-\text{poly(vinyl methyl ether)}} = 6.3^b$ )
$M_r$	average molecular weight of the repeating unit of the uncross-linked polymer	G1 = 335 Da
		G2 = 254.5 Da
$l$	carbon-carbon bond length	1.54 Å

<sup>a</sup>Gudeman et al. 1995, <sup>b</sup>Zeng et al. 2005

### 2.2.6 Drug release studies

FITC-dextran was used as a model drug. The absorbance of FITC-dextran in solution was measured by a UV-Vis spectrometer (Thermo Spectronic Genesys 6) at 497 nm. The absorbance difference of FITC-dextran-loaded hydrogel and FITC-dextran-unloaded hydrogel was recorded

to determine the drug release profile. The actual concentration was then determined by standard calibration curves.

#### **2.2.6.1 FITC-dextran loading**

A predetermined amount of FITC-dextran was added to a mixture of Glu-PMVE-MAc, PEG and water. FITC-dextran-loaded hydrogel was produced from the mixture following the previously described procedure. FITC-dextran unloaded hydrogel as control sample was prepared using the same Glu-PMVE-MAc.

#### **2.2.6.2 Preparation of enzyme-free simulated gastric fluid (SGF) (pH=1.2) and simulated intestinal fluid (SIF) (pH=6.8)**

Preparation of SGF: 2 g of sodium chloride and 7 mL of hydrochloric acid were dissolved in 500 mL of water. The solution was then diluted with water to 1 L and adjusted to a pH of 1.2.

Preparation of SIF: 6.8 g of monobasic potassium phosphate was first dissolved in 250 mL of water. 77 mL of 0.2 N sodium hydroxide and 500 mL of water were then added. The solution was finally diluted with water to 1 L and the pH was adjusted to be 6.8.

#### **2.2.6.3 *In vitro* release study**

Drug-loaded hydrogels were immersed in 10 mL of SGF (pH=1.2) or SIF (pH=6.8). At a predetermined time, 3 mL of the solution was analyzed by a UV-Vis spectrophotometer (Thermo Spectronic Genesys 6). The samples used for testing were then added back to the main solution. Absorbance of drug-unloaded hydrogels was tested at the same time as control. The absorbance difference of drug-loaded hydrogels and drug-unloaded hydrogels was the absorbance from

FITC-dextran. The cumulative amount of released drug was determined from the standard calibration curve and the percentage was calculated from division of the amount of released drug and loaded drug. All release tests were performed in triplicate on three dextran-loaded hydrogels and three dextran-unloaded hydrogels made from three individually synthesized glycopolymers (Glu-PMVE-MAc) for each kind of hydrogels.

## 2.3 Results and Discussion

### 2.3.1 FT-IR characterization of glucosamine grafted poly(methyl vinyl ether-alt-maleic acid) (Glu-PMVE-MAc)

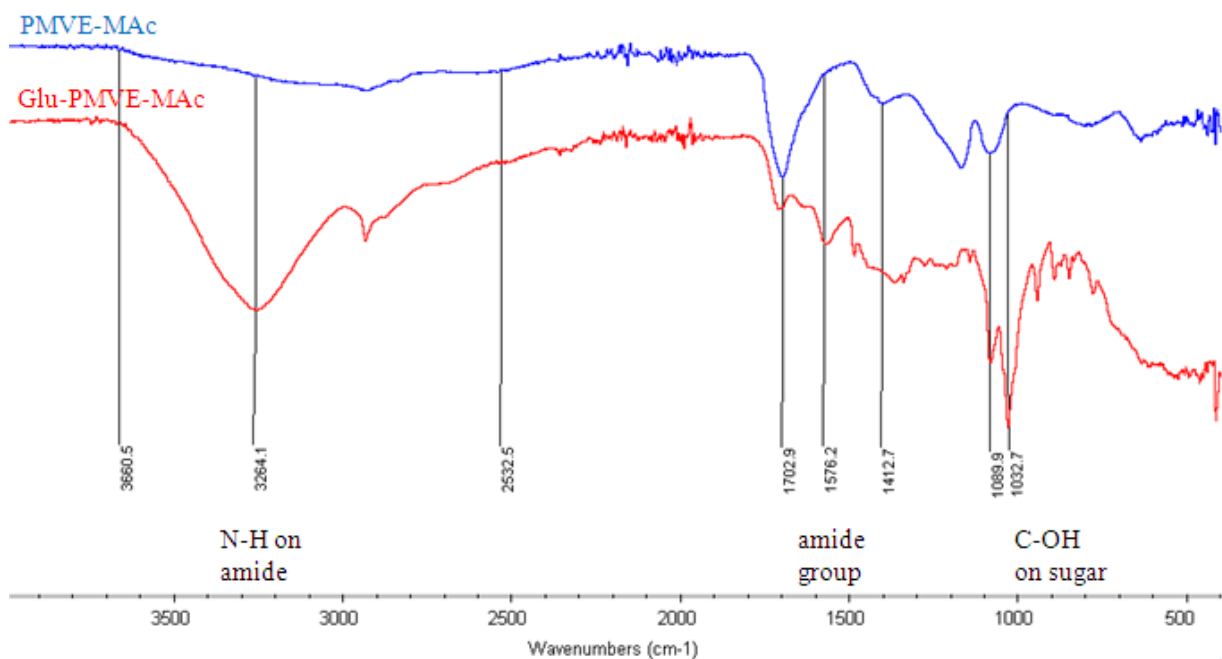


Figure 2-9 FT-IR spectra of glucosamine grafted poly(methyl vinyl ether-alt-maleic acid) (Glu-PMVE-MAc) (G1); Glu-PMVE-MAc: wavelength (cm<sup>-1</sup>): 1032.7 (C-OH on sugar), 1098.9 (ether group), 1576.2 (amide group), 1702.9 (C=O on carboxyl group), 2532.5 – 3660.5 (OH on sugar), 3264.1 (NH on amide group); in comparison PMVE-MAc: wavelength (cm<sup>-1</sup>): 1098.9 (ether group), 1412.7 (carboxylate anion), 1702.9 (C=O on carboxyl group)



The FT-IR spectra of glucosamine grafted poly(methyl vinyl ether-alt-maleic acid) (Glu-PMVE-MAc) and poly(methyl vinyl ether-alt-maleic acid) (PMVE-MAc) are shown in Fig. 2.9. The C-OH groups on sugar at  $1032.7\text{ cm}^{-1}$  and OH groups between  $2532.5.0\text{ cm}^{-1}$  and  $3660.5\text{ cm}^{-1}$  confirmed the sugar moiety on Glu-PMVE-MAc. Peaks for the amide group at  $1576.2\text{ cm}^{-1}$  and  $3264.1\text{ cm}^{-1}$  also proved the presence of the sugar moiety. The intensity was reduced for the carboxyl group at  $1702.8\text{ cm}^{-1}$  and the fact that the peak of the carboxylate anion at  $1412.7\text{ cm}^{-1}$  on Glu-PMVE-MAc disappeared indicated a lower amount of carboxyl groups on PMVE-MAc due to the successful grafting reaction.

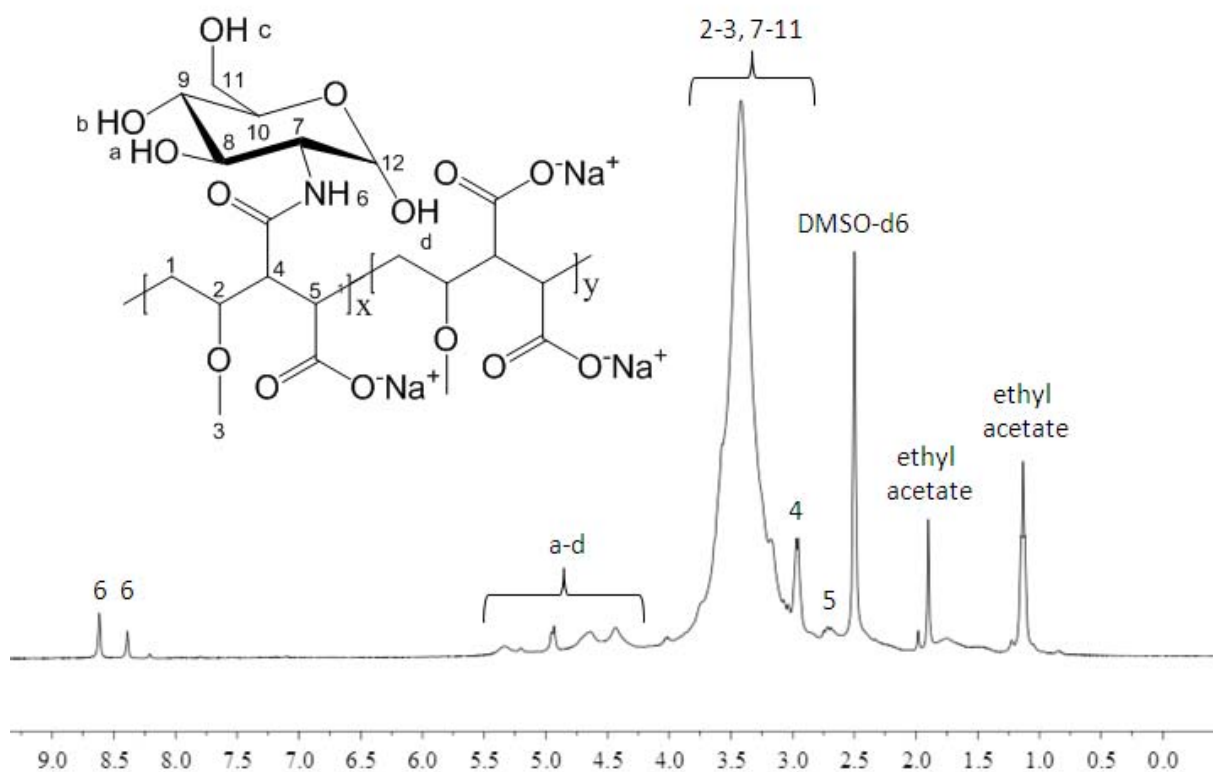


Figure 2-10  $^1\text{H-NMR}$  spectra of glucosamine grafted poly(methyl vinyl ether-alt-maleic acid) (Glu-PMVE-MAc) (G1); Glu-PMVE-MAc: (400MHz, DMSO-d),  $\delta(\text{ppm})$ : 1.13 (H-1), 2.72 (H-5), 2.96 (H-4), 3.03 – 4.13 (H-2, H-3, H-7 – H-11), 4.36-5.4 (H-a – H-d), 8.39, 8.62 (H-6)

### 2.3.2 <sup>1</sup>H-NMR characterization of glucosamine grafted poly(methyl vinyl ether-alt-maleic acid) (Glu-PMVE-MAc)

The chemical structure of glucosamine grafted poly(methyl vinyl ether-alt-maleic acid) (Glu-PMVE-MAc) was confirmed by <sup>1</sup>H-NMR analysis shown in Fig. 2.10. H-7 to H-11 and H-a to H-d proved the sugar moiety on Glu-PMVE-MAc. The H-6 which is the N-H on amide group indicated that the grafting reaction has occurred.

### 2.3.3 Glucosamine substitution rate on Glu-PMVE-MAc determined by elemental analysis

According to data from elemental analysis and further calculation, about 91.3% of maleic acid was grafted by one glucosamine in G1, and about 48.1% of maleic acid was grafted by one glucosamine in G2 (as expressed in the Table 2.3 and the Fig. 2.10 by x and y ratio). The result agreed well with the theoretically expected ratio based on the feed ratio.

Table 2.4 Glucosamine substitution rate on Glu-PMVE-MAc

	C	H	N	x : y (in Sch 2.1 )	x : y (theory)
Glu-PMVE-MAc (1:1) (G1)	46.57%	6.27%	3.98%	0.913 : 0.087	1 : 0
Glu-PMVE-MAc (1:2) (G2)	47.15%	6.09%	2.68%	0.481 : 0.519	1 : 1

### 2.3.4 Swelling behavior of Glu-PMVE-MAc and PMVE-MAc hydrogels in aqueous solution from pH of 1.2 to 7.4

Swelling curves were obtained for each of the hydrogels. Their equilibrium swelling ratios (ESR) in aqueous solution from pH of 1.2 to 7.4 are shown in Fig. 2.11. All Glu-PME-MAc hydrogels merely swelled in strong acidic solution. However, the ESR increased dramatically above a pH of 2.5 and reached equilibrium above pH of 3.5. The pH-responsive behavior could be due to the free carboxyl acid groups in the hydrogels. As introduced before, in acidic condition, most of the

carboxyl acid groups did not dissociate. However, at higher pH, negative charges on increasingly dissociated carboxyl acid groups repelled each other, thus the ESR increased remarkably. Interestingly, although there were more free carboxyl acid groups in PMVE-MAc hydrogels, those hydrogels did not show pH-responsive behavior. It might be due to lack of hydrophilic sugar groups in the matrix that boost water absorption.

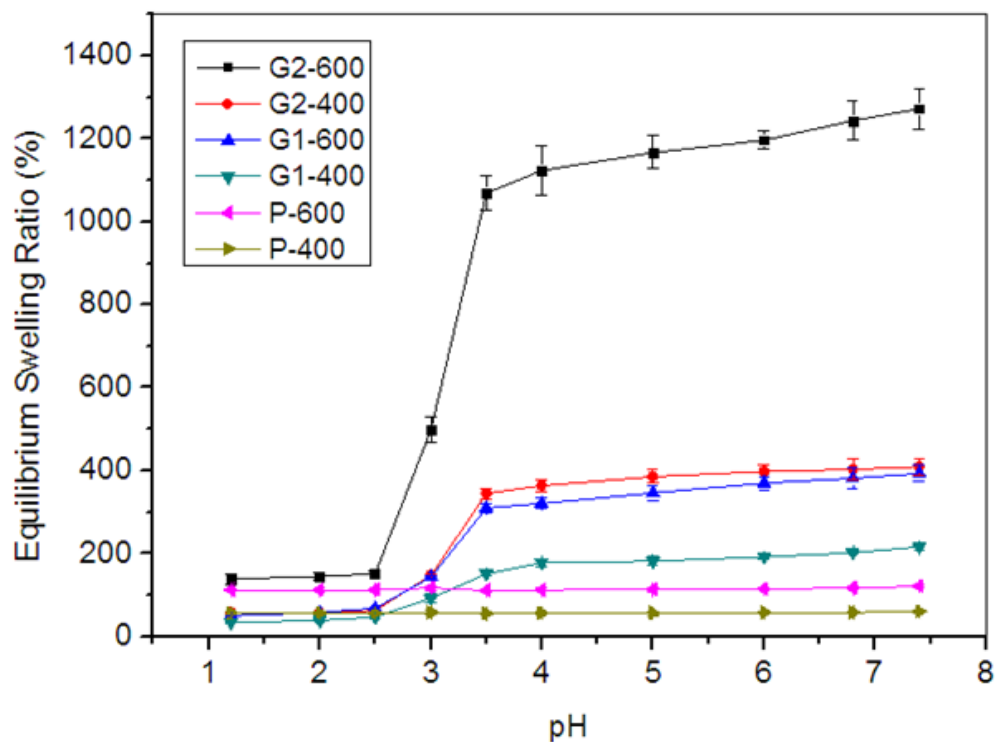


**Figure 2-11 Equilibrium swelling ratio of Glu-PMVE-MAc and PMVE-MAc hydrogels in aqueous solution from pH of 1.2 to 7.4**

The ESR was controlled by both of the glucosamine substitution rate on Glu-PMVE-MAc and the molecular weight of PEG. Low glucosamine substitution rate and higher molecular weight of PEG enhanced the ESR. As determined in elemental analysis, 91.3% of maleic acid was grafted by one glucosamine on G2 and 48.1% of maleic acid was grafted by one glucosamine on G1. Glucosamine reacted with carboxyl acid groups therefore reduced the amount of carboxyl acid groups available for the crosslinking reaction. For this reason, the crosslink density, which is

defined as moles of crosslinks per unit volume, of G1 hydrogels was higher than G2 hydrogels when crosslinked by the same type of PEG. From the definition of crosslink density, shorter PEG resulted in higher crosslink density therefore lower ESR.

### 2.3.5 Mesh size of Glu-PMVE-MAC hydrogels in aqueous solution from pH of 1.2 to 7.4

Data from the equilibrium swelling study were used to estimate the mesh size of hydrogels by the Peppas–Merrill equation. Fig. 2.12 shows the mesh size of Glu-PMVE-MAC hydrogels in aqueous solution from pH of 1.2 to 7.4. Mesh size of Glu-PMVE-MAC hydrogels reduced dramatically in acidic solution comparing to in higher pH solution.

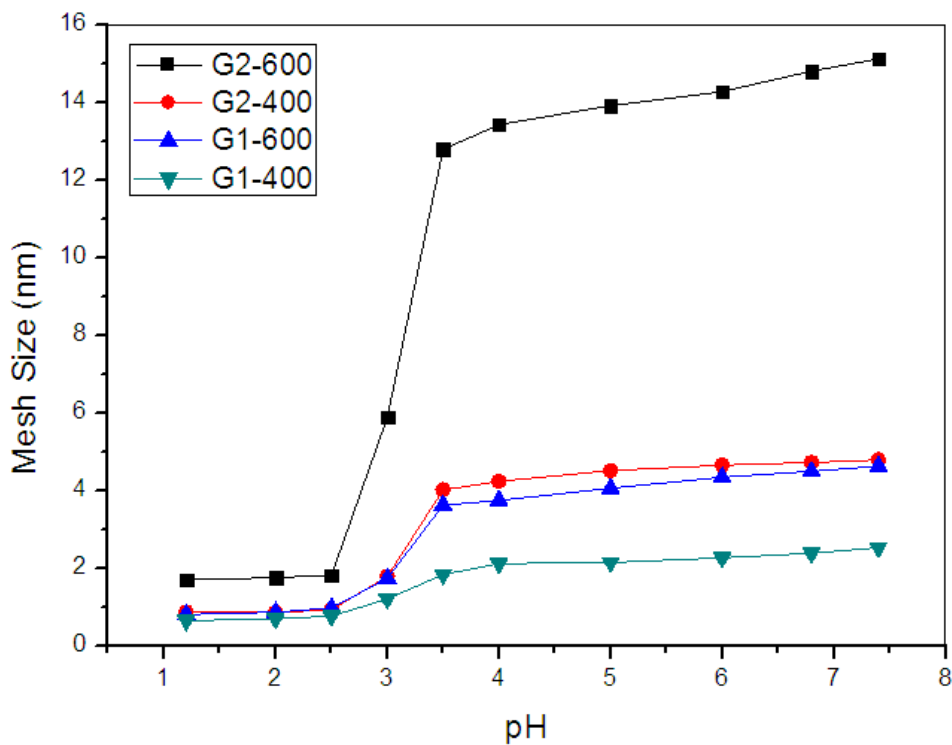


Figure 2-12 Mesh size of Glu-PMVE-MAC hydrogels in aqueous solution from pH of 1.2 to 7.4

### 2.3.6 *In vitro* release study of FITC-dextran-loaded Glu-PMVE-MAC hydrogels in enzyme-free simulated gastric fluid (SGF) (pH=1.2) and simulated intestinal fluid (SIF) (pH=6.8)

**Table 2.5 Actual weight and weight percentage of released Glu-PMVE-MAc of G2-400 hydrogels after immersing in SGF or SIF in 240 minutes**

In SGF (pH = 1.2) (10 mL)		
Sample	Weight of released Glu-PMVE-MAc (mg)	Weight of loaded FITC-dextran (mg)
FITC-dextran-unloaded hydrogel (control)	4.436	n/a
FITC-dextran-loaded hydrogel	4.404	1.029
Weight of hydrogels (mg)	Weight of total Glu-PMVE-MAc (mg)	Percentage of released Glu-PMVE-MAc (%)
FITC-dextran-unloaded hydrogel = 99.7	57.0	7.78
FITC-dextran-loaded hydrogel = 102.9	58.8	7.49
In SIF (pH = 6.8) (10 mL)		
Sample	Weight of released Glu-PMVE-MAc (mg)	Weight of loaded FITC-dextran (mg)
FITC-dextran-unloaded hydrogel	4.224	n/a
FITC-dextran-loaded hydrogel	3.995	1.145
Weight of hydrogels (mg)	Weight of total Glu-PMVE-MAc (mg)	Percentage of released Glu-PMVE-MAc (%)
FITC-dextran-unloaded hydrogel = 119.7	68.4	6.17
FITC-dextran-loaded hydrogel = 114.5	65.4	6.13

Drug release study of FITC-dextran-loaded Glu-PMVE-MAc hydrogels was conducted using a UV-Vis spectrometer. Fig. 2.13 shows the drug release profile of dextran-loaded G2-600 and

G2-400 hydrogels in enzyme-free simulated gastric fluid (SGF) (pH=1.2) and simulated intestinal fluid (SIF) (pH=6.8). In SIF, dextran was rapidly released from hydrogels at the same rate within 60 min and reached equilibrium after 120 min. After 240 min, 82.9% of dextran was released from G2-600 and 71.5% from G2-400. In SGF, none of dextran was released from G2-400 and G2-600. In fact, a slight negative value was detected due to the simultaneous release of a small amount of uncrosslinked Glu-PMVE-MAc from the hydrogel, which added to the absorbance difference of FITC-dextran-loaded hydrogel and FITC-dextran-unloaded hydrogel.

The actual amount of uncrosslinked Glu-PMVE-MAc was determined by standard calibration curve at 300 nm using a UV-Vis spectrometer. Data in Table 2.4 show actual weight and weight percentage of released Glu-PMVE-MAc was determined on G2-400 hydrogels. In SGF, 7.8% of Glu-PMVE-MAc was released from a FITC-dextran-unloaded hydrogel and 7.5% was discharged from a FITC-dextran-loaded hydrogel. From mesh size calculation, mesh size of G2-400 at pH of 1.2 was estimated to be about 0.9 nm. Since there was 1.029 mg of FITC-dextran ( $M_w=10000$  g/mol) in the hydrogel, the loaded FITC-dextran might have blocked the release of uncrosslinked Glu-PMVE-MAc from the relatively small cavities in the hydrogel. For this reason, absorbance of FITC-dextran-loaded hydrogel appeared lower than of the control hydrogel. In SIF, about 6.1% of uncrosslinked Glu-PMVE-MAc was discharged from both hydrogels. The loaded FITC-dextran could no longer hinder the release of uncrosslinked Glu-PMVE-MAc since the mesh size had increased to be about 4.7 nm. Interestingly, more uncrosslinked Glu-PMVE-MAc was released from G2-400 in SGF (pH =1.2) than in SIF (pH = 6.8), possibly because acid might have catalyzed the hydrolysis of ester bonds which served as crosslinks on the hydrogels. With less than 2%, however, it could safely be assumed that acid did not significantly damage the hydrogel.

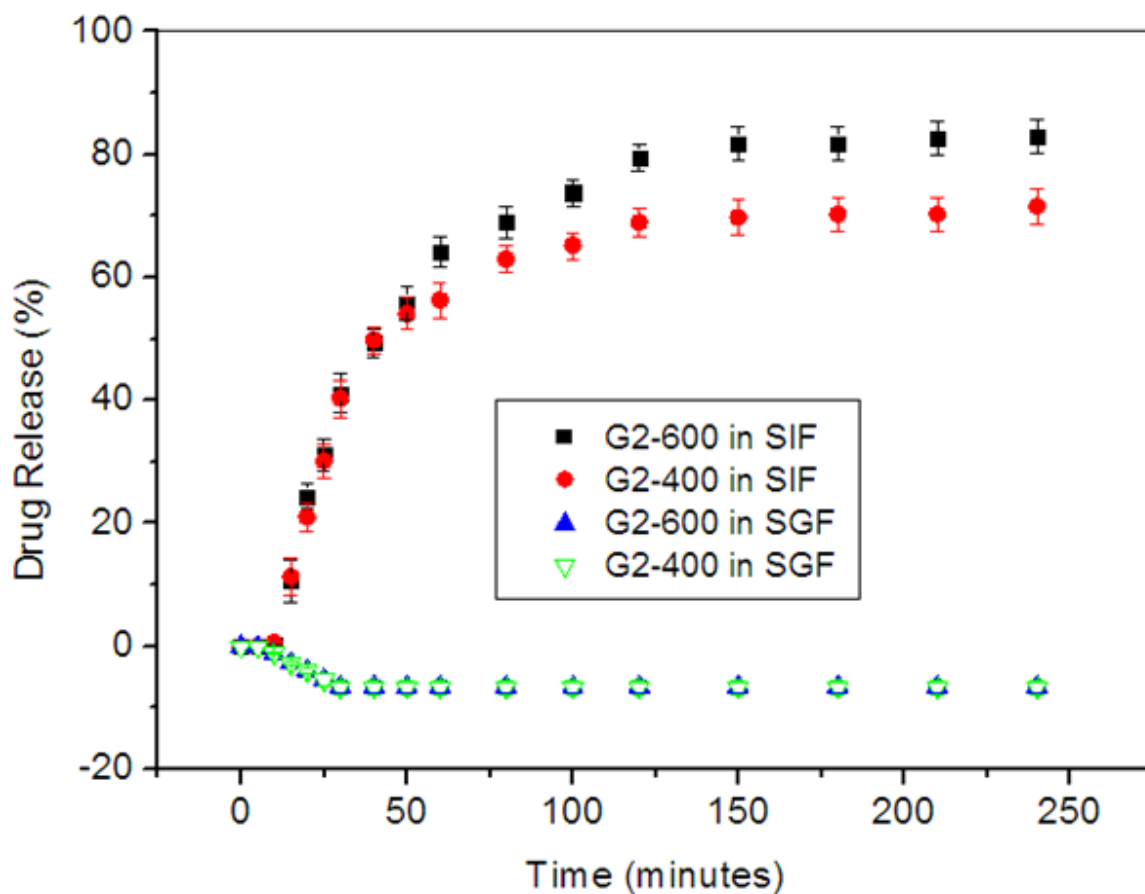


**Figure 2-13 Drug release profile of FITC-dextran-loaded Glu-PMVE-Mac hydrogels in enzyme-free simulated gastric fluid (SGF) (pH=1.2) or simulated intestinal fluid (SIF) (pH=6.8) within 240 min**

As expected, the drug release profile was clearly related to the estimated mesh size. It was reported from the manufacturer that the hydrodynamic diameter of FITC-dextran (MW 10,000) is about 4.6 nm. Obviously, dextran could not be released when the mesh size of hydrogels was less than 2 nm. When mesh size of hydrogels increased to 4.7 nm, most of dextran was discharged. More dextran was released when the mesh size increased to 14.8 nm. As shown in Fig. 2.14, 89.8% of dextran was released from G2-400 hydrogels with mesh size of 4.7 nm after 88 h and 98.8% of dextran was released from G2-600 hydrogels with mesh size of 14.8 nm after 52 h. The *in vitro* drug release study demonstrates that pH-sensitive drugs of an appropriate size

could potentially be retained in the hydrogel matrix in the stomach and released effectively in the small intestine.

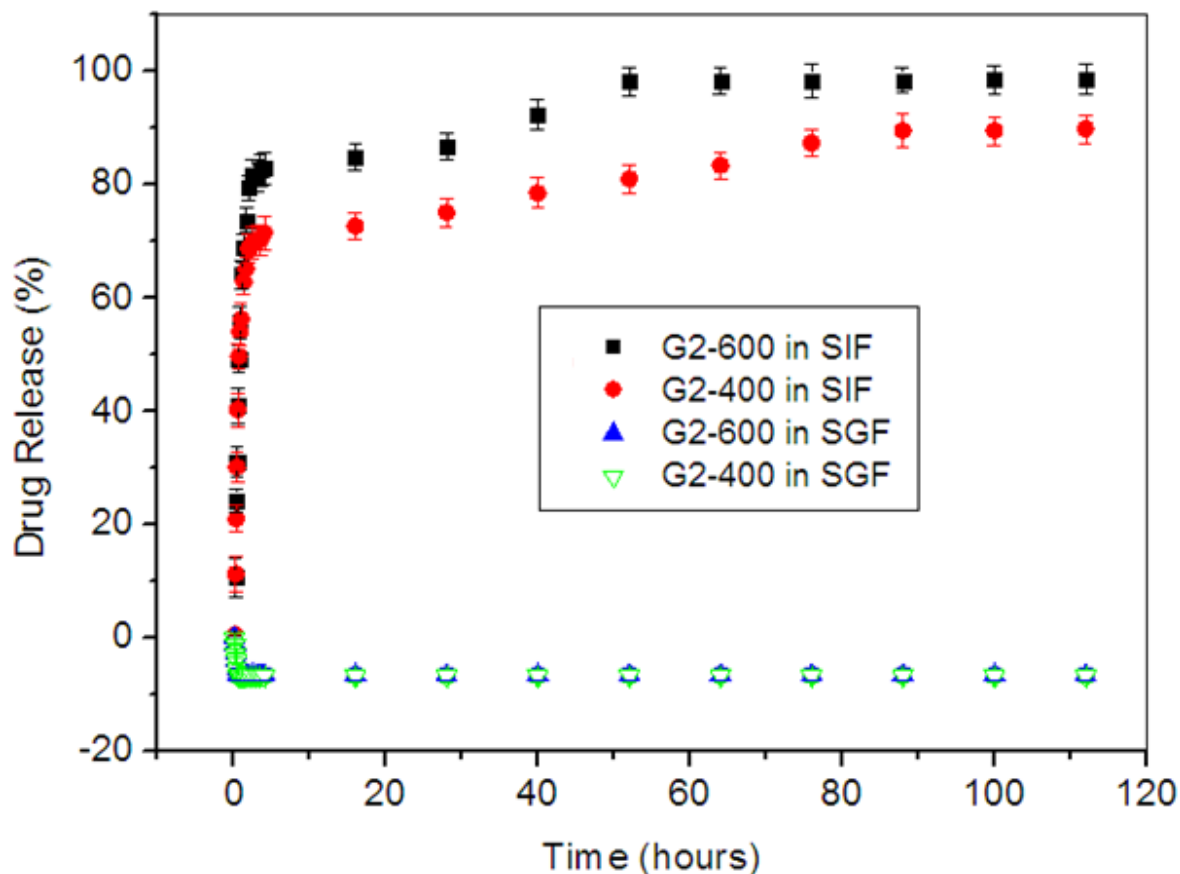


Figure 2-14 Drug release profile of FITC-dextran-loaded Glu-PMVE-MAc hydrogels in enzyme-free simulated gastric fluid (SGF) (pH=1.2) or simulated intestinal fluid (SIF) (pH=6.8) within 120 h

## 2.4 Conclusions

Glucosamine grafted glycopolymer poly(methyl vinyl ether-alt-maleic acid) (Glu-PMVE-MAc) was successfully synthesized with high yield. The structure of Glu-PMVE-MAc was confirmed by FT-IR and  $^1\text{H-NMR}$ . Elemental analysis was utilized to determine the amount of grafted glucosamine groups. A glycopolymer hydrogel was produced via crosslinking Glu-PMVE-MAc by PEG 400 or PEG 600. The swelling behavior in aqueous solution from pH of 1.2 to 7.4 was



studied. The mesh size was estimated from equilibrium swelling data using Peppas-Merrill equation. FITC-dextran with a molecular weight of 10,000 was used as a model drug to investigate the drug delivery profile in enzyme-free simulated gastric fluid (SGF) (pH=1.2) and enzyme-free simulated intestinal fluid (SIF) (pH=6.8). None of the dextran was released in SGF, however, most was discharged in SIF. Therefore, these hydrogels could potentially be used to transport drugs through the stomach and to be released in the intestinal tract.

## 2.5 References

Allard L, Cheynet V, Oriol G, Veron L, Merlier F, Scremin G, Mandrand B, Delair T, and Mallet F. *Bioconjugate Chemistry*, **2001**, 12, 972-979

Arakawa T, and Timasheff SN. *Biochemistry*, **1982**, 21, 6536-6544

Auzely-Velty R, Cristea M, and Rinaudo M. *Biomacromolecules*, **2002**, 3, 998-1005

Cade D, Ramus E, Rinaudo M, Auzely-Velty R, Delair T, and Hamaide T. *Biomacromolecules*, **2004**, 5, 922-927

Donati I, Gamini A, Vetere A, Campa C, and Paoletti S. *Biomacromolecules*, **2002**, 3, 805-812

Galgali P, Varma AJ, Puntambekar US, and Gokhale DV. *CHEM. COMMUN.* , **2002**, 2884-2885

Galgalia P, Puntambekarb US, Gokhaleb DV, and Varma AJ. *Carbohydrate Polymers*, **2004**, 55, 393-399

Galgali P, Agashe M, and Varma AJ. *Carbohydrate Polymers*, **2007**, 67, 576-585

Garland MJ, Raj-Singh TR, Woolfson AD, and Donnelly RF. *International Journal of Pharmaceutics*, **2011**, 406, 91-98

Goetz L, Mathew A, Oksman K, Gatenholm P, and Ragauskas AJ. *Carbohydrate Polymers*, **2009**, 75, 85-89

Goetz L, Foston M, Mathew AP, Oksman K, and Ragauskas AJ. *Biomacromolecules*, **2010**, 11, 2660-2666

Grombe R, Gouzy MF., Nitschke M, Komber H, and Werner C. *Colloids and Surfaces A: Physicochem. Eng. Aspects*, **2006**, 284–285, 295-300

Grombe R, Gouzy MF, Maitz MF, Freudenberg U, Zschoche S, Simon F, Pompe T, Sperling C, and Werner C. *Macromol. Biosci.*, **2007**, 7, 195-200

Gudeman LF and Peppas NA. *J. Appl. Polym. Sci.*, **1995**, 55, 919-928

Guo Xh, Deng F, Li L, and Prudhomme RK. *Biomacromolecules*, **2008**, 9, 1637-1642

Isosaki K, Seno N, and Matsumoto I. *Journal of Chromatography*, **1992**, 597, 123-128

Jeffrey PD. *Biochemistry*, **1974**, 13, 4441-4447

Kim B, and Peppas NA. *J. Biomater. Sci. Polymer Edn*, **2002**, 13, 1271-1281

Ladaviere C, Lorenzo C, Elaissari A, Mandrand B, and Delair T. *Bioconjugate Chemistry*, **2000**, 11, 146-152

Lee JC, Frigon RP, and Timasheff SN. *Ann N.Y. Acad. Sci.*, **1975**, 253, 284-291

Lee JC, and Timasheff SN. *J. Biol. Chem.*, **1981**, 256, 7 193-7201

Luppi B, Cerchiara T, Bigucci F, Di Pietra AM, Orienti I, and Zecchi V. *Drug Delivery*, **2003**, 10, 239-244

Mahkam M. *Drug Delivery*, **2007**, 14, 147-153

Miyata T, Jijihara A, and Nakamae K. *Macromol. Chem. Phys.* **1996**, 197, 1135-1146

Paraskar AS, Soni S, Chin KT, Chaudhuri P, Muto KW, Berkowitz J, Handlogten MW, Alves NJ, Bilgicer B, Dinulescu DM, Mashelkar RA, and Sengupta S. *PNAS*, **2010**, 107, 12435–12440

Paraskar A, Soni S, Roy B, Papa AL and Sengupta S. *Nanotechnology*, **2012**, 23, 75-103

Peppas NA, and Merrill EW. *J. Appl. Polym. Sci.*, **1977**, 21, 1763-1770

Polikarpov N, Kaufmann A, and Kluge J, *abstracts/ journal of controlled release*, **2010**, 148, 66-67

Raj-Singh TR, McCarron PA, Woolfson AD, and Donnelly RF. *European Polymer Journal*, **2009**, 45, 1239–1249

Raj-Singh TR, Woolfson AD, and Donnelly RF. *Journal of Pharmacy and Pharmacology*, **2010**, 62, 829–837

Su Rm, Li L, Chen Xp, Han Jh, and Han Sf. *Org. Biomol. Chem.*, **2009**, 7, 2040–2045

Uzawa H, Ito H, Izumi M, Tokuhisa H, Taguchi K, and Minoura N. *Tetrahedron*, **2005**, 61, 5895–5905

Varma AJ, Kennedy JF, and Galgali P. Carbohydrate Polymers, **2004**, 56, 429-445

Vetere A, Donati I, Campa C, Semeraro S, Gamini A, and Paoletti S. Glycobiology, **2002**, 12, 283-290

Zeng XG, Chen L, and Yang XZ. Chemical Journal of Chinese Universities, **2005**, 26, 1561-1564

Zhang YI, Yao Qj, Xia Cf, Jiang X, and Wang PG. ChemMedChem, **2006**, 1, 1361-1366

## **CHAPTER 3    SYNTHESIS OF AMPHIPHILIC GLYCOPOLYMER (PHEMAGI-PPO) USING ATOM TRANSFER RADICAL POLYMERIZATION (ATRP) FOR DRUG DELIVERY APPLICATION**

### **3.1 Introduction**

#### **3.1.1 Glycopolymers in micelle formation**

A micelle is an aggregate of amphiphilic molecules, which are molecules consisting of hydrophilic and hydrophobic blocks, dispersed in form of a liquid colloid. It has a hydrophobic core and a hydrophilic shell. As a drug delivery device, micelles minimize drug degradation and loss upon administration, lessen harmful or undesirable side-effects, increase drug bioavailability, and control drug release to maximize efficiency and minimize toxicity of the drug. In aqueous solution, the hydrophilic outer layer creates a highly water-bound barrier, which blocks the adhesion of opsonins. Therefore lower the impact of immune system. (Yamamoto et al. 2001). Imaging contrast agents and multiple drugs can be loaded into a single micelle, allowing both diagnosis and therapy (Ferrari 2005). Compared to micelles structured from smaller molecules, polymeric micelles have much lower critical micelle concentration (CMC), defined as the lowest concentration of amphiphilic molecules to form a micellar structure. Low CMC enhances the stability of drugs incorporated in the micelle. Moreover, the larger size of polymeric micelles retards the rate of body clearance by renal filtration. Therefore they can stay in the body for a longer time for long-term drug release.

If a sugar-containing block serves as the hydrophilic block, an amphiphilic polymer can be classified as glycopolymer. Glycopolymers are defined as synthetic polymers that incorporate carbohydrate groups. They may play an important role in a wide range of biomolecular events

such as cellular recognition, adhesion, cell growth regulation, cancer cell metastasis, and inflammation.

Lectins, which are sugar binding proteins, have been used as model receptor to evaluate the binding capacity of glycopolymers. They only recognize specific carbohydrates. For example, concanavalin A (Con A) has the ability to bind with glucose and mannose; wheat germ agglutinin (WGA) only binds with N-acetylglucosamine; and ricinus communis agglutinin (RCA) can bind with galactose and N-acetylgalactosamine. On molecular basis, interaction of lectin with carbohydrate includes polar and hydrophobic interactions. Polar interaction is usually induced by polar amino acid side chains of the lectin and polar carbohydrate groups. In some cases, lectin-bound water can serve as a bridge between the binding partners by hydrogen bonding. Metal ions such as  $\text{Ca}^{2+}$  or  $\text{Mg}^{2+}$  may be incorporated into lectin and interact with the hydroxyl groups on the sugar. In addition to polar interactions, carbohydrate containing hydrophobic groups, can interact with aromatic amino acids on some lectins through hydrophobic interaction.

It was found that galactose binding lectins are over-expressed in a variety of tumor cells (Lahm et al. 2001); receptors of galactose are also highly expressed in hepatocytes cells in the liver (Ashwell et al. 1982) and the lung (Powell 1980); Moreover, mannose receptors are expressed on macrophages, which are the host cells of parasites and bacteria in the bloodstream (Chellat et al. 2005) and dendritic cells, which are the immune cells in the mammalian immune system (Guermonprez et al. 2002).

A device which can bind with these carbohydrate receptors and release drugs could minimize the side effect on healthy cells in the body. In regard to receptor binding, carbohydrates fixed within

a glycopolymer structure are more efficient than free carbohydrates due to the multivalent effect of the clustered saccharide (Lee et al. 1995). Therefore, glycopolymer micelles have the potential to be used as targeted drug delivery carrier. With the sugar moieties on the hydrophilic block, glycopolymer micelles may interact with the receptors mentioned above, therefore enhancing the targeting efficiency of incorporated drugs.

### 3.1.2 Synthesis of amphiphilic glycopolymers

Amphiphilic glycopolymers were generally synthesized by controlled radical polymerization which can produce a nearly perfect amphiphilic structure. Controlled polymerization included atom transfer radical polymerization (ATRP), reversible addition-fragmentation chain transfer polymerization (RAFT) and nitroxide mediated radical polymerization (NMRP). In the following paragraphs, glycopolymers obtained by these methods are briefly introduced.

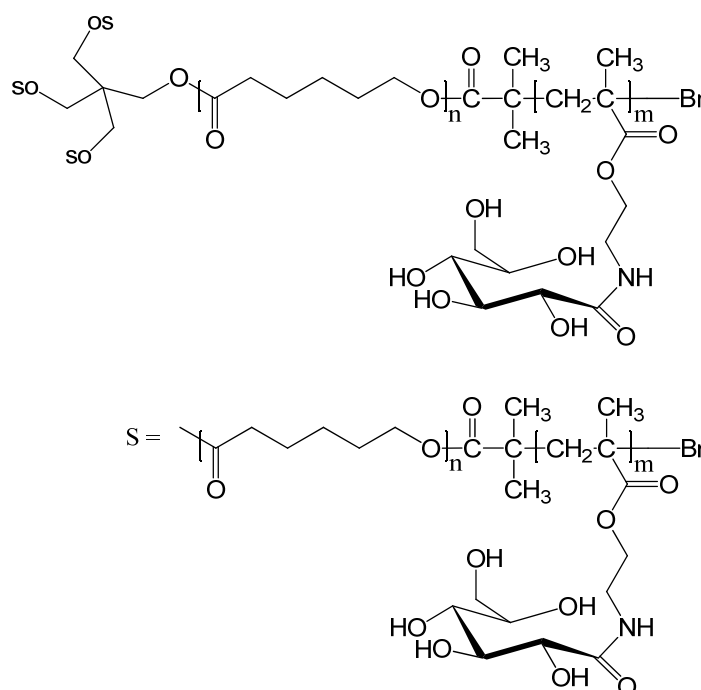
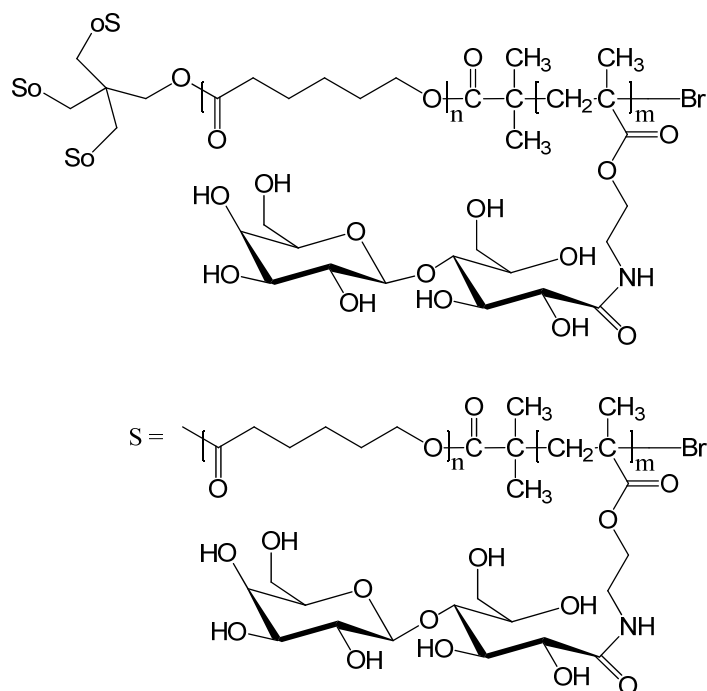


Figure 3-1 Star-shaped poly( $\epsilon$ -caprolactone)-b-poly(D-gluconamidoethyl methacrylate) glycopolymers (SPCL-PGAMA) (Dai et al. 2008)



**Figure 3-2 Star-shaped poly( $\epsilon$ -caprolactone)-b-poly(D-lactobionamidoethyl methacrylate) glycopolymers (SPCL-PLAMA) (Zhou et al. 2008)**

Several amphiphilic glycopolymers were produced by ATRP. Dai et al. (2008) synthesized a biodegradable star-shaped poly( $\epsilon$ -caprolactone)-b-poly(D-gluconamidoethyl methacrylate) glycopolymer (SPCL-PGAMA) (shown in Fig. 3.1) in 2008. Zhou et al. (2008) further reported a biodegradable star-shaped poly( $\epsilon$ -caprolactone)-b-poly(D-lactobionamidoethylmethacrylate) glycopolymer (SPCL-PLAMA) (Fig. 3.2) in the same year. Later on, an amphiphilic glycopolymer (shown in Fig. 3.3) consisting of poly(2-[(D-glucosamin-2N-yl)carbonyl]-oxy}ethyl methacrylate (PHEMAGI)) as hydrophilic block and poly(n-butyl acrylate) (PBA) as hydrophobic block were prepared by Leon et al. (2010). Amphiphilic glycopolymers synthesized by ATRP were also prepared by Narain et al. (2003), Qiu et al. (2009), and Dai et al. (2009). RAFT synthesized amphiphilic glycopolymers were reported by Liu et al. (2010), Hetzer et al. (2010), and Xiao et al. (2011). In 2009, Ting et al. (2009) obtained an amphiphilic diblock



glycopolymer: poly(2-( $\beta$ -D-galactosyloxy)ethyl methacrylate-co-styrene)-b-polystyrene (P(GalEMA-co-S)-b-PS) (Fig. 3.4) using NMRP.

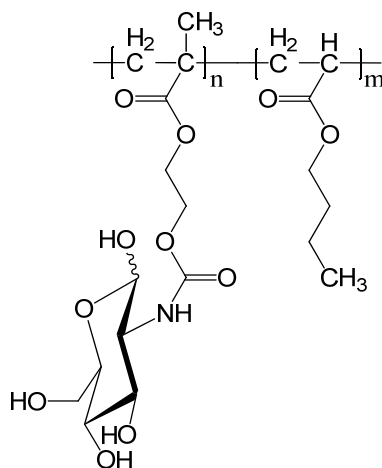


Figure 3-3 Poly(2-{{(D-glucosamin-2N-yl)carbonyl]-oxy}ethyl methacrylate-b-poly(n-butyl acrylate) (PHEMAGI-PBA) (Leon et al. 2010)

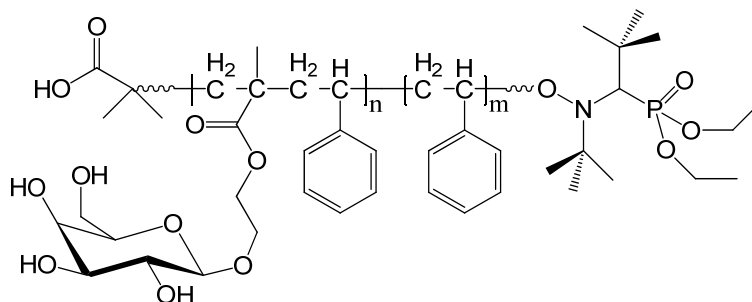
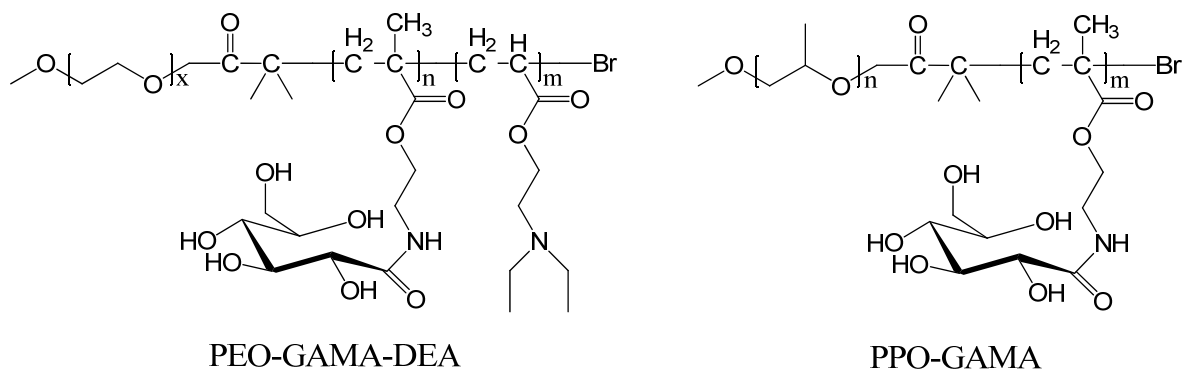


Figure 3-4 Poly(2-( $\beta$ -D-galactosyloxy)ethyl methacrylate-co-styrene)-b-polystyrene (P(GalEMA-co-S)-b-PS) (Ting et al. 2009)

### 3.1.3 Formation of glycopolymer micelles

Formation of most glycopolymer micelles was done by adding distilled water slowly into a glycopolymer organic solution followed by dialysis. In addition to dialysis stimulated micelles, there are some stimuli-responsive glycopolymers that could form when dissolving in a specific environment.

A poly(ethylene oxide)-b-poly(D-gluconamidoethyl methacrylate)-b-poly(2-(diethylamino)ethyl methacrylate) (PEO-GAMA-DEA) (Fig. 3.5) was synthesized by Narain et al. (2003). DEA homopolymer is a weak polybase with a  $\text{PK}_b$  of around 6.7 and is insoluble in neutral or alkaline aqueous solution.  $^1\text{H-NMR}$  spectra and surface tension measurements of the triblock copolymer showed the pH-responsive feature of DEA block. The amphiphilic copolymer formed micelles in alkaline aqueous solution. A poly(propylene oxide)-b-poly(D-gluconamidoethyl methacrylate) (PPO-GAMA) (Fig. 3.5) was also reported by Narain et al. in the same paper. The thermo-responsive feature of PPO block was determined by  $^1\text{H-NMR}$  spectra and surface tension measurement of the diblock copolymer. Below  $5\text{ }^\circ\text{C}$ , the PPO-GAMA diblock copolymer was molecularly dissolved. However, micelles were formed at  $20\text{ }^\circ\text{C}$ .



**Figure 3-5 Poly(ethylene oxide)-poly(D-gluconamidoethyl methacrylate)-poly(2-(diethylamino)ethyl methacrylate) (PEO-GAMA-DEA) and poly(propylene oxide)-poly(D-gluconamidoethyl methacrylate) (PPO-GAMA) (Narain et al. 2003)**

Liu et al. (2010) prepared a pH-responsive amphiphilic glycopolymer composed of a block of poly(2-(diethylamino)ethyl methacrylate) (PDEA) and a block of poly(3-O-methacryloyl- $\alpha,\beta$ -D-glucopyranose) (PMAGlc) (as shown in Fig. 3.6). The pH-responsive feature of DEA block was also confirmed by  $^1\text{H-NMR}$  spectra and transmittance measurement. The glycopolymer self-assembled at alkaline pH.

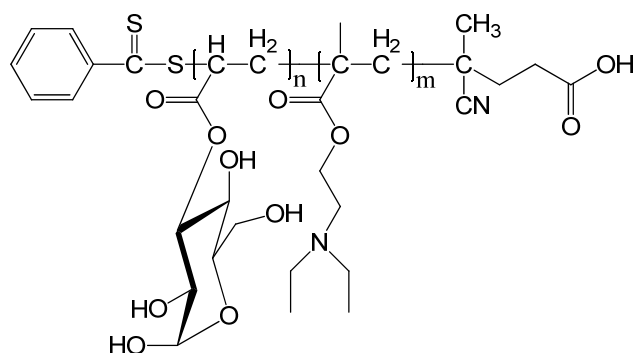


**Figure 3-6 Poly(3-*O*-methacryloyl- $\alpha,\beta$ -D-glucopyranose)-b-poly(2-(diethylamino)ethyl methacrylate) (PMAGlc-PDEA) (Liu et al. 2010)**

Hetzer et al. (2010) synthesized a thermo-responsive amphiphilic glycopolymer: poly(2'-(4-vinyl-[1,2,3]-triazol-1-yl)ethyl-*O*- $\alpha$ -D-mannopyranoside)-b-poly(*N*-isopropyl acrylamide) (Fig. 3.7). Poly(*N*-isopropyl acrylamide) (NIPAAm) is a common thermo-responsive polymer which is water-soluble at room temperature. However, it becomes water-insoluble above 32°C. Therefore, the amphiphilic glycopolymer formed micelles at the elevated temperature above 40°C. The formation of micelles was confirmed by measuring the micelle size by dynamic light scattering (DLS) at different temperatures.

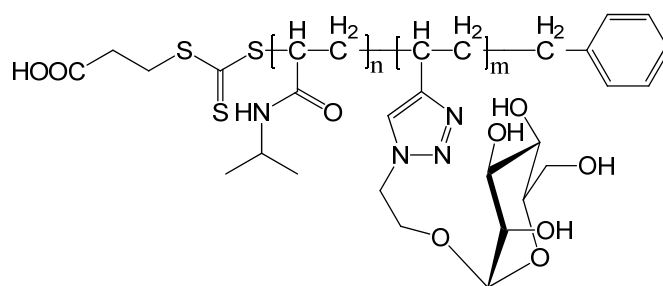


**Figure 3-7 Poly(2'-(4-vinyl-[1,2,3]-triazol-1-yl)ethyl-*O*- $\alpha$ -D-mannopyranoside)-b-poly(*N*-isopropyl acrylamide) (Hetzer et al. 2010)**

A thermo-responsive amphiphilic glycopolymer (AcMH-b-PEtOz-b-AcMH) (as shown in Fig. 3.8), based on peracetylated maltoheptaose (AcMH) and poly(2-ethyl-2-oxazoline) (PEtOz), was prepared by Chen et al. (2010). Poly (2-ethyl-2- oxazoline) (PEtOz) is a thermo-sensitive

polyelectrolyte with good biocompatibility and biodegradability. The thermo-responsive feature of the glycopolymer was determined by optical transmittance measurement from 25 °C to 65 °C. Micelles were prepared by direct dissolution in water at room temperature.

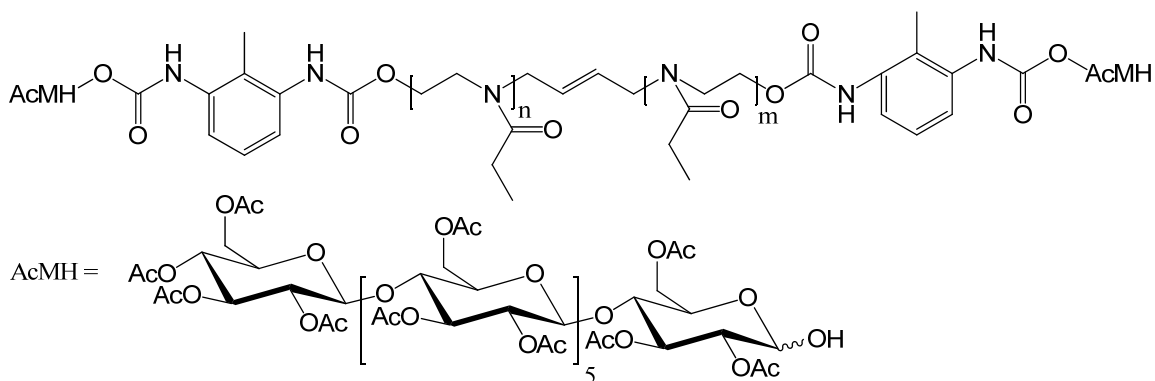


**Figure 3-8 Peracetylated maltoheptaose-b-poly(2-ethyl-2-oxazoline)-b-peracetylated maltoheptaose (AcMH-b-PEtOz-b-AcMH) (Chen et al. 2010)**

### 3.1.4 CMC of amphiphilic glycopolymers

**Table 3.1 CMC of amphiphilic glycopolymers and common surfactant**

Amphiphilic Glycopolymers			
Author	Year	Composition	CMC ( $\mu\text{M}$ )
Dai et al.	2008	SPCL15-PGAMA7	1.886
		SPCL15-PGAMA18	1.409
Zhou et al.	2008	SPL15-PLAMA7	0.422
		SPL15-PLAMA3	0.35
		SPL75-PLAMA5	0.0751
Qiu et al.	2009	SPBLG36-PGAMA7	0.411
		SPBLG30-PGAMA13	0.62

		SPBLG36-PGAMA39	0.417
Dai et al.	2009	PAMAM-PCL28-PGAMA3	0.125
		PAMAM-PCL28-PGAMA28	0.0423
Chen et al.	2010	AcMH-b-PEtOz50-b-AcMH	0.241
		AcMH-b-PEtOz80-b-AcMH	0.376
Common Surfactants			
Name		Type	CMC ( $\mu\text{M}$ )
Sodium dodecyl sulfate (SDS)		Anionic	8200
Cetyltrimethylammonium bromide (CTAB)		Cationic	920
Polysorbate 20 (Tween 20)		Nonionic	42
Polysorbate 80 (Tween 80)		Nonionic	28

As shown in Table 3.1, the CMC of amphiphilic glycopolymers was determined to be in the magnitude of  $10^1$  to  $10^{-2}$   $\mu\text{M}$ ; however, the CMC of common surfactants was much larger. As mentioned above, the smaller CMC of the micelles increases the stability of drugs incorporated in them.

### **3.1.5 Hydrodynamic diameter ( $D_h$ ) of glycopolymer micelles and their interaction with lectins**

Data in Table 3.2 show that the  $D_h$  of glycopolymer micelles formed from amphiphilic glycopolymers are much greater than micelles structured by common surfactants. As mentioned above, the larger size of polymeric micelles makes it possible for these micelles to remain in the body for a longer time and thus for an extended drug release.

**Table 3.2 D<sub>h</sub> of glycopolymer aggregates determined by DLS and lectins that can interact with them**

Amphiphilic Glycopolymers					
Author	Year	Composition	D <sub>h</sub> (nm)	Aggregate type	Lectin
Dai et al.	2008	SPCL15-PGAMA11	25.5	spherical micelle	Con A
		SPCL15-PGAMA7	n/a	worm-like micelle	
		SPCL50-PGAMA5	200.6	vesicle	
Zhou et al.	2008	SPCL15-PLAMA3	109.5	micellar aggregate	RCA <sub>120</sub>
		SPCL15-PLAMA11	432.3	micellar aggregate	
		SPCL75-PLAMA11	148.0	small vesicle	
			742.9	big vesicle	
Leon et al.	2010	PHEMAGI46-b-PBA20	141.8	micellar aggregate	Con A
		PHEMAGI46-b-PBA162	141.8	micellar aggregate	
Ting et al.	2009	P(GalEMA <sub>0.9</sub> -co-S <sub>0.1</sub> )-b-PS	35	spherical micelle	PNA
Narain et al.	2003	PPO33-LAMA50	38	spherical micelle	n/a
Liu et al.	2010	PDEAEMA18-PMAGlc19	22	spherical micelle	Con A
			233	micellar aggregate	
Hetzer et al.	2010	n/a	22.5	spherical micelle	Con A
Qiu et al.	2009	SPBLG36-PGAMA7	161.2	micellar aggregate	Con A
		SPBLG36-PGAMA39	274.3	micellar aggregate	
Dai et al.	2009	PAMAM-PCL28-PGAMA3	102.2	vesicle	Con A
		PAMAM-PCL28-PGAMA9	146.3	spherical micelle	
		PAMAM-PCL28-PGAMA28	305.4	micellar aggregate	
		AcMH-b-PEtOz50-b-AcMH	126.5	spherical micelle	

Chen et al.	2010	AcMH-b-PEtOz80-b-AcMH	133.1	spherical micelle	n/a
Common Surfactants					
Name		Type		$D_h$ (nm) of micelle	
Sodium dodecyl sulfate (SDS)		Anionic		1.7	
Cetyltrimethylammonium bromide (CTAB)		Cationic		3	
Polysorbate 20 (Tween 20)		Nonionic		8.5	
Polysorbate 80 (Tween 80)		Nonionic		10.7	

It should be noted that, as the molecular ratio of hydrophobic to hydrophilic segment varies, the amphiphilic glycopolymer may aggregate in a different manner and form worm-like micelles or vesicles rather than micelles of spherical shape (Dai et al. 2008 and Dai et al. 2009). Small vesicles may further aggregate to become big vesicles (Zhou et al. 2008,). With hydrogen bonding and van der Waals forces among the hydrophilic shell, single micelles can aggregate to become spherical aggregates (Zhou et al. 2008, Leon et al. 2010, Liu et al. 2010, Qiu et al. 2009, and Dai et al. 2009). The two species could be observed in the same TEM image (Liu et al. 2010). Most amphiphilic glycopolymers can be recognized by lectins.

### 3.1.6 Drug-loaded glycopolymer micelles

Drugs can be incorporated into micelles by chemical conjugation or by physical entrapment. Chemical conjugation implies the formation of a covalent bond, such as an amide group (Yoo and Park 2001 and Hruby et al. 2005), or an ester group (Zhang et al. 2005 and Xie et al. 2007) between specific groups on the drug and the hydrophobic core of the micelles. Cleavage of such bonds is the result from hydrolysis or pH change (Bae et al. 2003, 2005<sup>a</sup>, and 2005<sup>b</sup>). Physical entrapment of drugs is generally achieved by dialysis or oil-in-water emulsion procedure. For the

dialysis method, the drug and amphiphilic copolymer are first dissolved in a solvent in which they are both soluble. The solution is added to a solvent that is selective only for the hydrophilic part of the polymer. As the good solvent is replaced by the selective one, the drug is incorporated while forming micelles. In the oil-in-water emulsion method, an aqueous solution of the copolymer is added to a solution of the drug in a water-insoluble volatile solvent to form an oil-in-water emulsion. The drug-loaded micelles are formed as the solvent evaporates. The physically entrapped drug is released from the micelle by diffusion and upon dissociation of micelle. Micelle dissociation may result from physical stimuli such as pH (Lee et al. 2003), temperature (Wei et al. 2006, Nakayama et al. 2006), ultrasound (Husseini et al. 2000 and 2007, Pruitt et al. 2002, Gao et al. 2005), ultraviolet (Lepage et al. 2007), and near-infrared light (Goodwin et al. 2005). The incorporated drug may be released at the specific site where those physical stimuli are applied.

Drug-loaded glycopolymer micelles have been reported by several research groups. A star-shaped glycopolymer composed of poly( $\gamma$ -benzyl L-glutamate) and poly(D-gluconamidoethyl methacrylate) (SPBLG-PGAMA) (shown in Fig. 3.9) was reported by Qiu et al. (2009). An anticancer drug: doxorubicin was loaded into the micelle aggregates via dialysis method with loading efficiency of about 20%.  $D_h$  of doxorubicin-loaded micelles were found to be more than twice compared to the blank micelles. Doxorubicin was released *in vitro* for 1000 h in a triphasic pattern. About 15% of drug was discharged in 15 h, about 45% of drug was released in 12 days, and about 20% of drug was delivered within 1 month.



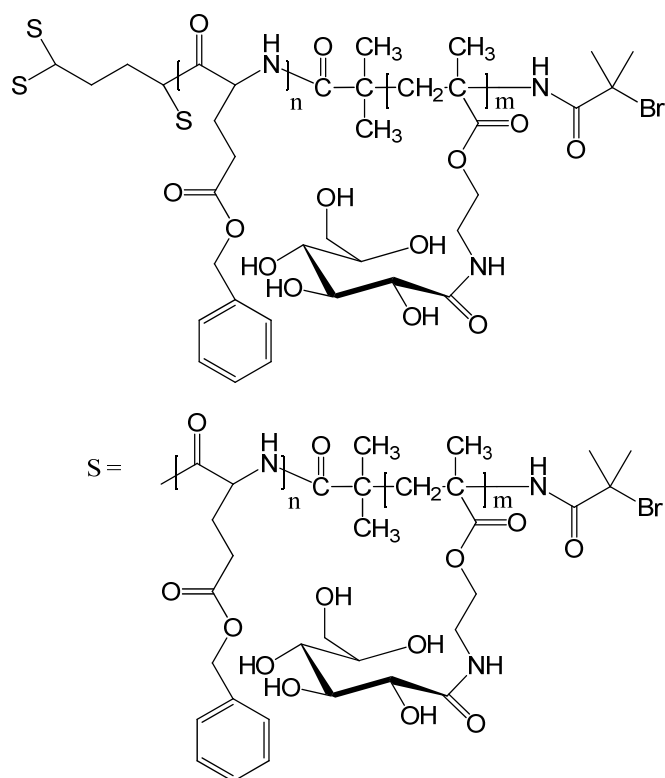


**Figure 3-9 Star-shaped poly( $\gamma$ -benzyl L-glutamate)-b-poly(D-gluconamidoethyl methacrylate) (SPBLG-PGAMA) (Qiu et al. 2009)**

A star poly(amido amine)-b-poly( $\epsilon$ -caprolactone)-b-poly(D-gluconamidoethyl methacrylate) (PAMAM– PCL–PGAMA) (Fig. 3.10) block glycopolymer with a dendrimer core was prepared by Dai et al. (2009). Nimodipine-loaded micelle aggregates were fabricated by dialysis method. A high drug loading efficiency of 74.1% was reported. The *in vitro* drug release underwent a burst release for about 10 h and a slow release for about 160 h.

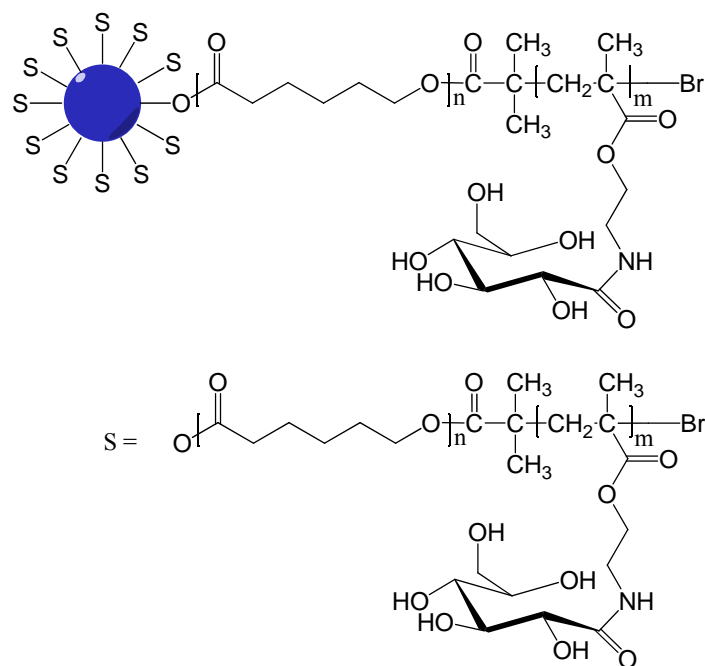


**Figure 3-10 Star poly(amido amine)-b-poly( $\epsilon$ -caprolactone)-b-poly(D-gluconamidoethyl methacrylate) (PAMAM– PCL–PGAMA) (Dai et al. 2009)**

Indomethacin was incorporated into the thermo-responsive amphiphilic glycopolymer (AcMH-b-PEtOz-b-AcMH) (Fig. 3.8) mentioned above (Chen et al. 2010). The formation of indomethacin-loaded micelles was achieved by adding distilled water to ethanol solution of glycopolymer and indomethacin. Unloaded indomethacin was removed by centrifugation and filtration. The incorporation of indomethacin was confirmed by determining the chemical structure by  $^1\text{H}$  NMR, and measuring the size by DLS and TEM. *In vitro* drug release profiles were obtained at different temperatures. The indomethacin release profile was apparently different at 25°C and 37°C compared to that at 45°C and 55°C due to the thermo-responsive property.

The biodegradable and biocompatible aldehyde-functionalized glycopolymer poly(6-*O*-(2'-formyl-4'-vinylphenyl)-D-galactopyranose-b-5,6-benzo-2-methylene-1,3-dioxepane) (PVDG-BMDO) (Fig. 3.11) was synthesized by Xiao et al. (2011). Doxorubicin was conjugated onto the glycopolymer bearing highly reactive aldehyde groups via an acid-labile Schiff base linkage. The

drug efficiency was determined to be as high as 14%. The doxorubicin-loaded micelles exhibited an average hydrodynamic diameter of about 125 nm determined by DLS. TEM images showed a slightly smaller diameter. Lower cytotoxicity of doxorubicin-loaded micelles than free doxorubicin was reported. *In vitro* release studies indicated that only about 10% of doxorubicin was released at pH of 7.4 in 120 h. However, about 63% of doxorubicin was discharged at a pH of 5.0 in the same time period. The pH dependent release profile was attributed to the acid-cleavable Schiff base linkage. This feature might be useful since tumor sites and inflammatory tissues have a more acidic environment (Ulbrich et al. 2000, Etrych et al. 2002, Ulbrich et al. 2004, Hruby et al. 2005, and Chytil et al. 2006).

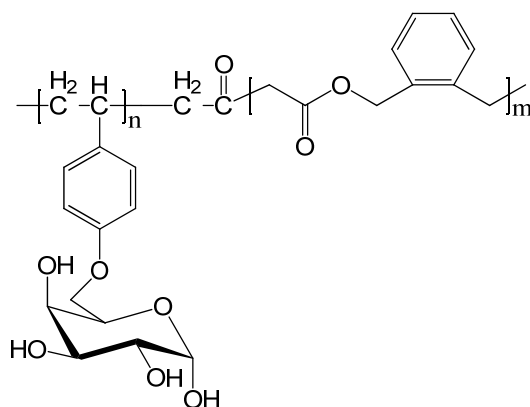


**Figure 3-11 Poly(6-*O*-(2'-formyl-4'-vinylphenyl)-*D*-galactopyranose-*b*-5,6-benzo-2-methylene-1,3-dioxepane) (PVDG-BMDO) (Xiao et al. 2011)**

As mentioned above, glycopolymer micelles which are mostly biocompatible, have lower CMC values and larger sizes than their smaller molecule counterparts (e.g., common surfactant micelles). Most glycopolymer micelles can be recognized by lectin. Drugs can be incorporated into the glycopolymer micelles and be released in a controlled manner. In addition, drugs could be released from stimuli-responsive glycopolymer micelles upon environmental changes. All

these features might result in a stable drug-carrying device which could stay in the body for a longer period of time and release drugs to a targeted site in a regulated manner.

### **3.1.7 Approach**

In this work, a thermo-responsive amphiphilic glycopolymer: poly(2-[(D-glucosamin-2N-yl)carbonyl]-oxy}ethylmethacrylate)-b-poly(propylene oxide) (PHEMAGI-PPO) was synthesized via atom transfer radical polymerization (ATRP). The chemical structure of glycomonomer (HEMAGI), macroinitiator (PPO-Br), and glycopolymer was confirmed by <sup>1</sup>H-NMR or <sup>13</sup>C-NMR spectra. Degree of functionalization of PPO-Br was determined to be more than 99%. Molecular weight of glycopolymers was estimated from integral ratio of specific peaks on NMR spectra. The CMC of the glycopolymer was measured by dye micellization method and the diameter of the formed particles was determined by DLS. The lectin recognition property was determined using Con A as a model lectin.

## **3.2 Experimental part**

### **3.2.1 Materials**

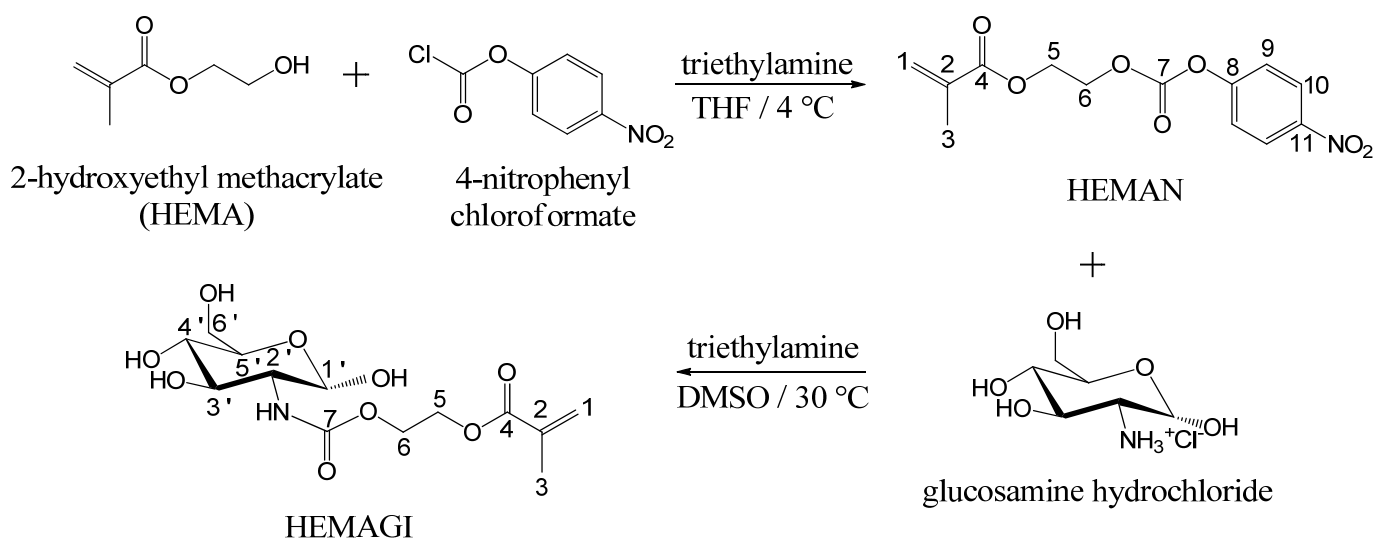
2-Hydroxyethyl methacrylate (97%), triethylamine (99%), tetrahydrofuran (THF) (99%), 4-nitrophenyl chloroformate (97%), dimethyl sulfoxide (DMSO) (99%), diethyl ether (99%), dichloromethane (99.5%) were all from Alfa Aesar and used without further purification. Anhydrous magnesium sulfate (MgSO<sub>4</sub>) (99%, Strem Chemicals), D-glucosamine hydrochloride (99.9%, Calbiochem), dimethylformamide (99.9%, Fisher), methanol (99.8%, EMD), phosphorus pentoxide (98%, Spectrum), mono-capped poly(propylene oxide) (Mn=2500, Sigma-Aldrich), toluene (99.9%, Fisher), 2-bromoisobutyryl bromide (97%, TCI), decolorizing

charcoal (Sigma-Aldrich), Eosin Y (0.5% w/v, Sigma-Aldrich), and Concanavalin A (Sigma-Aldrich) were used as received.

### 3.2.2 Synthesis of 2- $\{[(D\text{-glucosamine-}2N\text{-yl)carbonyl]oxy\}$ ethyl methacrylate (HEMAGI)

The glycomonomer, HEMAGI was synthesized by modifying the procedure previously reported (Leon, et al., 2010; shown in Scheme 3.1). Briefly, 2-hydroxyethyl methacrylate (HEMA) (0.021 mol, 2.73 g), triethylamine (0.025 mol, 2.52 g), anhydrous magnesium sulfate (1.5 g), and THF (10 ml) were placed in a 50 mL flask, which was entirely isolated from the outside to avoid any contact with humidity. Once the solution was equilibrated at 4°C, 4-nitrophenyl chloroformate (0.021 mol, 5.076 g) in pre-dried THF (10 mL) was successively added while stirring. The reaction was performed at 4°C for 24 h. The formed triethyl amine chlorohydrate and magnesium sulfate were filtered off. The product was poured into 100 mL water and separated by separatory funnel. (Yield: 82.2 %)

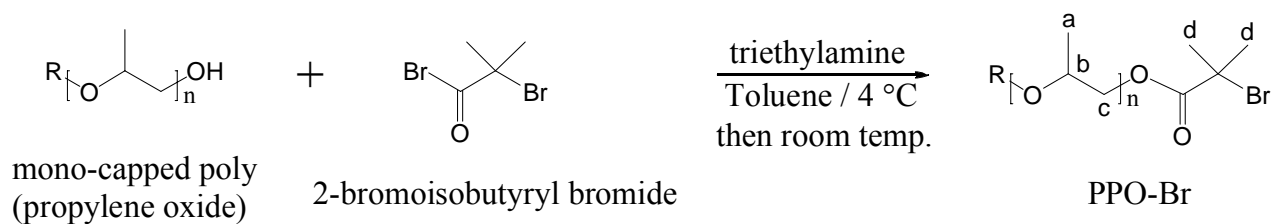
Subsequently, the modified monomer with p-nitrophenylcarbonate groups, HEMAN, (0.0085 mol, 2.51 g) was dissolved in 10 mL anhydrous DMSO at 30°C. Triethylamine (0.01275 mol, 1.288 g), D-glucosamine chloride (0.0085 mol, 1.832 g) and anhydrous magnesium sulfate (1.5 g) were then added while stirring. The reaction was maintained for 24 h at 30°C. After that, magnesium sulfate was filtered off. The glycomonomer, HEMAGI, was poured into 100 mL diethyl ether/dichloromethane mixture (4:1, v/v) and isolated by separatory funnel. The product was purified by solubilization in DMF/methanol (1:4, v/v) and reprecipitation in diethyl ether/dichloromethane mixture (4:1, v/v). The resulting product was dried in vacuum at room temperature in the presence of phosphorus pentoxide until constant weight was reached (Yield: 58.6 %).



**Scheme 3.1 Synthesis of glycomonomer: 2-[(D-glucosamine-2N-yl)carbonyl] oxy}ethyl methacrylate (HEMAGI)**

### 3.2.3 Synthesis of end-group bromized poly(propylene glycol) (PPO-Br) as macroinitiator

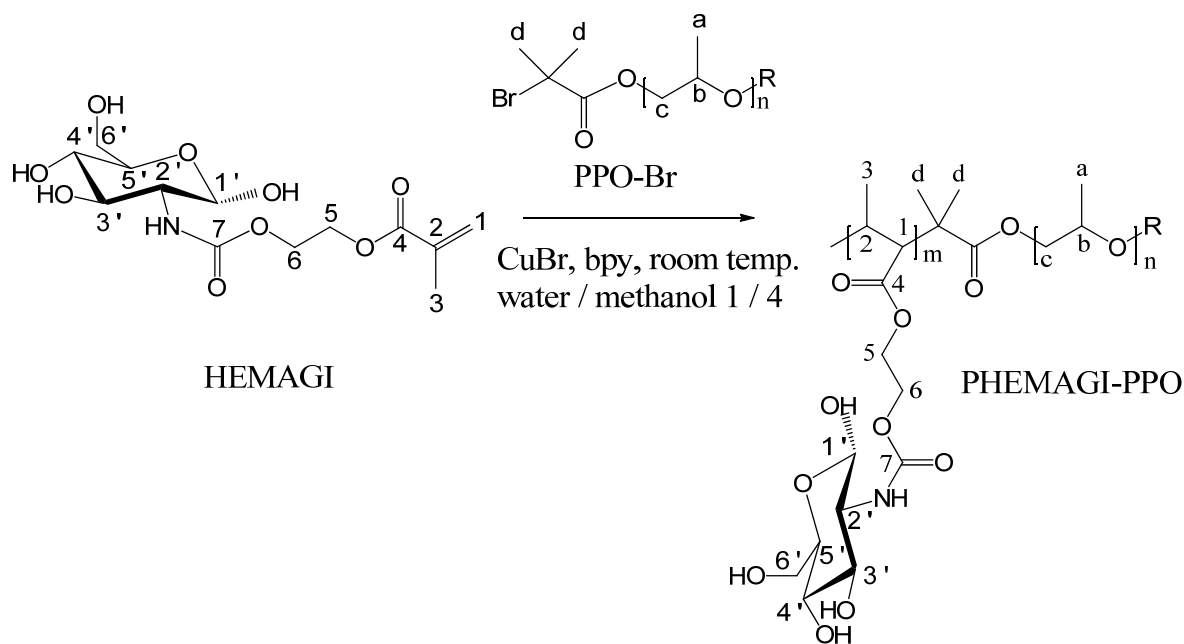
For the synthesis of the macroinitiator, the procedure described in Li et al. (2005) was followed. The reaction is shown in Scheme 3.2. Mono-capped poly(propylene oxide) (PPO) ( $M_n=2500$ ) (3.2 mmol, 8 g) and triethylamine (6.5 mmol, 0.6565 g) were dissolved in 20 mL anhydrous toluene and the solution mixture was cooled to 4°C. 2-bromoisobutyryl bromide (6.5 mmol, 1.495 g) in 5 mL anhydrous toluene was added dropwise via a syringe over about one hour. The temperature was slowly raised to room temperature and stirred for 48 h. The reaction mixture was filtered and the filtrate treated with decolorizing charcoal for 12 h, dried over anhydrous  $\text{MgSO}_4$  for 1 h, and then filtered again. The resulting product was dried using a rotary evaporator to get the final PPO-Br macroinitiator. (Yield: 51.5 %)



Scheme 3.2 Synthesis of macroinitiator poly(propylene oxide)-Br (PPO-Br)

### 3.2.4 Atom transfer radical polymerization of amphiphilic glycopolymer PHEMAGI-PPO

HEMAGI was dissolved in a methanol/water (4/1, v/v) mixed solvent (10 mL). Then PPO-Br macroinitiator was added and the solution was degassed via argon gas purge. After 30 min, the copper(I) bromide (CuBr) catalyst and 2,2'-bipyridine (bpy) were added to the reaction solution, which turned dark brown. After reacting at 20 °C for 24 h, the solution was exposed to air and diluted with methanol, which led to aerial oxidation of the ATRP catalyst. The final product was obtained by drying under vacuum using rotary evaporator. Scheme 3.3 illustrates the process. The amount of utilized reagents is listed in Table 3.3.



Scheme 3.3 Atom transfer radical polymerization of amphiphilic glycopolymer: PHEMAGI-PPO

**Table 3.3 Amount of utilized reagents for synthesis of PHEMAGI-PPO**

HEMAGI	PPO-Br	CuBr	bpy	Targeted Composition
1.35 g, 4.03 mmol	0.1625 g, 0.065 mmol	9.5 mg, 0.065 mmol	20 mg, 0.13 mmol	PHEMAGI <sub>62</sub> -PPO <sub>41</sub>
1.35g 4.03 mmol	0.219 g 0.088 mmol	12.86 mg 0.088 mmol	27.08 mg 0.176 mmol	PHEMAGI <sub>46</sub> -PPO <sub>41</sub>
1.35 g, 4.03 mmol	0.325 g, 0.013 mmol	19 mg, 0.013 mmol	40 mg, 0.026 mmol	PHEMAGI <sub>31</sub> -PPO <sub>41</sub>
1.35 g, 4.03 mmol	0.65 g, 0.026 mmol	38 mg, 0.026 mmol	80 mg, 0.052 mmol	PHEMAGI <sub>15</sub> -PPO <sub>41</sub>

### 3.2.5 Characterization

#### 3.2.5.1 Structural characterization by nuclear magnetic resonance (NMR) spectroscopy

<sup>1</sup>H and <sup>13</sup>C NMR were used to determine the structure of the synthesized products. Spectra were recorded at room temperature on solution in deuterated dimethyl sulfoxide (DMSO-d<sub>6</sub>) or deuterated chloroform (CDCl<sub>3</sub>) with a Bruker 400 spectrometer at 400 MHz. Typical parameters for the proton spectra were a 15 s pulse delay, a 3 s acquisition time, a 20.68 ppm spectral width, and 16 scans.

#### 3.2.5.2 Critical micelle concentration (CMC) determination using UV-Vis spectroscopy

The CMC was measured by dye micellization method (Patist et al. 2000) with Eosin Y as indicator. Absorbance of solutions which contained equal amounts of Eosin Y but increasing amounts of PHEMAGI-PPO at 542 nm was measured by UV-Vis spectroscopy (Thermo



Spectronic Genesys 6). The straight line portion was linear-fitted by Origin 8.0. The interception of the fitted line and the baseline which was the absorbance without PHEMAGI-PPO in solution was determined to be the critical micelle concentration.

### **3.2.5.3 Thermo-responsive behavior of PHEMAGI-PPO micelles**

Thermo-responsive behavior of the micelles (2 mg/ml) was measured on a UV-Vis spectroscopy (Thermo Spectronic Genesys 6) incorporated with a thermocouple. Optical transmittance at wavelength of 600 nm from 8 °C to 22 °C was recorded. Temperature at which the transmittance is 50% of original was defined as the lower critical solution temperature (LCST) (Wang et al. 2003, Weberm et al. 2009).

### **3.2.5.4 Micellar size measurement in aqueous solution by transmission electron microscopy (TEM)**

The particle size was measured using a Zeiss EM 10CR transmission electron microscopy. One drop of micellar solution was deposited onto the surface of 300 mesh Formvar-carbon film-coated copper grids. Excess solution was removed by filter paper. Negative staining using phosphotungstic acid (0.5 wt %) was carried out to increase the contrast of the specimens. Thirty micelles each were measured from the images. The average diameter and average deviation was calculated.

To induce the desired micelle formation, PHEMAGI-PPO was dissolved in water at 4°C, and the temperature was slowly increased within 1 h to reach room temperature.

### **3.2.5.5 Interaction of PHEMAGI-PPO micelles with Con A**

The lectin recognition property was evaluated by changes in the solution turbidity. Buffer solution (pH = 7.2) was prepared by adding 0.01 M  $\text{KH}_2\text{PO}_4$ , 1 mM  $\text{MnCl}_2$ , 1 mM  $\text{CaCl}_2$ , and 0.5 M  $\text{NaCl}$  in deionized water. Glycopolymer micelles were formed in the buffer solution by cooling method described above. Con A buffer solution at 0.5 mg/mL was added to buffer solutions of glycopolymer micelles with various concentration. The solution was stirred intensively 1 h after adding Con A buffer solution. Then, the turbidity was measured by a UV-Vis spectrometer (Thermo Spectronic Genesys 6) at 360 nm and room temperature.

### 3.3 Results and Discussion

#### 3.3.1 $^{13}\text{C}$ -NMR characterization of HEMAN

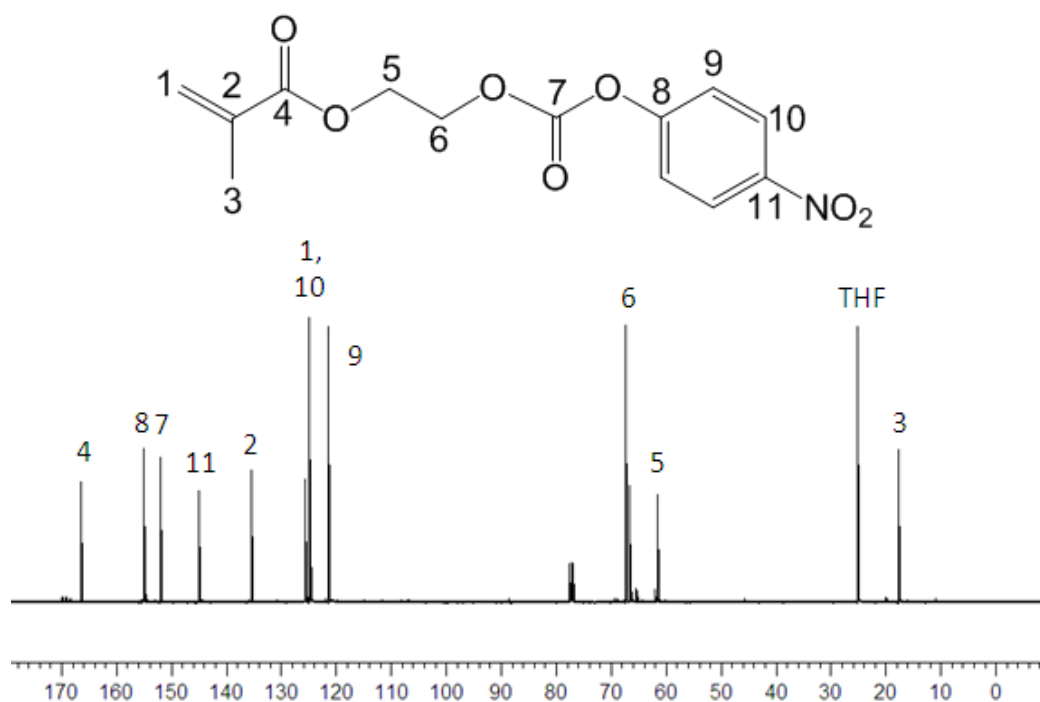


Figure 3-12  $^{13}\text{C}$ -NMR spectra of HEMAN, HEMAN: (400MHz,  $\text{CDCl}_3$ ),  $\delta(\text{ppm})$ : 17.7 (C-3), 61.6 (C-5), 66.6 (C-6), 121.5 (C-7), 124.3 (C-8), 125.7 (C-1), 135.5 (C-2), 145.0 (C-11), 152.0 (C-7), 155.1 (C-8), and 166.4 (C-4)

The chemical structure of HEMAN was confirmed by  $^{13}\text{C}$ -NMR spectra shown in Fig. 3.12. The signal of C-7 at 121.5 ppm confirmed the success of the reaction. Signals of C-8 to C-11 represent the benzene ring. Signals of C-1 and C-3 indicated that the vinyl group in the structure was still present, thus the ability of polymerization remained.

### 3.3.2 $^1\text{H}$ -NMR characterization of the glycomonomer HEMAGI

Signals of H-4', H-3', H-5', H-6', H'-1, OH, and NH suggest that glucosamine has been linked to HEMAN (See Fig. 3.13). Signals of H-1 and H-3 indicated that the vinyl group remained, and thus the ability for future polymerization was preserved.

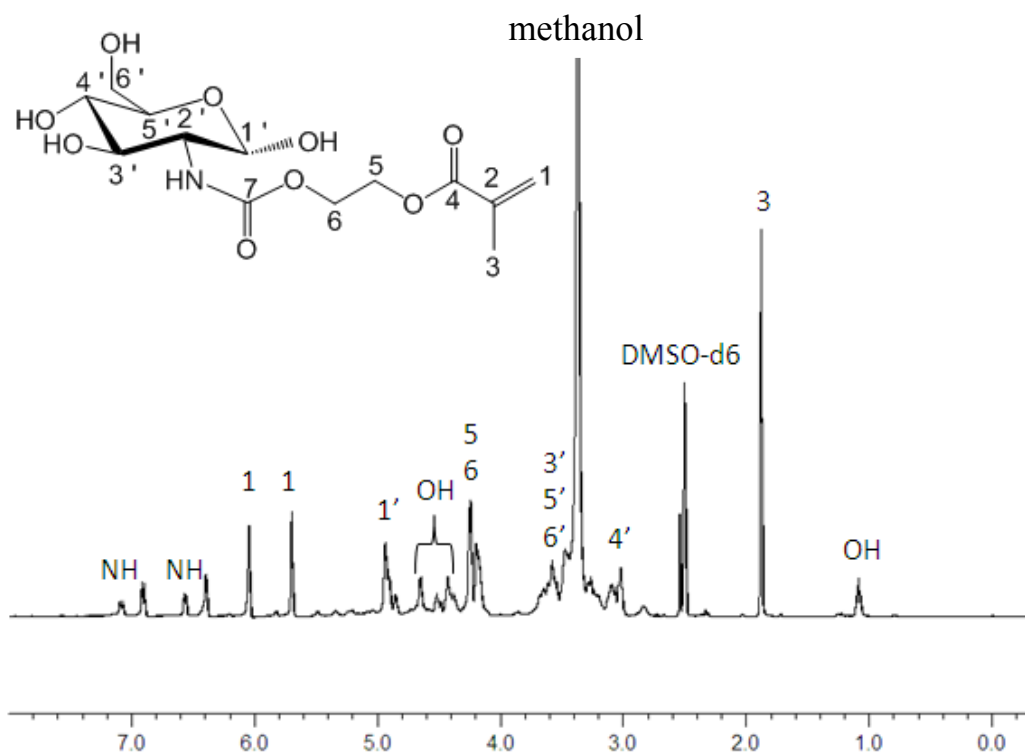


Figure 3-13  $^1\text{H}$ -NMR spectra of HEMAGI, HEMAGI: (400MHz, DMSO-d6),  $\delta$ (ppm): 1.08 (OH), 1.88 (H-3), 2.99-3.16 (H-4'), 3.38-3.71 (H-3', H-5', H-6'), 4.12-4.29 (H-5, H-6), 4.33-4.71 (OH), 4.92 (H-1'), 5.70 (H-1), 6.04 (H-1), and 6.56 (NH), 7.08 (NH)

### 3.3.3 $^1\text{H-NMR}$ characterization of macroinitiator: PPO-Br

As shown in Fig. 3.14, the signal of H-d at 1.94 ppm is the evidence that 2-bromosiobutyryl bromide was linked to PPO via the hydroxyl end group. The degree of bromide functionalization was estimated to be more than 99% from the integral ratio of H-d and H-a.

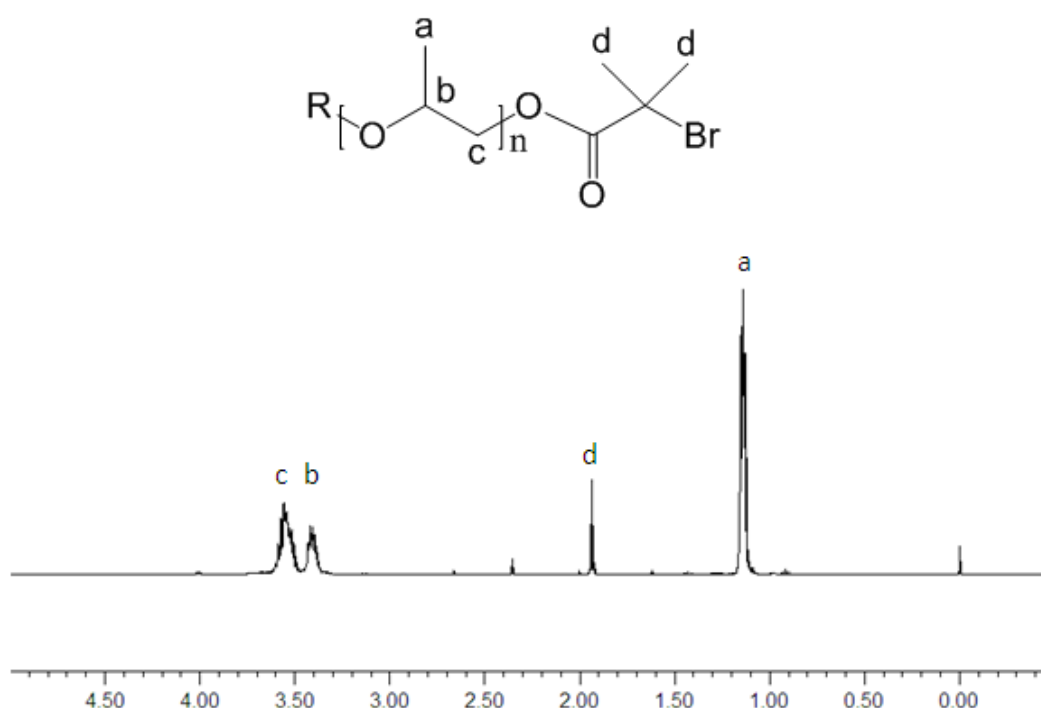
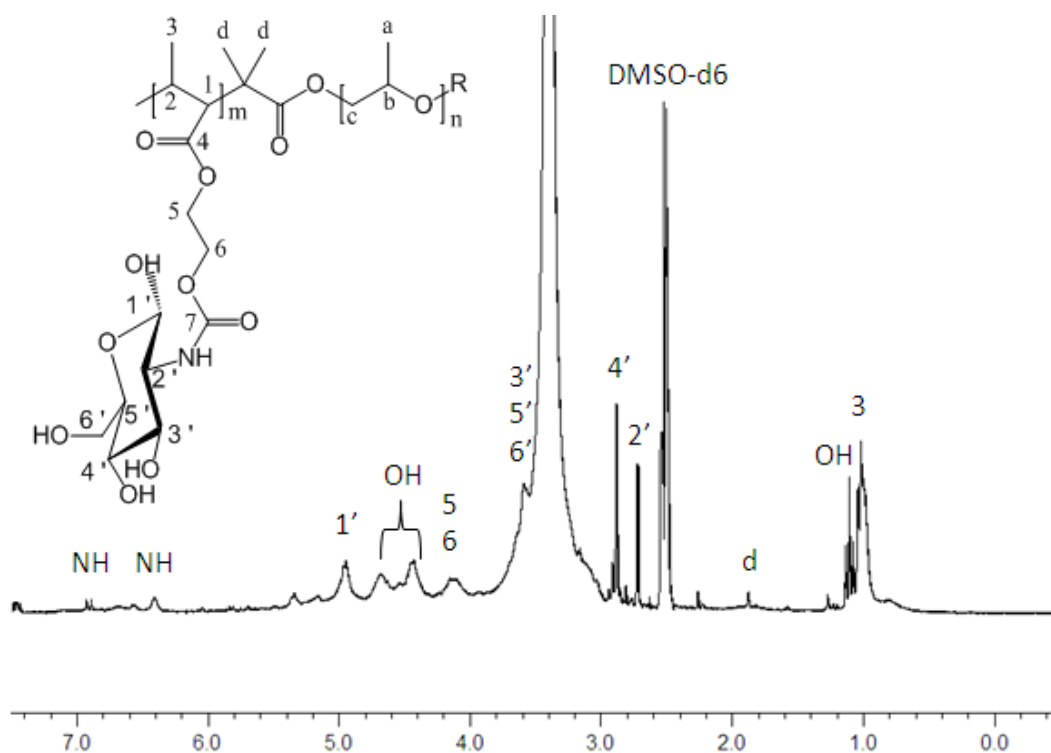


Figure 3-14  $^1\text{H-NMR}$  spectra of PPO-Br, PPO-Br: (400MHz,  $\text{CDCl}_3$ ),  $\delta(\text{ppm})$ : 1.14 (H-a), 1.94 (H-d), 3.41 (H-b), and 3.55 (H-c)

### 3.3.4 $^1\text{H-NMR}$ characterization of amphiphilic glycopolymer PHEMAGI-PPO

The signals of H-3 at 1.88 ppm and H-1 at 5.7 ppm and 6.04 ppm of HEMAGI disappeared in the spectra of PHEMAGI-PPO (Fig. 3.15). It indicated that HEMAGI reacted completely during the polymerization. The integral ratio of H-d at 1.94 ppm and H-3 from 0.61 to 1.06 ppm could be used to estimate the molecular weight of the glycopolymer.



**Figure 3-15**  $^1\text{H-NMR}$  spectra of PHEMAGI-PPO, PHEMAGI-PPO: (400MHz, DMSO- $d_6$ ),  $\delta$ (ppm): 0.61-1.06 (H-3), 1.08 (OH), 1.94 (H-d), 2.65-3.16 (H-2', H-4'), 3.38-3.71 (H-3', H-5', H-6'), 4.12-4.29 (H-5, H-6), 4.33-4.71 (OH), 4.95 (H-1'), and 6.41, 6.89 (NH)

### 3.3.5 Molecular weight and yield of PHEMAGI-PPO glycopolymer

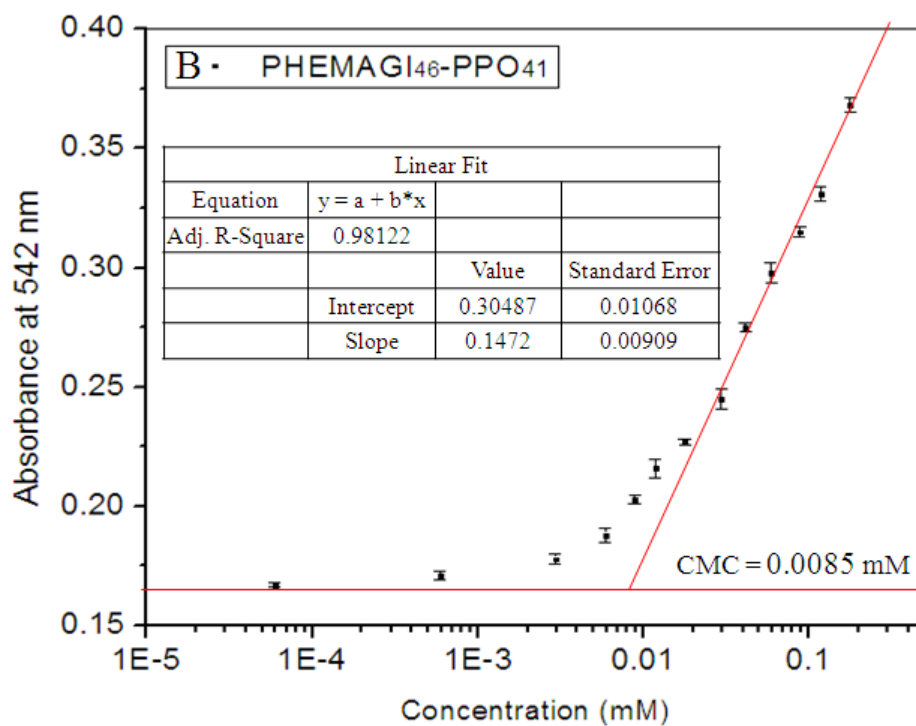
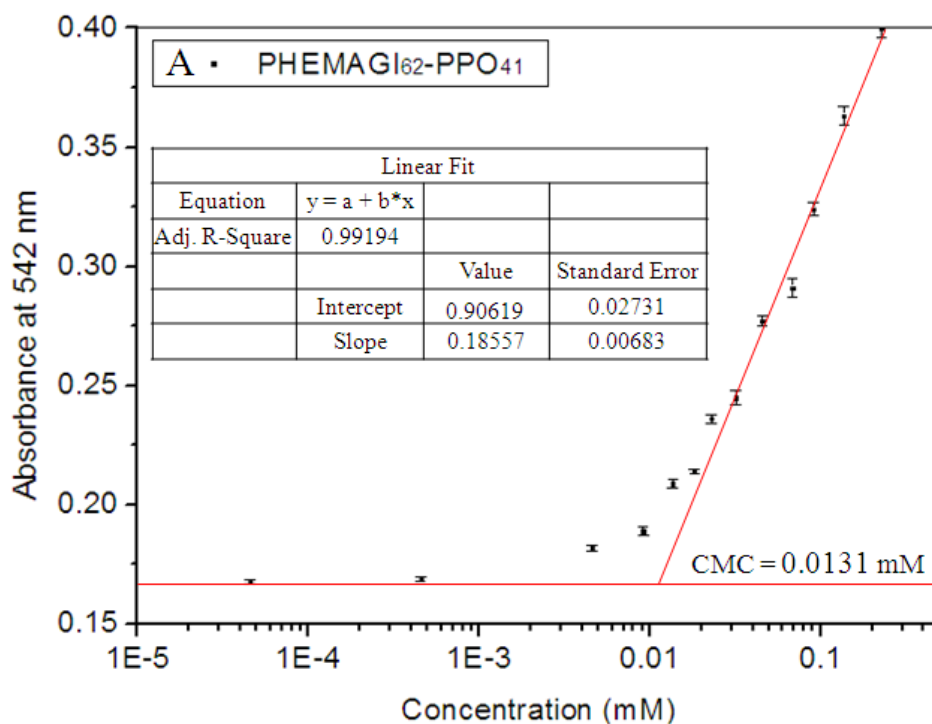
As shown in Table 3.4, PHEMAGI-PPO glycopolymers were synthesized with high yield. The molecular weight of the glycopolymers calculated from the integral ratio of specific peaks on  $^1\text{H-NMR}$  spectra agreed well with the theoretical molecular weight.

**Table 3.4 Characteristics of PHEMAGI-PPO glycopolymers synthesized by ATRP**

Composition	Mn, NMR (g/mol)	Mn, Theo (g/mol)	Yield (%)
PHEMAGI <sub>62</sub> -PPO <sub>41</sub>	21930	23270	92.1
PHEMAGI <sub>46</sub> -PPO <sub>41</sub>	16905	17910	87.9
PHEMAGI <sub>31</sub> -PPO <sub>41</sub>	11880	12885	90.4
PHEMAGI <sub>15</sub> -PPO <sub>41</sub>	7190	7525	89.3

### 3.3.6 Critical micelle concentration (CMC) determination for PHEMAGI-PPO

CMC is an important parameter for the thermodynamic stability of micelles in aqueous solution (Du et al. 2006). As determined by dye micellization method, the relationship of the absorbance intensity as a function of glycopolymer concentration at room temperature is shown in Fig. 3.16. It can be seen that after reaching a certain concentration, the absorbance intensity increased linearly. The concentration at the on-set of the linear increase began and the critical micelle concentration (CMC) of PHEMAGI<sub>62</sub>-PPO<sub>41</sub>, PHEMAGI<sub>46</sub>-PPO<sub>41</sub>, PHEMAGI<sub>31</sub>-PPO<sub>41</sub>, and PHEMAGI<sub>15</sub>-PPO<sub>41</sub> are recorded in Table 3.5. With the same hydrophobic block, the CMC reduced from 12.4  $\mu$ M to 6.4  $\mu$ M, however, increased to 13.8  $\mu$ M with the decreasing length of the hydrophilic segment. Concentration at which linear increase began also followed a similar trend. As mentioned by Zhou et al. (2008) and Dai et al. (2009), the CMC decreased with the decreasing length of the hydrophilic segment. A micelle has a hydrophobic core and a hydrophilic shell. Thus, a higher amount of PHEMAGI<sub>15</sub>-PPO<sub>41</sub> might be necessary to form a micelle since the short PHEMAGI block on PHEMAGI<sub>15</sub>-PPO<sub>41</sub> may not cover the relatively large PPO core efficiently to form the core-shell structure.



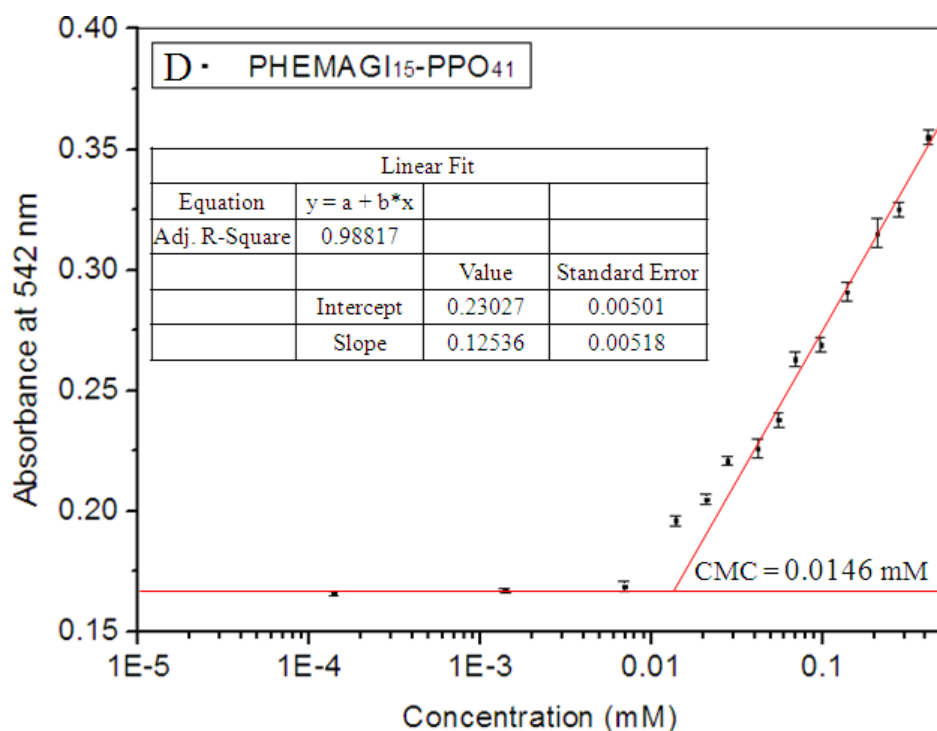
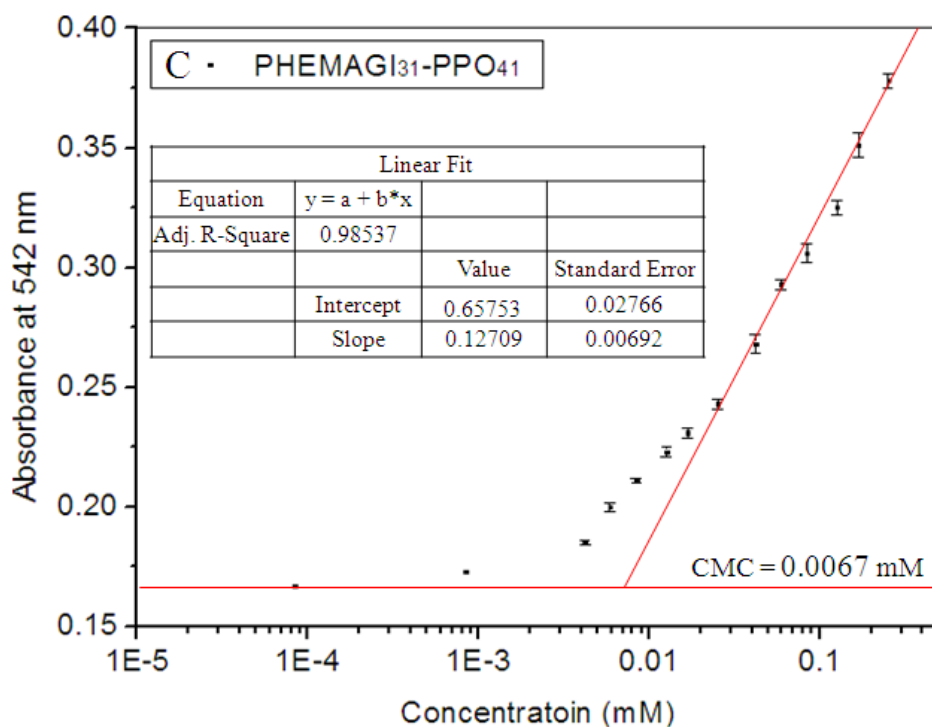


Figure 3-16 CMC determination of PHEMAGI<sub>62</sub>-PPO<sub>41</sub> (A), PHEMAGI<sub>46</sub>-PPO<sub>41</sub> (B), PHEMAGI<sub>31</sub>-PPO<sub>41</sub> (C), and PHEMAGI<sub>15</sub>-PPO<sub>41</sub> (D), (two individually synthesized samples of each glycopolymer were used to determine the CMC, only one sample is shown in the figure. Average value is listed in table 3.5)



**Table 3.5 CMC and concentration at onset of linear course**

Composition	CMC ( $\mu\text{M}$ )	Concentration at onset of linearity ( $\mu\text{M}$ )
PHEMAGI <sub>62</sub> -PPO <sub>41</sub>	12.4 $\pm$ 0.7	31.9
PHEMAGI <sub>46</sub> -PPO <sub>41</sub>	8.1 $\pm$ 0.4	29.6
PHEMAGI <sub>31</sub> -PPO <sub>41</sub>	6.4 $\pm$ 0.3	25.3
PHEMAGI <sub>15</sub> -PPO <sub>41</sub>	13.8 $\pm$ 0.8	41.7

### 3.3.7 Thermo-responsive behavior of PHEMAGI-PPO micelles

Fig. 3-17 demonstrates the optical transmittance of PHEMAGI-PPO solutions as a function of temperature. Initially, the transmittance was higher than 90% at 8 °C. However, after reaching a certain temperature, transmittance reduced dramatically and then equilibrated at room temperature. It indicated that PHEMAGI-PPO was molecularly dissolved in the solution at 8 °C; however, micelles were formed at room temperature. Such thermo-responsive feature could be utilized for facile formation of micelles while maintaining stability of the micelles at room temperature. The LCST of PHEMAGI<sub>62</sub>-PPO<sub>41</sub>, PHEMAGI<sub>46</sub>-PPO<sub>41</sub>, PHEMAGI<sub>31</sub>-PPO<sub>41</sub>, and PHEMAGI<sub>15</sub>-PPO<sub>41</sub> are recorded in Table 3.6. It was known that PPO exhibited a LCST in the range of 10 °C – 20 °C, depending on concentration of polymer (Alexandridis et al. 1995). At 2 mg/ml, LCST of PPO was about 10 °C. The LCST of all glycopolymers lied between 11 °C to 14 °C, which showed that the hydrophilic block played a minor role in phase transition. Among all glycopolymers, PHEMAGI<sub>15</sub>-PPO<sub>41</sub> had slightly lower LCST than others. It was due to inefficient coverage of the short hydrophilic block to hydrophobic block as discussed above.

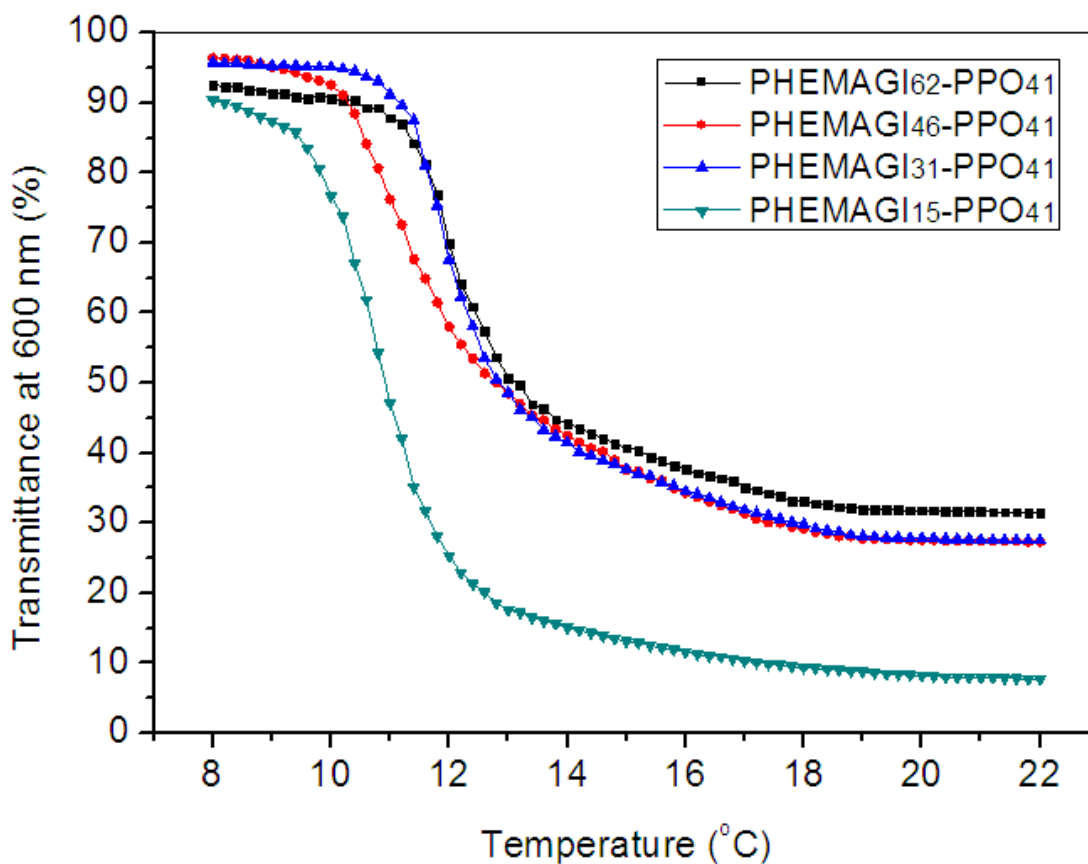


Figure 3-17 Optical transmittance measurement as a function of temperature for PHEMAGI-PPO micelles (two individually synthesized samples of each glycopolymer were used to determine the LCST, only one sample is shown in the figure. Average value is listed in table 3.7)

Table 3.6 Lower critical solution temperature (LCST) of PHEMAGI-PPO

Composition	LCST (°C)
PHEMAGI <sub>62</sub> -PPO <sub>41</sub>	13.8 ± 0.2
PHEMAGI <sub>46</sub> -PPO <sub>41</sub>	13.4 ± 0.1
PHEMAGI <sub>31</sub> -PPO <sub>41</sub>	13.2 ± 0.1
PHEMAGI <sub>15</sub> -PPO <sub>41</sub>	11.2 ± 0.2

### 3.3.8 Size study of PHEMAGI-PPO micelles in aqueous solution

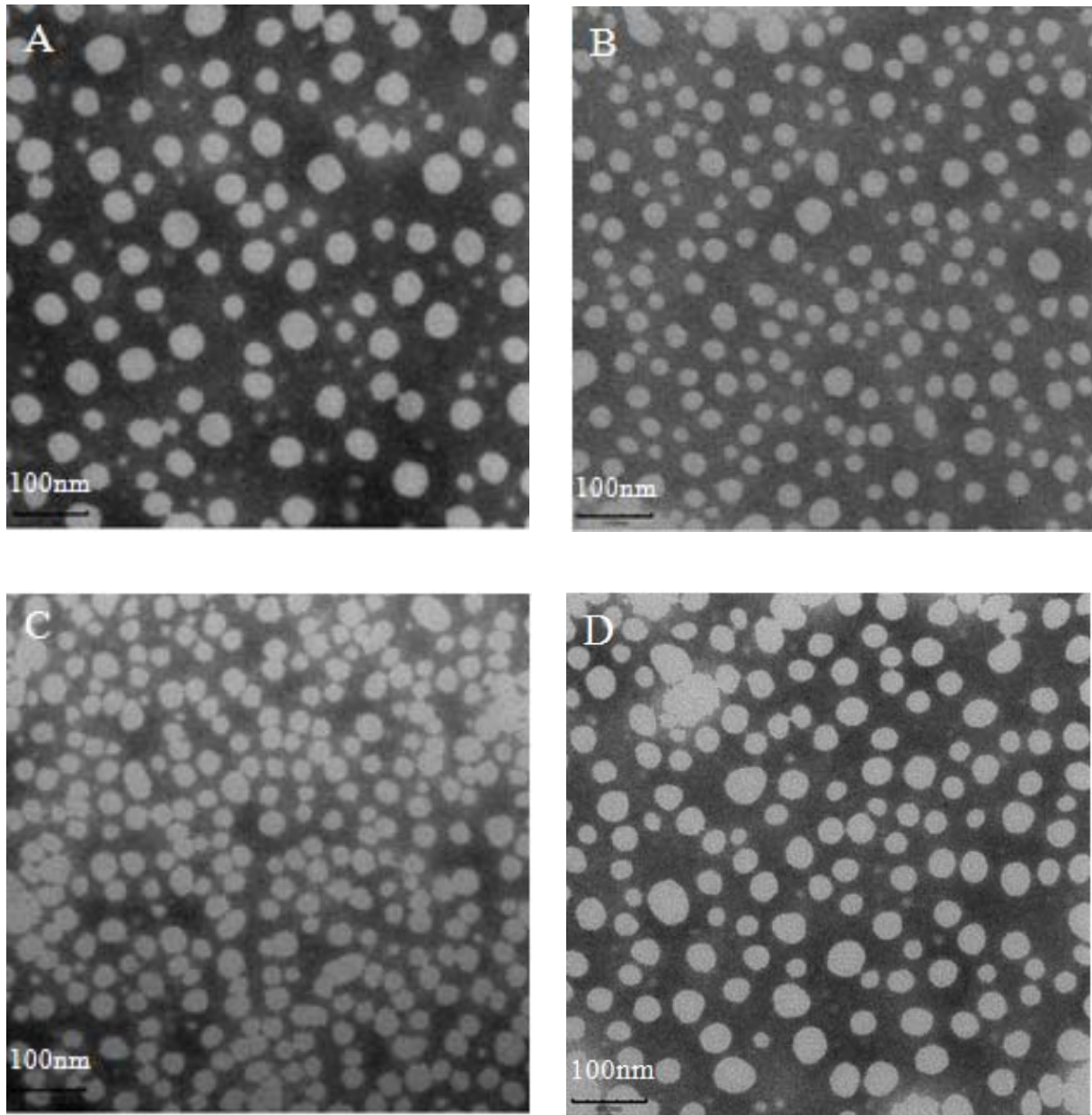


Figure 3-18 TEM images of PHEMAGI<sub>62</sub>-PPO<sub>41</sub> (A), PHEMAGI<sub>46</sub>-PPO<sub>41</sub> (B), PHEMAGI<sub>31</sub>-PPO<sub>41</sub> (C), and PHEMAGI<sub>15</sub>-PPO<sub>41</sub> (D), scale bar: 100 nm

**Table 3.7 Size of the micelles and the concentration of the glycopolymer solutions**

Composition	Size (nm)	Concentration ( $\mu\text{M}$ )
PHEMAGI <sub>62</sub> -PPO <sub>41</sub>	$43.8 \pm 3.0$	13.7
PHEMAGI <sub>46</sub> -PPO <sub>41</sub>	$32.2 \pm 2.2$	11.8
PHEMAGI <sub>31</sub> -PPO <sub>41</sub>	$29.7 \pm 1.9$	8.4
PHEMAGI <sub>15</sub> -PPO <sub>41</sub>	$37.8 \pm 2.7$	13.9

The self-assembly behavior of PHEMAGI-PPO in aqueous solution was studied by transmission electron microscopy (TEM). The glycopolymer solutions were prepared and the concentration was slightly higher than the CMC determined above. Morphology of the micellar structure from PHEMAGI-PPO was investigated by TEM, as shown in Fig. 3.18. The size of the micelles and the concentration of the glycopolymer solutions are listed in Table 3.7. TEM images demonstrated the spherical shape of the micelles. As the length of hydrophilic PHEMAGI segment was reduced, the size of the resulting micelles also decreased. However, the size of PHEMAGI<sub>15</sub>-PPO<sub>41</sub> (D) which had larger diameter than PHEMAGI<sub>46</sub>-PPO<sub>41</sub> (B) and PHEMAGI<sub>31</sub>-PPO<sub>41</sub> (C), didn't follow the trend. As discussed in section on CMC, more PHEMAGI<sub>15</sub>-PPO<sub>41</sub> may be required to form the core-shell structure because of inefficient coverage of the short hydrophilic block to hydrophobic block. Therefore, the diameter of the resulting micelles was larger than expected. Overall, micelles with diameters ranging from 30 to 50 nm may be suitable for drug delivery (Haag, 2004).

### 3.3.9 Interaction of PHEMAGI-PPO micelles with Con A

The lectin binding ability was measured by using Con A as a model lectin. Con A is well-known for binding specifically to  $\alpha$ -mannosyl and  $\alpha$ -glucosyl residues (Liener et al. 1986). In this test, Con A interacts with the already formed glycopolymer micelles and is precipitated out of the solution together with the micelle. After 1 h, the solution was stirred and the turbidity was measured. Fig. 3.19 presents the turbidity variation with the glycopolymer concentration. Absorbance indicated the amount of Con A-glycopolymer micelles aggregates. As it can be observed, the absorbance intensity initially increased with increasing concentration, then reached a plateau which showed the limitation of binding ability of glycopolymer micelles. By comparing PHEMAGI<sub>31</sub>-PPO<sub>41</sub> and PHEMAGI<sub>62</sub>-PPO<sub>41</sub>, it could be found that PHEMAGI<sub>31</sub>-PPO<sub>41</sub> with shorter HEMAGI blocks and containing less sugar moieties bound with more Con A than PHEMAGI<sub>62</sub>-PPO<sub>41</sub> at the same concentration. As the glycopolymers already self-assembled to micelles in the buffer solution, Con A only interacted with sugar moieties on the surface of micelles. Therefore, the length of HEMAGI blocks played a minor role for the interaction of Con A with the micelles. Considering that CMC of PHEMAGI<sub>31</sub>-PPO<sub>41</sub> was about half of the PHEMAGI<sub>62</sub>-PPO<sub>41</sub>'s, more micelles were formed in the PHEMAGI<sub>31</sub>-PPO<sub>41</sub> buffer solution. Thus, more Con A-micelle aggregates precipitated out of the solution. Interaction of Con A with PHEMAGI<sub>46</sub>-PPO<sub>41</sub> also depended on its CMC value. The Con A binding ability test demonstrated the potential application of PHEMAGI-PPO micelles as a targeted drug delivery device.

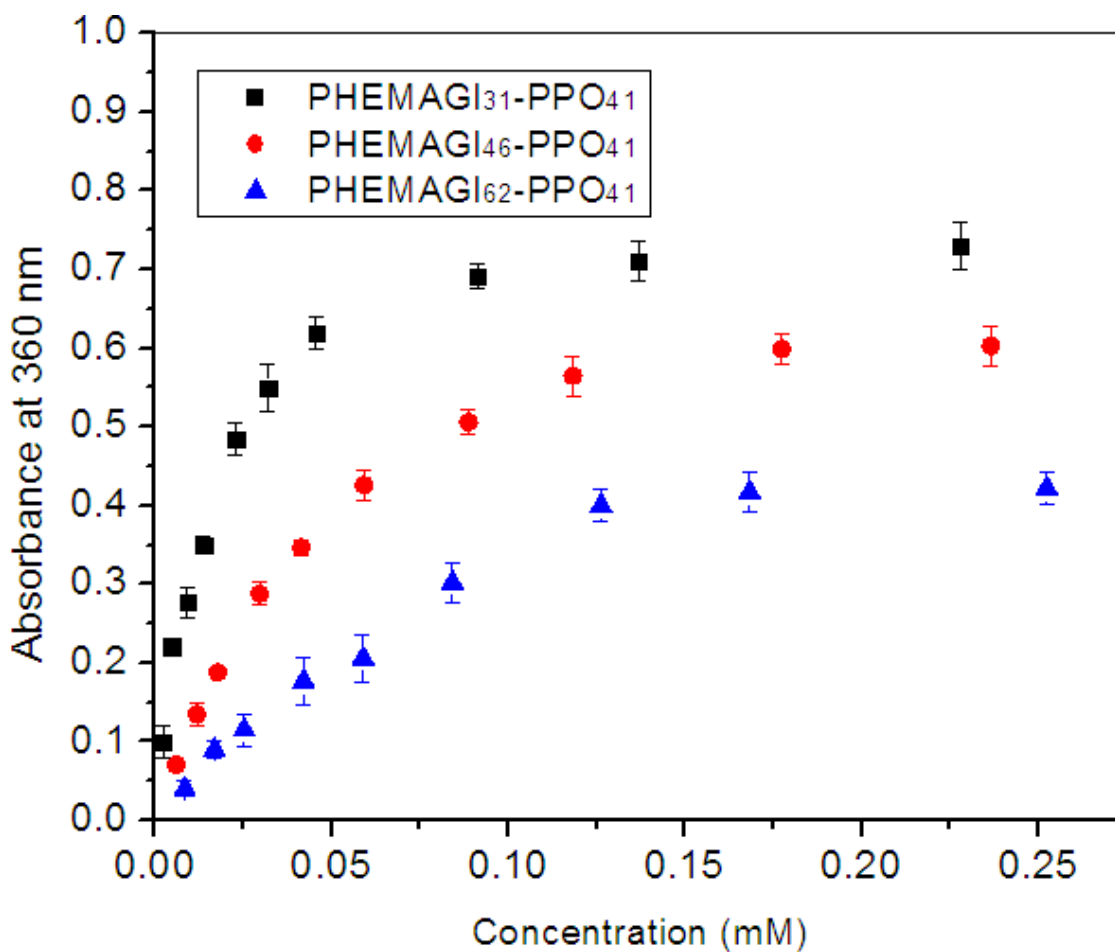


Figure 3-19 Lectin binding ability test of PHEMAGI-PPO using Con A (0.5 mg/mL) as the model lectin

### 3.4 Conclusions

Amphiphilic glycopolymers PHEMAGI-PPO with different compositions were successfully synthesized by ATRP. The chemical structure was confirmed by NMR spectra. Molecular weight of the glycopolymers, estimated from integral ratio of specific peaks on NMR spectra, agreed well with the theoretical value. Critical micelle concentration was determined to be low. Large diameter of self-assembly in micellar solution indicated that single micelles arranged to form larger aggregates because of hydrogen-bonding ability of the hydrophilic segment. The micelles were found to bind to Con A which shows that the system could find applications as drug delivery vehicle.

### 3.5 References

Alexandridis P and Hatton TA. *Colloids Surf. A*, **1995**, 96, 1-46

Ashwell G, and Harford J. *Annual Review of Biochemistry*, **1982**, 51, 531–554

Bae Y, Fukushima S, Harada A, and Kataoka K. *Angew Chem Int Ed Engl.*, **2003**, 42, 4640–4643

Bae Y, Nishiyama N, Fukushima S, Koyama H, Matsumura Y, and Kataoka K. *Bioconjugate Chem.*, **2005<sup>a</sup>**, 16, 122–130

Bae Y, Jang W, Nishiyama N, Fukushima S, and Kataoka K. *Mol Biosyst.*, **2005<sup>b</sup>**, 1, 242–250

Chellat F, Merhi Y, Moreau A, and Yahia LH. *Biomaterials*, **2005**, 26, 7260–7275

Chen Lq, Zhang Lm, Chen Jj, Yang J, and Li Rx. *Chinese Sci Bull.*, **2010**, 55, 4187–4196

Chytil P, Etrych T, Konak C, Sirova M, Mrkvan T, Rihova B, and Ulbrich K. *J. Controlled Released*, **2006**, 115, 26-36

Dai Xh, and Dong Cm. *Journal of Polymer Science: Part A: Polymer Chemistry*, **2008**, 46, 817–829

Dai Xh, Zhang Hd, and Dong Cm. *Polymer*, **2009**, 50, 4626–4634

Du Jz, Chen Dp, Wang Yc, Xiao Cs, Lu Yj, Wang J, and Zhang GZ. *Biomacromolecules*, **2006**, 7, 1898–1903

Etrych T, Chytil P, Jelinkova M, Rihova B, and Ulbrich K. *Macromol. Biosci.*, **2002**, 2, 43-52

Ferrari M. *Nat Rev Cancer*, **2005**, 5, 161-171

Gao Z, Fain H, and Rapoport N. *J Control Release*, **2005**, 102, 203–221

Goodwin AP, Mynar JL, Ma Y, Fleming GR, and Frechet JM. *J Am Chem Soc.*, **2005**, 127, 9952–9953

Guermonprez P, Valladeau J, Zitvogel L, Thery C, and Amigorena, S. *Annual Review of Immunology*, **2002**, 20, 621–667

Haag R, *Angew Chem Int Ed*, **2004**, 43, 278-282.

Hetzer M, Chen Gj, Barner-Kowollik C, and Stenzel MH. *Macromol. Biosci.*, **2010**, 10, 119–126

Hruby M, Konak C, and Ulbrich K. *Journal of Controlled Release*, **2005**, 103, 137–148

Husseini GA, Myrup GD, Pitt WG, Christensen DA, and Rapoport NY. *J Control Release*, **2000**, 69, 43–52

Husseini GA, Diaz DL, Rosa MA, Gabuji T, Zeng Y, Christensen DA, and Pitt WG. *J Nanosci Nanotechnol.*, **2007**, 7, 1028–1033

Lahm H, Andre S, Hoeflich A, Fischer JR, Sordat B, and Kaltner, H. *Journal of Cancer Research and Clinical Oncology*, **2001**, 127, 375–386

Lee CY, and Lee TR. *Accounts of chemical research*, **1995**, 28, 321-327

Lee E, Shin H, Na K, and Bae Y. *J Control Release*, **2003**, 90, 363–374

Leon O, Bordege V, Munoz-Bonilla A, Sanchez-Chaves M, and Fernandez-Garcia M. *Journal of*



Polymer Science: Part A: Polymer Chemistry, **2010**, 48, 3623–3631

Lepage M, Jiang J, Babin J, Qi B, Tremblay L, and Zhao Y. *Phys Med Biol.*, **2007**, 52, 249–255

Li Cm, Buurma NJ, Haq I, Turner C, and Armes SP. *Langmuir*, **2005**, 21, 11026-11033

Liener I, Sharon N, and Goldstein I. *The Lectins: Properties, Functions, and Applications in Biology and Medicine*; Academic Press: San Diego, **1986**

Liu L, Zhang Jc, Lv Wh, Luo Y, and Wang Xj. *Journal of Polymer Science: Part A: Polymer Chemistry*, **2010**, 48, 3350–3361

Nakayama M, Okano T, Miyazaki T, Kohori F, Sakai K, and Yokoyama M. *J Control Release*, **2006**, 115, 46–56

Narain R, and Armes SP. *Biomacromolecules*, **2003**, 4, 1746-1758

Patist A, Bhagwat SS, Penfield KW, Aikens P, and Shah DO. *J. Surfactants & Detergents.*, **2000**, 3, 53-58

Powell JT. *Biochemical Journal*, **1980**, 187, 123–129

Pruitt JD, and Pitt WG. *Drug Deliv.*, **2002**, 9, 253–258

Qiu S, Huang H, Dai Xh, Zhou W, and Dong Cm. *Journal of Polymer Science: Part A: Polymer Chemistry*, **2009**, 47, 2009–2023

Serizawa T, Yasunaga S, and Akashi M. *Biomacromolecules*, **2001**, 2, 469-475

Ting SR S, Min EH, Escale P, Save M, Billon L, and Stenzel MH. *Macromolecules*, **2009**, 42, 9422–9434

Ulbrich K, Subr V, Strohalm J, Plocova D, Jelinkova M, and Rihova B. *J. Controlled Release*, **2000**, 64, 63-79

Ulbrich K, Etrych T, Chytil P, Pechar M, Jelinkova M, and Rihova B. *Int. J. Pharm.*, **2004**, 277, 63-72

Wang CH and Hsiue GH. *Biomacromolecules*, **2003**, 4, 1487–1490

Weberm C, Becer CR, and Hoogenboom R. *Macromolecules*, **2009**, 42, 2965–2971

Wei H, Zhang Xz, Zhou Y, Cheng Sx, and Zhuo Rx. *Biomaterials*, **2006**, 27, 2028–2034

Xiao Ny, Liang H, and Lu J. *Soft Matter*, **2011**, 7, 10834-10842

Xie Zg, Lu Tc, and Chen Xs. *J. Appy Polym Sci.*, **2007**, 105, 2271-2279

Yamamoto Y, Nagasaki Y, and Kato Y. *J Control Release*, **2001**, 77, 27-338

Yoo HS, and Park TG. *Journal of Controlled Release*, **2001**, 70, 63–70

Zhang Xf, Li Yx, and Chen Xs. *Biomaterials*, **2005**, 26, 2121-2128

Zhou W, Dai Xh, Dong Cm. *Macromol. Biosci.*, **2008**, 8, 268–278